Journal of Medicinal Chemistry

Article

The Optimisation of a Novel, Weak Bromo and Extra Terminal Domain (BET) Bromodomain Fragment Ligand to a Potent and Selective Second Bromodomain (BD2) Inhibitor

Jonathan Thomas Seal, Stephen J. Atkinson, Helen Aylott, Paul Bamborough, Chun-wa Chung, Royston C. B. Copley, Laurie J. Gordon, Paola Grandi, James R. J. Gray, Lee A Harrison, Thomas G Hayhow, Matthew Lindon, Cassie Messenger, Anne-Marie Michon, Darren J Mitchell, Alex Preston, Rab K. Prinjha, Inmaculada Rioja, Simon Taylor, Ian D. Wall, Robert J Watson, James M. Woolven, and Emmanuel H Demont

J. Med. Chem., **Just Accepted Manuscript** • DOI: 10.1021/acs.jmedchem.0c00796 • Publication Date (Web): 23 Jul 2020

The Optimisation of a Novel, Weak Bromo and Extra Terminal Domain (BET) Bromodomain Fragment Ligand to a Potent and Selective Second Bromodomain (BD2) Inhibitor

Jonathan T. Seal[†], Stephen J. Atkinson*[□], Helen Aylott[†], Paul Bamborough[§], Chun-wa Chung[§], Royston C. B. Copley[§], Laurie Gordon[§], Paola Grandi[¥], James R. J. Gray[//], Lee A. Harrison[†], Thomas G. Hayhow[†□], Matthew Lindon[†#], Cassie Messenger[§], Anne-Marie Michon[¥], Darren Mitchell[†], Alex Preston[†], Rab K. Prinjha[†], Inmaculada Rioja[†], Simon Taylor[// *], Ian D. Wall[§], Robert J. Watson[†], James M. Woolven[§], Emmanuel H. Demont[†]*

[†]Epigenetics Discovery Performance Unit; Quantitative Pharmacology, Immunoinflammation Therapy Area Unit; [§]Platform Technology and Science, GlaxoSmithKline, Medicines Research Centre, Gunnels Wood Road, Stevenage, Hertfordshire, SG1 2NY, U.K; [¥]IVIVT Cellzome, Platform Technology and Science, GlaxoSmithKline, Meyerhofstr. 1, 69117 Heidelberg, Germany.

Abstract:

The profound efficacy, yet associated toxicity of pan-BET inhibitors is well documented. The possibility of an ameliorated safety profile driven by significantly selective (>100 fold) inhibition of a sub-set of the 8 bromodomains is enticing, but challenging given the close homology. Herein, we describe the X-ray crystal structure-directed optimisation of a novel weak fragment ligand with a pan-second bromodomain (BD2) bias, to potent and highly BD2 selective inhibitors. A template hopping approach,

enabled by our parallel research into an orthogonal template (**15,** GSK046) was the basis for the high selectivity observed. This culminated in two tool molecules **20** (GSK620) and **56** (GSK549) which showed an anti-inflammatory phenotype in human whole blood, confirming their cellular target engagement. Excellent broad selectivity, developability and *in vivo* oral pharmacokinetics characterize these tools, which we hope will be of broad utility to the field of epigenetics research.

Introduction:

The bromodomain and extra terminal (BET) family of proteins, comprising the ubiquitous BRD2, 3 and 4 and the testis restricted BRDT, are epigenetic readers whose tandem bromodomains (BDs: N terminus, BD1 and C-terminus, BD2) recognise and bind acetylated lysine histone tail peptides of nucleosomes. Once bound to chromatin these proteins recruit transcriptional complexes and therefore play a key role in gene transcription.[1] The therapeutic potential of a pan-Bromo and Extra Terminal Domain inhibitor (iBET), binding equipotently to the eight bromodomains of the family, has now been extensively reported both in oncology[2-11] and immunoinflammation.[12-23] Moreover, iBET are actively progressing in the clinic for oncology indications, illustrating the tremendous potential of this epigenetic reader family as a therapeutic target.[24-26] Nevertheless it is also well known that a number of non-clinical toxicities and dose-limiting clinical findings have been associated with pan-inhibition of the BET family.[25, 27-29] There have been far fewer reports of selective BET bromodomain inhibitors, although these are now starting to emerge in the patent[30-37] and publication literature. Both BD1 (**1**-**7**)[38-44] and BD2 (**8**-**12**)[45-50] selective (>5 fold) inhibitors , binding to either the four BD1 or the four BD2 domains of the BET proteins have been published and the structures are shown in Figure 1 with the acetylated lysine mimetics highlighted in blue. Despite the emergence of such inhibitors, there is some debate as to whether 50-100 fold selective inhibitors are really capable of teasing out the relative roles of BD1 and BD2, due to the profound effects offered by iBET. Notwithstanding this, the recent disclosure that BD2-biased inhibitors such as RVX-297 (**9b**),[51] maintain a range of immune relevant efficacies *in vitro* and *in vivo* is noteworthy.[52] In parallel to our own research,[53] AbbVie recently

published ABBV-744 (**12**),[48-49] a highly selective BD2-inhibitor which retains some of the anti-proliferative activity of pan-BET inhibitors, albeit restricted largely to acute myeloid leukaemia and certain prostate cancer cell lines. Furthermore, there have been a number of studies detailing the different roles in chromatin binding that the BD1 and BD2 domains have.[54-57] The multivalent interaction between the BET family and chromatin or other binding partners is complex and context-dependent, and remains poorly understood. It is difficult to predict what different efficacy or safety profiles might be found when domain-selective inhibitors are compared to pan-BET inhibitors. We hope that the publication of potent, highly selective BD1 and BD2 domain-selective BET inhibitors will enable advances in our biological understanding of the mechanism of these highly important and disease-relevant targets.

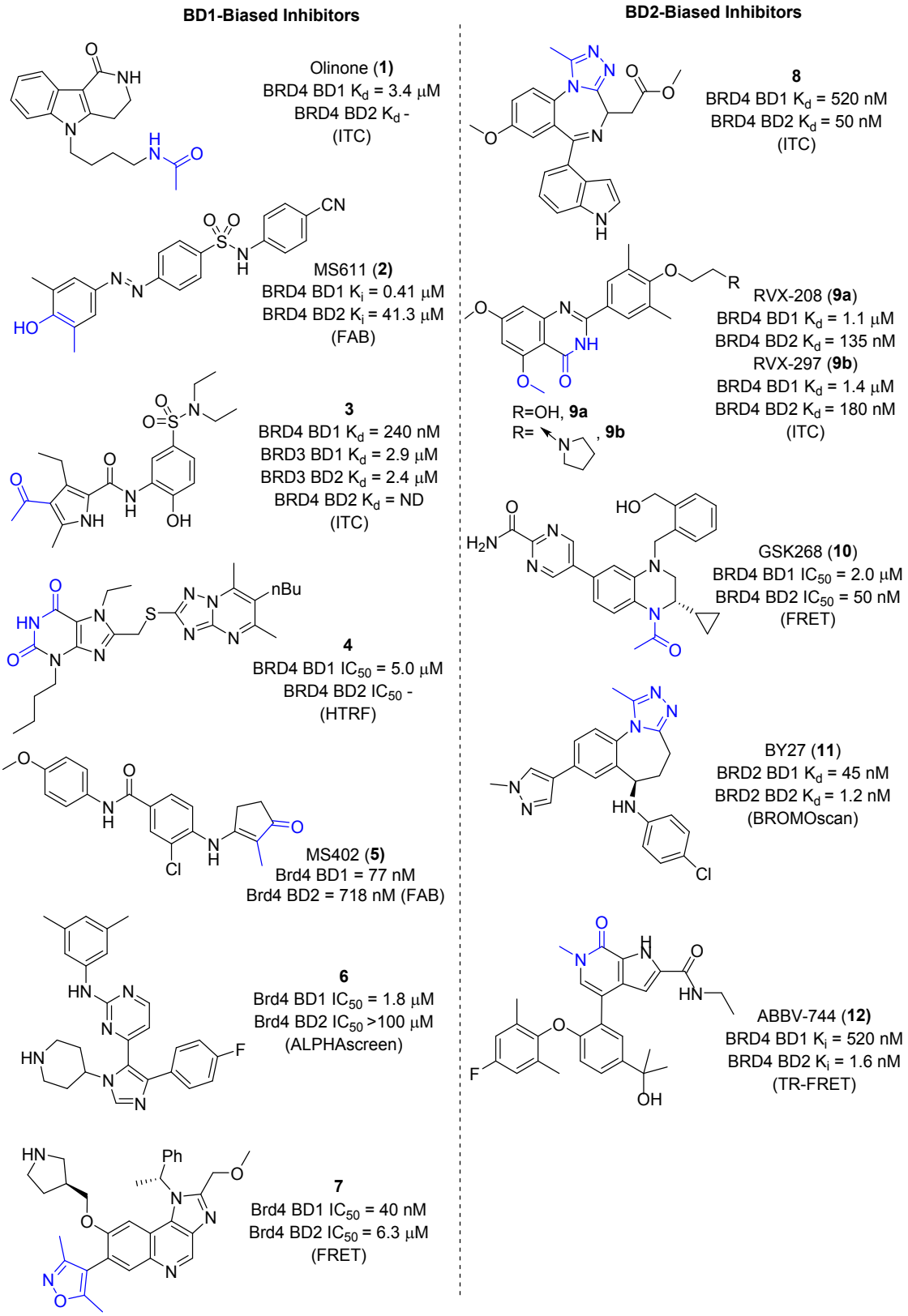

Figure 1. Published Domain Selective BET Bromodomain Inhibitors and their Literature Potencies / Affinities to the BD1 and BD2 Bromodomain of BRD4 with the acetylated lysine mimetic coloured blue.

Results

As part of our strategy to understand and profile more pan-BD2 inhibitors, a programme of hit finding was undertaken targeting inhibitors of the second bromodomain ultimately aiming for a pIC_{50} >7 and selectivity over the first bromodomain of at least 100 fold. This approach was driven by the high degree of sequence homology in the acetylated lysine (KAc) binding region for the BD2 (second) domain across the BRD 2,3,4 and T proteins. This is in contrast to reduced homology between the first (BD1) and second domains for the same proteins (Figure S3 a-c, Supporting Information); it was reasoned that pan-BD2 selectivity had a higher probability of success (*versus* single isoform selectivity). Accordingly, an HTS screen was initiated where the entire GSK compound collection (over 2M compounds) was screened at single concentration *versus* the BRD4 dual domain truncated protein construct, considered as representative of the BET family. Here the BD1 domain was mutated (Y390A) to prevent binding of acetyl lysine mimetics at this site and allow evaluation of potency exclusively at the second domain. Following the single concentration screen (TR-FRET assay format), a triaging strategy, including an orthogonal BD2 biochemical assay (FP assay format), full curve follow up against BRD4 BD2 and BD1 and SPR biophysical characterisation, led to real and robust hits. A focus on high ligand efficiency (LE^{58-59}/LLE_{AT}[60]), a minimum of 3 fold selectivity over BD1 and CHROMlogD[61] <4 led to the identification of **13a** (Table 1) as one of our preferred hits. Given the molecule contained only 2 aromatic rings and had a BRD4 BD2 derived LE of 0.35 and LLE_{AT} of 0.34, this was an appealing start point, especially given the level of BRD4 BD2 selectivity was already >10 fold. Whilst **13a** contained a potentially metabolically vulnerable methyl amide warhead, initial microsomal clearance in both rat and human was <1 mL/min/g tissue. The BD2 selectivity for BRD3 and BRDT was similar for **13a**, but the selectivity profile for BRD2 was somewhat lower and would therefore be monitored as we optimised this start point. The physicochemical profile was further improved by removal of the Br and F atoms to give **13b**, with no deleterious effect on potency and a large improvement in LLE_{AT} (0.43). As part of generating an understanding of the key core functionality required for potency and selectivity, screening of the corresponding 2-pyridone **14a** led to 10 fold increase in potency for BRD4

BD2, albeit accompanied with a similar rise in the BRD4 BD1 potency. Notably, an equivalent potency and selectivity was observed against BRD2, 3, T BD2, suggestive that this series was capable of generating pan-BD2 inhibitors. With a BRD4 BD2 derived LE of 0.45 and LLE_{AT} of 0.51, this represented a highly efficient start point to begin optimisation. When the methyl group of the amide was replaced with an ethyl (**14b**), a reduction of almost 1 log in potency was observed, together with reduced BD2 selectivity, suggestive that the methyl group plays an important and specific role in the binding of this template.

Table 1. Structure and Properties of BD2 HTS hit **13a** and Optimised Fragments **13b, 14a** and **14b**.

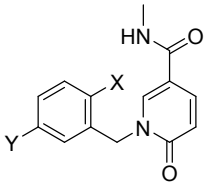

X = F, Y = Br, **13a**
X = Y = H, **13b**

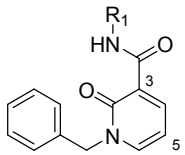

R_1 = Me, **14a**
R_1 = Et, **14b**

Compound	**13a**	**13b**	**14a**	**14b**
BRD4 BD2 / BD1 pIC_{50} (n)[a]	5.1 (6) / 4.0 (1[b])	4.9 (5) / <4.3 (5)	5.9 (9) / 5.1 (9)	5.2 (4) / 4.8 (4)
BRD2 BD2 / BD1 pIC_{50} (n) [a]	4.6 (6[c]) / 4.5 (2[d])	4.6 (8[f]) / 4.8 (2[e])	5.6 (8) / 4.8 (8)	-
BRD3 BD2 / BD1 pIC_{50} (n) [a]	5.0 (6) / <4.3 (6)	5.0 (4) / 4.8 (2[c])	6.3 (4) / 4.9 (4)	-
BRDT BD2 / BD1 pIC_{50} (n) [a]	4.9 (5[c]) / 4.4 (2[e])	4.7 (6[c]) / 4.5 (2[e])	5.7 (6) / 5.0 (6)	-
BRD4 BD2 selectivity (fold)	13	>4	7	3
BRD4 BD2 LE / LLE_{AT}	0.35 / 0.34	0.37 / 0.43	0.45 / 0.51	0.37 / 0.40
CHROMlogD (pH 7.4) / clogP	2.6 / 1.6	1.6 / 0.6	3.0 / 0.6	3.7 / 1.1
CLND[g] (µg/mL) / AMP[h] (nm/sec)	≥143 / 260	≥108 / 58	78 / 595	- / 790
Microsomal Cli (rat, hu, mL/min/g tissue)	0.76 / 0.53	-	-	-

[a] In all tables, the activity of the inhibitors has been determined using a TR-FRET assay, see experimental section for details. The average standard deviation for pIC_{50} is 0.1; [b]also tested <4.3

(n=5); [c]also tested <4.3 (n=2); [d]also tested <4.3 (n=8); [e]also tested <4.3 (n=6); [f]also tested <4.3 (n=1); [g]CLND = chemiluminescent nitrogen detection; [h]AMP = artificial membrane permeability.

There is a wealth of structural information concerning the binding mode of a variety of pan-BET inhibitors to their target proteins.[3, 62-64] Indeed, an X-ray crystal structure of **14a** in BRD2 BD2 was soon solved (Figure 2, a) revealing the key interactions. The pendant methyl amide serves as the KAc-mimetic, its carbonyl oxygen forming hydrogen-bonds to Asn429 and the conserved water network in an analogous manner to the carbonyl of the acetylated histone. The amide hydrogen-bonds internally to the pyridone 2-carbonyl oxygen, while its methyl group fills the KAc-methyl pocket. Ligand-efficient fragments containing related aryl amides have been shown to bind relatively weakly to other bromodomains in a similar way, but so far these have been limited to examples outside the BET family such as BAZ2B.[65] The benzyl group occupies the hydrophobic "WPF" shelf, packing against Val435 and Trp370. It also contacts a histidine residue (His433) in an edge-to-face interaction. A similar interaction has been noted between His433 and the shelf group of other inhibitors.[45] In BD1 this histidine is replaced with an aspartic acid residue, and this "Asp/His switch" and the differing interactions of the shelf aromatic ring as a result could account for the BD2-domain selectivity observed for **14a**.

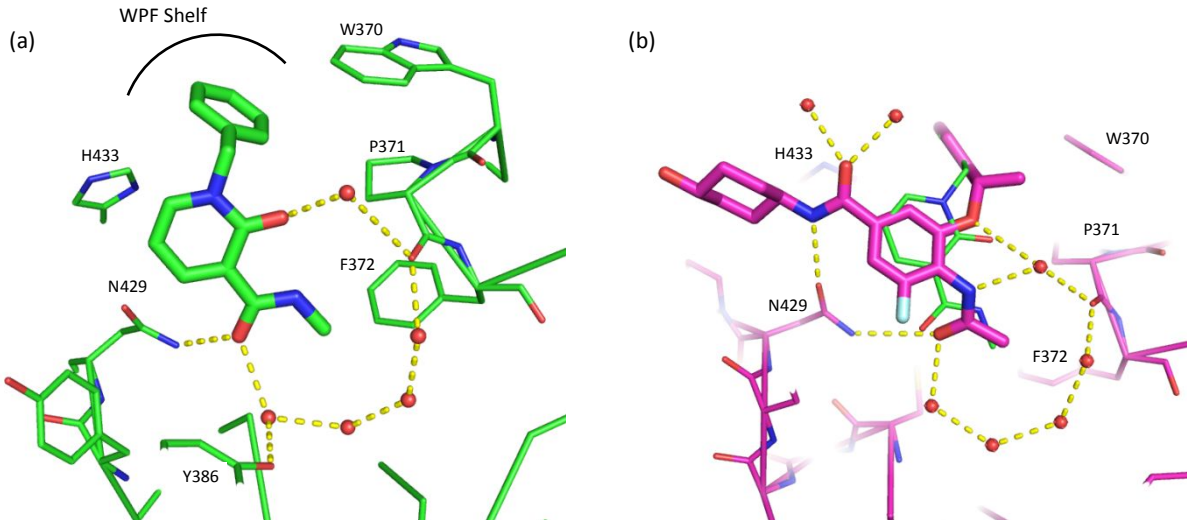

Figure 2. (a) X-ray Structure of **14a** in BRD2 BD2 (PDB 6ZB0) showing key interactions with Asn429 and a network of 5 water molecules, the benzyl group occupies the "WPF" shelf; (b) **14a** (green) overlaid with alternate tool **15** (magenta) in BRD2 BD2 (PDB 6SWP[53]) highlighting the additional vector and interaction with Asn429 utilised by **15**.

Despite the excellent efficiency of **14a**, the compound remained a relatively weak inhibitor, with a large increase in BD2 potency required. Amongst the published pan-BET inhibitors, almost all series gain potency by occupying three key regions of the BET binding site: a potent, often heteroaromatic warhead which serves as the KAc-mimetic, the WPF shelf and/or the ZA channel. In this case, we believed we had achieved BD2 bias by starting from a relatively weak non-aromatic warhead and engaging the shelf of the protein. Whilst the benzylic methylene offered a vector to enter the ZA channel, this did not lead to the required level of potency and selectivity (data not shown) and an alternative growth vector was sought.

Table 2. Structure and BRD4 Potency and Selectivity of GSK046 (**15**).[53, 66]

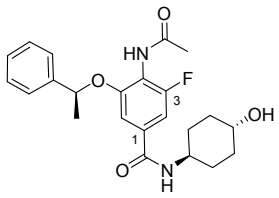

Profile	**15**
BRD4 BD2 pIC_{50} (n)	7.3 (14)
BRD4 BD1 pIC_{50} (n)	4.2 (3[a])
Selectivity (fold)	1400

[a]also tested <4.3 (10)

In parallel to our efforts on this series, a second HTS hit was being elaborated and SAR-driven optimisation had led to the tool **15** (GSK046, Table 2).[53, 66] The acetamide warhead of **15** and its "WPF shelf" benzyl group bound in an analogous manner to **14a**, but **15** offered >1000 fold selectivity for

BRD4 BD2 over BD1. The increase in potency and selectivity was believed to be due to the addition of a second amide substituent entering a cleft in the binding site formed by Leu383, Tyr428 and Asn429 (see Figure 2, b). Additionally, the NH of the C1 amide substituent made a hydrogen bond with the carbonyl of Asn429 (which also interacts with the warhead carbonyl, *vide supra*). Comparing the X-ray structures of bound compounds **14a** with **15**, we considered that adding an amide group to the 5-position of the pyridone core may lead to a similar increase in potency and selectivity.

The installation of an amide group at C5 of **14a** (*cf.* Table 1 & 3) delivered potent and highly selective inhibitors, whilst also improving the physicochemical properties of the series (i.e. lower CHROMlogD and higher CLND solubility *vs* **14a**). Table 3 shows that increasing the size of the amide from primary (**16**, R^2 = H) to a secondary methyl (**17**, R^2 = Me) and ethyl amide (**18**, R^2 = Et) offers a stepwise increase in both potency and selectivity compared to **13**. **16**-**18** maintain excellent binding efficiency, with similar LE values and an increase in LLE_{AT} *vs* fragment **13**. Ethyl amide **18** in particular is close to 100 nM, with >100 fold selectivity and an LE of 0.41 and LLE_{AT} of 0.52. These data validated both our hit finding approach of starting with a small and efficient fragment, and of working on multiple templates in parallel during the hit-to-lead phase.

To assess the SAR at R^2 a range of logical modifications were investigated. For example, branching of the ethyl amide to iPr (**19**) was less well tolerated, however, small cyclic alkyl groups proved optimal, with cPr and cBu (**20** and **21**) boasting selectivity levels of 200 fold. Larger rings were less well tolerated (e.g. THP **22**). This is in contrast to acetamide **15** (Table 2) and represents divergent SAR between the series.[66] Searching for additional affinity, the effect of growing from the promising ethyl amide was also investigated; the installation of polarity from the beta-carbon, such as for **23** and **24**, was poorly tolerated with a loss of >3 fold of potency relative to **18**. Indeed, branching from this carbon of the amide was also deleterious (**25**). Potency could be restored through gamma-branched examples **26** and **27** although this appeared to offer no advantage to the smaller derivatives of similar potency already identified where both the LE and LLE_{AT} values were significantly higher (*cf*. **18** and **20**). Whilst a basic amine was not tolerated in example **28**, extending the carbon chain further did provide a BRD4

BD2 potency boost and led to the most selective compounds prepared yet (>300 fold over BD1). Piperidine **29**, expectedly showed poor predicted permeability in an artificial membrane high throughput assay,[67] by virtue of its high basicity, although this was somewhat attenuated in the less-basic morpholine **30**. Nevertheless it was clear that the small and neutral ethyl and cyclopropyl amides **18** and **20** offered the best balance of potency, selectivity and physicochemical properties. Indeed, cPr analogue **20** had a low clogP and CHROMlogD, was predicted to be permeable and was soluble in our high throughput CLND kinetic solubility assay (conducted from DMSO solution).[68]

Table 3. SAR for the amide vector (R^2)

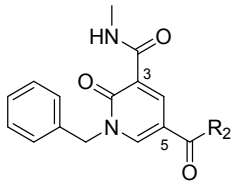

Compound	R^2	BRD4 BD2 / BD1 pIC_{50} (n)	Selectivity (fold)	BRD4 BD2 LE / LLE_{AT}	CHROMlogD (pH 7.4) / clogP	CLND (µg/mL) / AMP (nm/s)
16	NH_2	6.4 (4) / 5.1 (6)	20	0.42 / 0.58	2.0 / -0.7	71 / 110
17	NHMe	6.8 (3) / 5.1 (3)	50	0.42 / 0.56	2.4 / -0.5	≥118 / 130
18	NHEt	6.8 (5) / 4.8 (4[a])	120	0.41 / 0.51	3.0 / 0.0	≥144 / 245
19	NH*i*Pr	6.2 (3) / 5.0 (1[b])	15	0.35 / 0.44	3.6 / 0.3	≥136 / 330
20	NHcPr	7.1 (16) / 4.8 (14)	220	0.40 / 0.51	3.1 / 0.1	≥154 / 200
21	NHcBu	7.0 (8) / 4.7 (5[c])	220	0.39 / 0.47	3.8 / 0.4	28 / 427
22	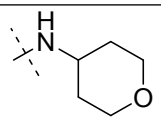	6.6 (4) / 4.9 (3)	60	0.34 / 0.49	2.8 / -0.9	≥174 / 110

23	$NH(CH_2)_2OMe$	6.2 (4) / 5.1 (3)	10	0.34 / 0.46	2.7 / -0.3	≥164 / 110
24	$NH(CH_2)_2OH$	6.2 (4) / 4.7 (3)	30	0.35 / 0.52	1.9 / -1.1	≥140 / 22
25	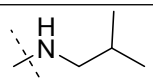	6.3 (3) / <4.3 (3)	>100	0.34 / 0.40	4.3 / 1.0	43 / 510
26	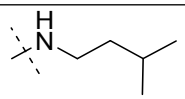	6.9 (3) / 4.5 (3)	210	0.36 / 0.39	4.8 / 1.5	10 / 530
27	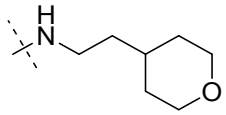	6.7 (3) / 4.6 (3)	120	0.31 / 0.41	3.6 / 0.3	≥127 / 170
28	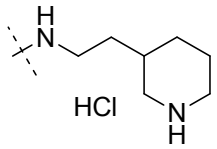	4.6 (3) / <4.3 (3)	>2	0.22 / 0.32	1.6 / 0.3	≥146 / <3
29	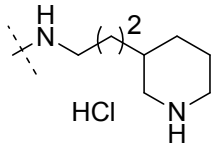	7.8 (3) / 5.2 (3)	370	0.36 / 0.43	2.0 / 0.8	156 / <3
30	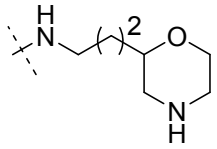	7.7 (2) / 5.1 (2)	340	0.35 / 0.48	1.4 / -0.6	≥194 / 15

[a]also tested <4.3 (n=1); [b]also tested <4.3 (n=2); [c]also tested <4.3 (n=3)

20 was soaked into the BRD2 BD2 construct and bound as shown in Figure 3, a. In addition to the interactions of the KAc mimetic and shelf groups, already described for **14a**, the additional hydrogen bond between the amide NH and Asn429 that we had hoped to engage, was indeed observed. The cPr group shows excellent shape complementarity with a narrow groove created by His433 and Pro430 on one side and Tyr428 and Leu383 on the other (Figure 3,b). This may explain why larger groups in this position are less well tolerated. The origin of BD2 selectivity arises from residue differences between BD1 and BD2 as highlighted in Figure 3, d. The key residue changes are His433 and Pro430 (BRD2 BD2 numbering) to Asp144 and Lys141 (BRD4 BD1 numbering). Both changes affect the shape of the groove that the cyclopropyl group occupies. As described earlier, in BD2 His433 makes a key

edge-to-face interaction with the shelf benzyl group. In addition, the tight-packed arrangement of the cyclopropyl amide and His433 adds significantly to the surface area of this residue buried by **20**. The combination of all these positive interactions which are absent in BD1 are likely to drive the observed selectivity.

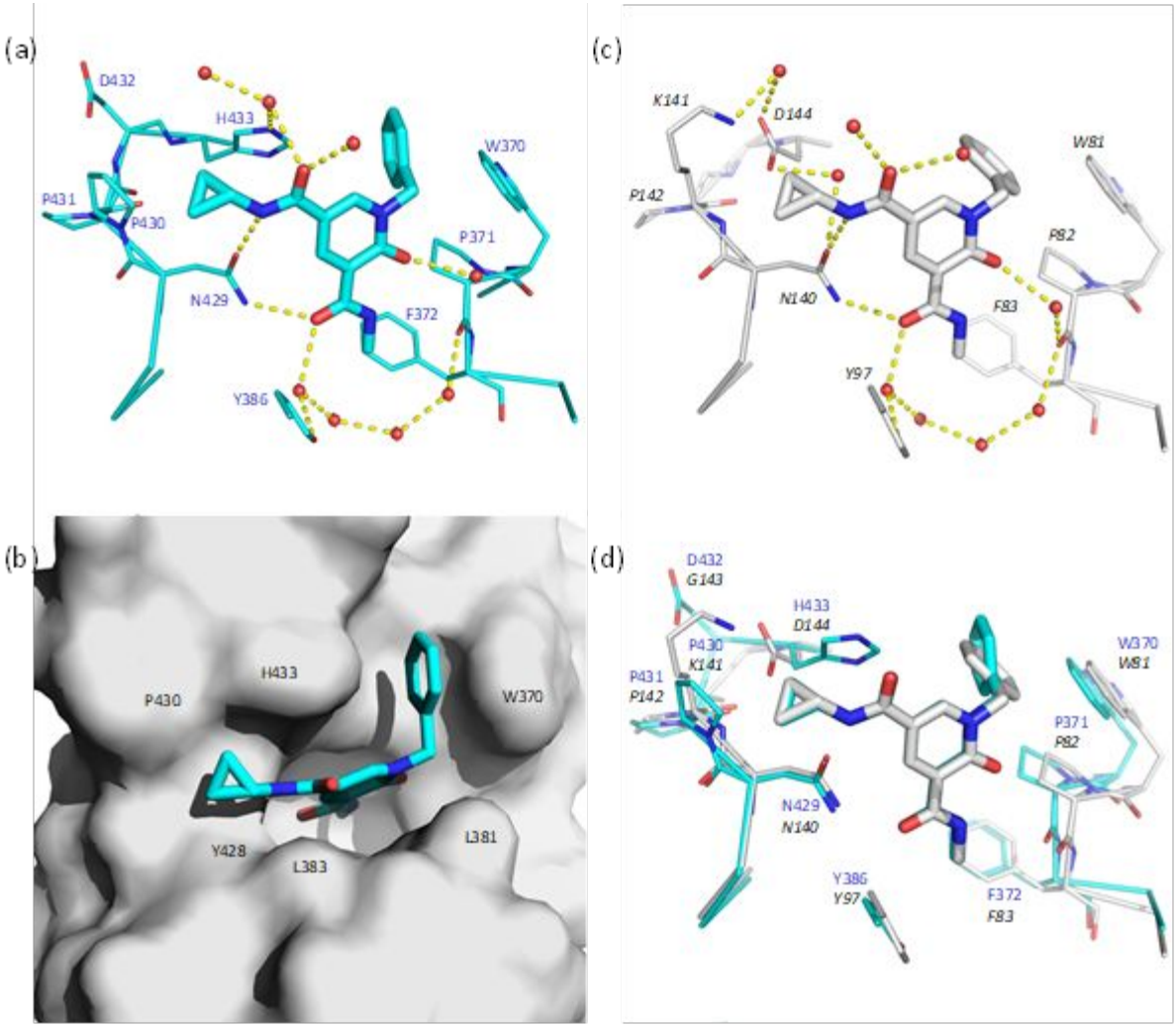

Figure 3. (a) Key interactions of GSK620 (**20**) with BRD2 BD2 (PDB 6ZB1, cyan); (b) GSK620 shown with the protein surface representation of BRD2 BD2; (c) Key interactions of GSK620 (**20**) with BRD4 BD1 (PDB 6ZB3, white); (d) Overlay of GSK620 (**20**) in BRD2 BD2 (cyan) and BRD4 BD1 (white) providing a rationale for the domain selectivity.

It is important to realise that this "Asp/His switch" involves conformational differences as well as an amino acid exchange. In BRD2 BD2, His433 points towards the KAc site and the bound inhibitor **20**,

whereas in BRD4 BD1 the equivalent Asp144 sidechain points away (Figures 3 a,c). This is consistent with systematic differences found in deposited Protein Data Bank crystal structures, where the BET BD1 domain aspartic acids typically lie in *gauche*(+) chi1 rotameric states while the BD2 histidines are predominantly seen in the *trans* rotamer with minor *gauche*(+) components (Figure S3 e-g, Supporting Information). In this conformation, the imidazole of BRD4 His433 is able to accept a helix-capping hydrogen-bond from the Val435 backbone NH. In BRD4 BD1, the Asp144 sidechain forms a conserved hydrogen-bond with the free backbone NH of Lys141, perhaps explaining the prevalence of its *gauche*(+) conformation. The substitution of Lys141 for Pro430 in BRD2 BD2 makes this interaction impossible and may sterically restrict the loop, encouraging the histidine to lie in its *trans* conformation. The Asp144/Lys141 and His433/Pro430 combinations are conserved in all BET BD1 and BD2 domains (Figure S3 d, Supporting Information) so this rationalisation of BD2 over BD1 selectivity extends across the family.

The potency and physicochemical properties of amides **18** and **20** looked highly promising and indeed the CLND solubility was towards the maximum limit of the high throughput assay for the vast majority of analogues. However, upon crystallisation of cPr amide **20** [confirmed by X-Ray Powder Diffraction (XRPD) analysis] and evaluation of its fasted-state simulated intestinal fluid (FaSSIF) solubility, a far more relevant end point for an orally-targeted inhibitor, its solubility was only moderate (13-35 µg/mL, Table 4). Given the attractive physicochemical space occupied by this inhibitor, it was likely this low solubility was being driven by its highly crystalline nature. To investigate this further, a small molecule crystal structure was determined for **20** (Figure 4, a). The Me-amide group forms an intramolecular N-H···O hydrogen bond with the pyridone oxygen atom, O14. The cPr-amide forms an intermolecular N-H···O hydrogen bond with the oxygen atom of the Me-amide, O16. These intermolecular hydrogen bonds between the two pivotal amides connect molecules of **20** into columns (Figure 4, b) that extend in the direction of the crystallographic *b*-axis. There are no pi-stacking interactions in this structure. Given the amide groups of **20** make important hydrogen bonds to the BD2 domain and were therefore considered non-replaceable, we interrogated the other

proximal interactions within the small molecule crystal structure. It was noteworthy that the benzylic methylene resided in close proximity to the carbonyl oxygen of the cPr-amide in an adjacent molecule, whilst the 6-position of the pyridone core also sits close to the same CH of its neighbour (Figure 4, c). We hypothesised that adding substituents to these positions may be sufficient to disrupt the packing and lead to increased solubility. As shown in Table 4, this hypothesis proved correct and crystalline (by XRPD) single enantiomer **31**, not only showed a markedly increased FaSSIF solubility of 815 µg/mL, but was well tolerated in terms of potency and selectivity. Interestingly, further additions to the cleft region offered no advantage to **20** and **31** in terms of potency or selectivity. Unfortunately, whilst crystalline (by XRPD) 6-methylpyridone **32** also had an excellent FaSSIF solubility, this substituent impacted binding at BD2, with a low BRD4 BD2 pIC_{50} of 5.7 resulting and was not progressed further.

Table 4. The Potency, Selectivity and Solubilities of Methylated Derivatives of **20**

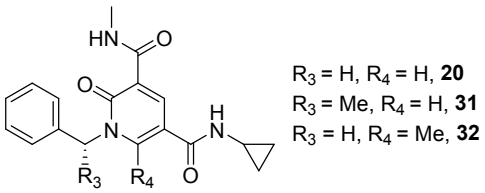

Compound	**20**	**31**	**32**
BRD4 BD2 / BD1 pIC_{50} (n)	7.1 (16) / 4.8 (14)	7.1 (4) / 4.9 (4)	5.7 (5) / <4.3 (4)
BRD4 BD2 Selectivity (fold)	220	170	>30
CHROMlogD (pH 7.4) / clogP	3.1 / 0.1	3.5 / 0.4	2.9 / 0.2
CLND[a] (µg/mL) / AMP[b] (nm/s)	≥154 / 200	≥168 / 300	≥126 / 110
FaSSIF[c] (µg/mL)	13 – 35	815	577

[a]CLND = chemiluminescent nitrogen detection solubility; [b]AMP = artificial membrane permeability; [c]FaSSIF = fasted state simulated intestinal fluid solubility

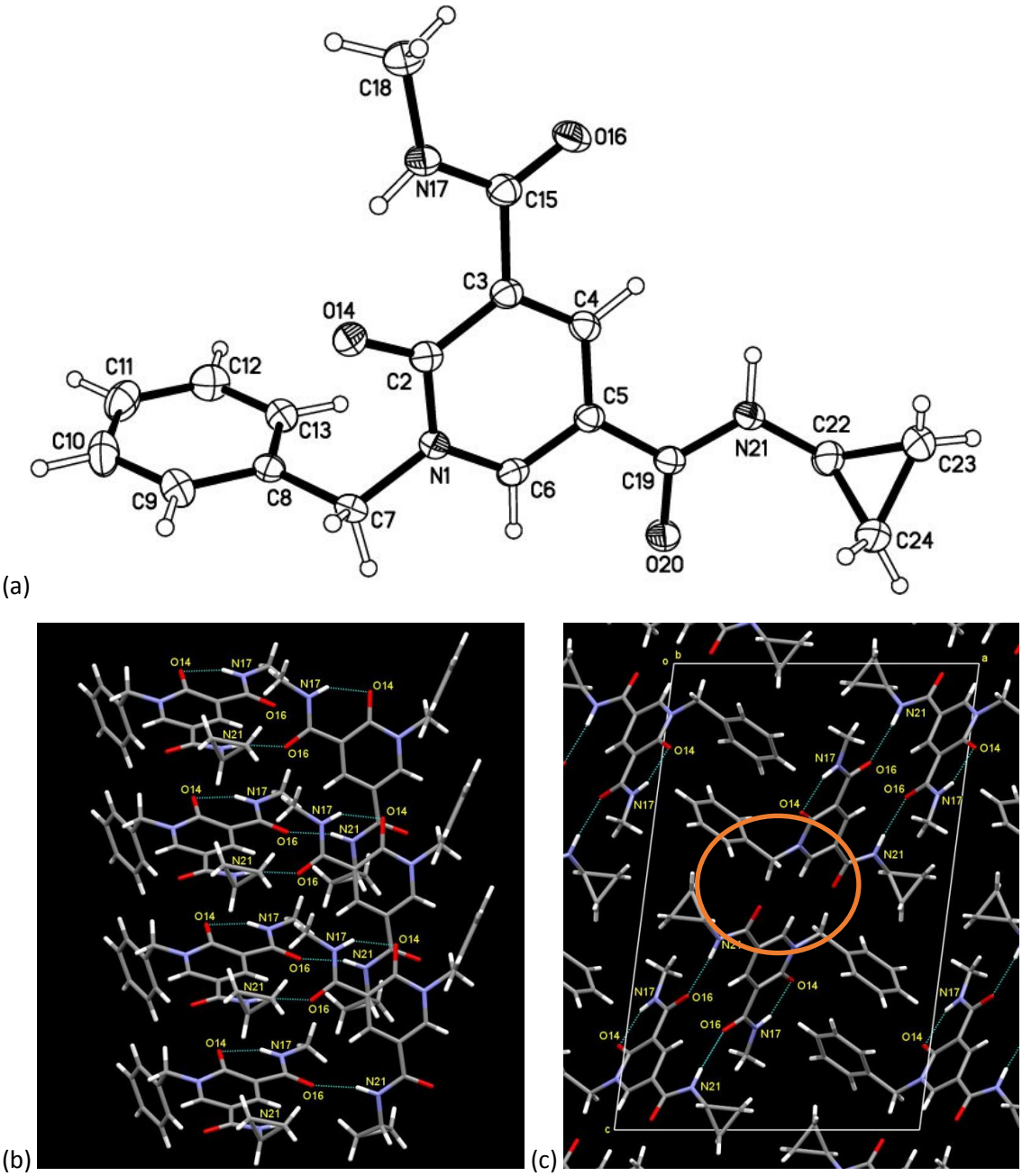

Figure 4. (a) A view of a molecule of **20** from the crystal structure, showing the numbering scheme employed. Anisotropic atomic displacement ellipsoids for the non-hydrogen atoms are shown at the 50% probability level. Hydrogen atoms are displayed with an arbitrarily small radius. (b) Molecules of **20** forming part of a hydrogen bonded column within the crystal structure. Hydrogen bonds are displayed as dashed lines with the donors and acceptors labelled. (c) Packing plot of the crystal structure of **20** viewed down the crystallographic *b*-axis showing the close proximity of the benzylic

methylene and 6-pyridone hydrogens to an adjacent molecule (circled). Hydrogen bonds are displayed as dashed lines with the donors and acceptors labelled.

Further profiling of **20** and **31** will be discussed subsequently, but it was also important to evaluate the SAR of the shelf region of the template. Due to its key role in BD2 binding, further affinity may be possible in this region, whilst diversity could also be valuable for physicochemical properties and metabolic stability. As shown in Table 5, the replacement of the phenyl ring of **20** with cyclohexyl **33** was tolerated. Given the edge-to-face interactions observed for **20**, this was somewhat surprising – but later rationalised by crystallography: the cyclohexyl ring adopts a different conformation to the phenyl group and packs nicely against the tryptophan. Unfortunately, capitalising on this observation was problematic. Cyclohexyl **33** itself offered no benefit in terms of lipophilicity (CHROMlogD = 4 *vs* 3.1 for **20**) and attempts to insert polarity either onto or into this ring led to a significant reduction in potency (e.g. THPs **34-36**). It would have been similarly desirable to increase the polarity of the aromatic ring, but unfortunately pyridyls **37-39** showed a 10 fold reduction in potency, with no obvious means of obtaining this back elsewhere in the inhibitor. A range of electron withdrawing groups (EWG) and electron donating groups (EDG) were then prepared but as **40**-**46** show, the potency and selectivity SARs were flat with no compound offering an advantage in these terms over the unsubstituted lead **20**. The incorporation of a 3-CN group (**47**) proved detrimental, whilst in contrast, the addition of solubilising groups such as secondary alcohol **48,** or morpholine **49** were well tolerated and led to a large increase in FaSSIF solubility. Morpholine **49** had sub-optimal *in vitro* clearance data in rat (14.7 mL/min/g tissue), however alcohol **48** was worthy of further evaluation and will be discussed further alongside our other preferred inhibitors.

The addition of a *meta*-aniline (**50**) appeared to offer a small selectivity advantage over **20**. Hoping to capitalise on this observation and given that a free aniline was not desired from a genetic toxicity viewpoint,[69] it was hypothesised that bicyclic motifs bearing an appropriate H-bond donor at this position were worthy of investigation. Cyclisation of the *meta*- and *para*-positions to provide benzimidazole **51** showed a reduction in potency relative to aniline **50**, however cyclisation of the

ortho- and *meta*-positions looked more encouraging, with benzimidazole **52** equipotent to the aniline. Preparation of regioisomeric indazoles **53** and **54** was also tolerated, though in both cases selectivity was reduced relative to the benzimidazole. Benzofuran **55**, lacking any H-bond donor was only moderately potent and selective. This was in contrast to indole **56** which was not only 3 fold more potent at BRD4 BD2 than any other example tested, but also exquisitely selective versus BD1 (>1000 fold). Interestingly, the same potency increase was not observed with regioisomeric indole **57**. A crystal structure in BRD2 BD2 for **56** was solved and provided a rationale for its high potency. As shown in Figure 5, the indole group, as expected, still occupies the WPF shelf. However, the additional pi-system of the pyrrole ring now appears to engage in a more optimal edge-to-face interaction with His433 (which remains in the same place as observed for **20** (Figure 3). The NH of the indole also makes a through water H-bond with Asp434. It is hypothesised that it is this combination of interactions which drives the additional BD2 potency of **56**.

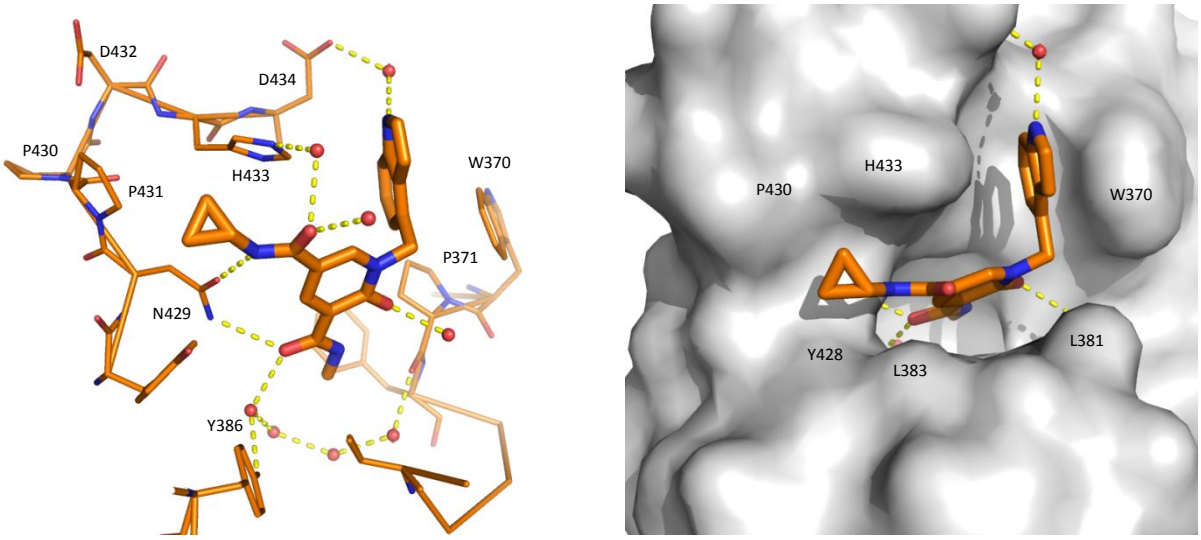

Figure 5. X-ray Structure of **56** in BRD2 BD2 (PDB 6ZB2) showing: (a) the key interactions with His433, Asp434 and Trp370 on the WPF shelf; (b) the binding mode with a surface to highlight its optimal position on the WPF shelf.

Given the excellent potency of **56**, it was postulated that further polarity might be able to be incorporated in the Ph ring. 5-aza-indole **58** was prepared and whilst a 1 log drop-off in biochemical potency was observed (in accord with ***o*-37** *vs* **20**), **58** still had a reasonable potency / selectivity profile,

given the highly polar nature of the compound. Finally, to understand the effect of the second pi-system on the enhanced potency of indole **56**, the corresponding indoline **59** was prepared. In this instance, 3 fold potency was lost versus BD2, supporting the binding hypothesis in Figure 5, that the extended pi-system, as well as the *meta*-hydrogen bond donor, has a role in the high potency of **56**. Nevertheless, given indoline **59** has one less aromatic ring, has a reduced CHROMlogD of 2.1 (*vs* 3.1 for **20** and 2.9 for **56**), and a BD2 selectivity of 415 fold and an enhanced solubility, this analogue was also worthy of further investigation.

Table 5. SAR for the "WPF shelf" vector (R_5).

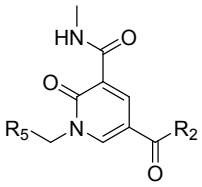

Compound	R_2	R_5	BRD4 BD2 / BD1 pIC_{50} (n)	Selectivity (fold)	CHROMlog D (pH 7.4) / clogP	CLND (µg/mL) / FaSSIF (µg/mL) / AMP (nm/s)
20	NHcPr	Ph	7.1 (16) / 4.8 (14)	220	3.1 / 0.1	≥154 / 13-35 / 200
21	NHcBu	Ph	7.0 (8) / 4.7 (5[a])	220	3.8 / 0.4	28 / 24 / 427
33	NHcPr	cHex	6.9 (3) / 5.0 (3)	85	4.0 / 1.3	≥148 / - / 190
***o*-34**	NHcPr	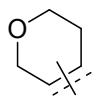	6.4 (3) / 4.5 (1[b])	70	2.6 / -0.5	≥149 / - / 46
***m*-35**			5.6 (3) / 4.4 (1[b])	14	2.0 / -1.1	≥131 / - / 22
***p*-36**			5.5 (3) / 4.6 (3)	10	1.5 / -1.1	≥165 / - / 12
***o*-37**	NHcBu		5.9 (3) / <4.3 (3)	>40	2.2 / -1.1	≥103 / 920 / 51

Compound	R_2	R_5	BRD4 BD2 / BD1 pIC_{50} (n)	Selectivity (fold)	CHROMlog D (pH 7.4) / clogP	CLND (µg/mL) / FaSSIF (µg/mL) / AMP (nm/s)
***m*-38**			6.0 (3) / <4.3 (3)	>50	1.8 / -1.1	≥99 / 189 / 130
***p*-39**			5.6 (3) / <4.3 (3)	>20	1.7 / -1.1	≥118 / 121 / 130
***o*-40**	NHcPr	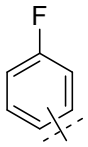	6.9 (3) / 4.8 (3)	120	3.0 / 0.2	≥145 / 88 / 220
***m*-41**			6.9 (4) / 4.7 (3)	170	3.2 / 0.2	≥133 / 31 / 300
***p*-42**			7.1 (5) / 5.0 (4)	120	3.2 / 0.2	≥162 / 84 / 300
***m*-43**	NHcPr	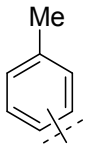	7.2 (5) / 4.8 (4[c])	250	3.6 / 0.6	≥205 / 88 / 440
***p*-44**			7.0 (3) / 5.0 (3)	100	3.5 / 0.6	24 / 11 / 350
***m*-45**	NHcPr	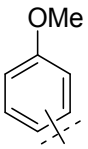	6.8 (4) / 4.4 (1[c])	240	3.0 / 0.0	79 / 582 / 220
***p*-46**			7.0 (4) / 4.7 (4)	190	3.0 / 0.0	≥143 / 263 / 220
47	NHcPr	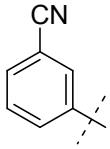	6.1 (5) / 4.4 (2[b])	50	2.6 / -0.5	≥148 / - / 100
48	NHcPr	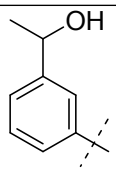	7.0 (4) / 4.1 (2[a])	690	2.2 / -0.6	≥131 / 495 / 34
49	NHcPr	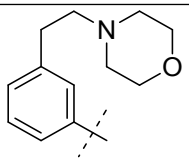	7.0 (3) / 4.1 (2[a])	800	2.3 / 0.2	≥185 / 887 / 68

Compound	R_2	R_5	BRD4 BD2 / BD1 pIC_{50} (n)	Selectivity (fold)	CHROMlog D (pH 7.4) / clogP	CLND (µg/mL) / FaSSIF (µg/mL) / AMP (nm/s)
50	NHcBu	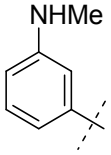	7.2 (3) / 4.6 (2[c])	450	3.6 / -0.1	≥155 / - / 430
51	NHcPr	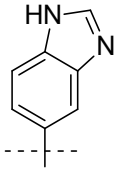	6.6 (4) / 4.4 (2[b])	180	1.2 / -0.5	≥163 / 225 / <3
52	NHcPr	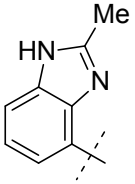	7.3 (4) / 4.4 (4)	800	1.5 / -0.2	≥198 / - / 24
53	NHcPr	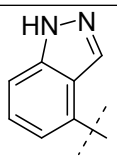	7.1 (3) / 4.5 (1[b])	390	1.5 / -0.4	10 / 4 / 38
54	NHcPr	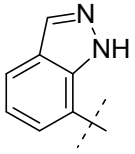	6.8 (3) / <4.3 (3)	>320	2.2 / -0.4	≥181 / 131 / 190
55	NHcPr	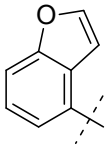	6.9 (4) / 4.4 (4[c])	300	3.4 / 0.6	≥110 / 74 / 410
56	NHcPr	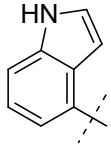	7.8 (8) / 4.7 (8)	1150	2.9 / 0.1	78 / 17-23 / 178
57	NHcPr	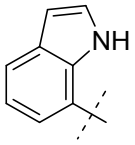	7.0 (3) / 4.6 (3[c])	200	3.7 / 0.1	≥144 / 11 / 480

Compound	R_2	R_5	BRD4 BD2 / BD1 pIC_{50} (n)	Selectivity (fold)	CHROMlog D (pH 7.4) / clogP	CLND (µg/mL) / FaSSIF (µg/mL) / AMP (nm/s)
58	NHcPr	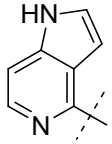	6.7 (4) / <4.3 (4)	>230	1.7 / -0.9	73 / - / 7
59	NHcPr	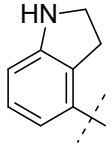	7.2 (7) / 4.6 ([a]4)	415	2.1 / -0.3	≥184 / 100 / 140

[a]also tested <4.3 (n=3); [b]also tested <4.3 (n=2); [c]also tested <4.3 (n=1)

With the desired level of potency and selectivity in hand, and having controlled the physicochemical properties closely (lipophilicity, permeability and solubility) a diverse set of optimised inhibitors remained. In search of an orally bioavailable molecule, a selection of lead compounds were evaluated for their pharmacokinetics *in vivo*. Before committing to such studies, all compounds were evaluated *in vitro* using isolated hepatocytes. As indicated in Table 6, the ethyl and cPr amides **18** and **20** have low measured *in vitro* Cl_i in hepatocytes for rat, human and dog (all <1 mg/mL/g tissue). This translated into low *in-vivo* clearance for both compounds in the rat and when dosed orally, excellent oral bioavailability. Given **20** had slightly superior selectivity, this example was also profiled in the dog, with a blood clearance (Cl_b) of 2 mL/min/kg and an oral bioavailability (F%) of 57. It was also notable that both compounds had high free fractions in rat and dog, illustrating that unbound clearances are also low and high *free* blood concentrations *in vivo* are achievable.[70] A number of the more selective biaryl shelf examples were also profiled. Whilst indazole **53** had raised Cl_b *in vivo* (in contrast to its *in vitro* rat profile) and poor oral bioavailability (likely driven by poor absorption), the highly selective indole **56** and indoline **59** both had low/moderate rat Cl_b of 23 and 16 mL/min/kg respectively. In the case of indoline **59** this translated into an oral bioavailability of 53%. Whilst the oral leg of the rat study for **56** was run in a different species (female Lewis) and so the bioavailability cannot be calculated, **56**

also had good oral exposure as shown by an AUC/D of 23.6 min.kg/L. Finally, two examples where increased FaSSIF solubility had been achieved were tested. Secondary alcohol **48** unfortunately showed high Cl_b in rat *in vivo*, which correlated with raised *in vitro* clearance in hepatocytes in that species. Interestingly, this compound is predicted to have low clearance in dog and human, however, given the improved rat Cl_b profile of other analogues, this was not tested further. Finally, the addition of the methyl group to the benzylic methylene to provide **31** unfortunately resulted in high rat Cl_b. Overall, the excellent pharmacokinetics of **20**, together with the enhanced potency and selectivity of **56** allowed us to select these as our two preferred BD2-selective and *in vivo* capable tools.

Table 6. The pharmacokinetic profile of selected BD2 inhibitors following intravenous infusion and oral administration in the Male Wistar Han Rat and Beagle Dog

Compound	Species	Hepatocyte CL_{int} (mL/min/g tissue)	Dose iv (n) / po (n) (mg/kg)	CL_b (mL/min/kg)	V_{ss} (L/kg)	$t_{½}$ (h)	F_{po} (%)	fu_b
20	Rat Human Dog	0.95 <0.45 <1.26	1 (1) / 3 (3) 0.5 (1) / 1 (1)	12 2	0.8 1.0	1.1 5.7	67 57	0.16 0.38
18	Rat Human Dog	<0.80 <0.87 <1.26	1 (3) / 3 (3)	12	0.8	0.6	104	0.16
53	Rat Human	<0.80 <0.45	1.5 (1) / 3 (3)	42	1.2	0.4	14	0.22
56	Rat Human Dog	1.70 <0.45 <1.26	1 (1) / 10 (3[a])	23	1.3	0.8	ND[a]	0.18
59	Rat Human Dog	<0.80 <0.45 <1.26	1 (1) / 3 (3)	16	0.9	0.6	53	0.53

48	Rat Human Dog	3.0 <0.45 <1.26	1.4 (1) / -	74	1.7	0.4	-	0.48
31	Rat Human	1.50 <0.87	1.4 (1) / -	72	1.6	0.4	-	0.27

[a]F% cannot be calculated as po dosing carried out using alternate female Lewis rat strain, po AUC/D = 23.6 min.kg/L.

Chemistry

In order to synthesise this series of analogues, a plan was envisaged which commenced from commercial pyridone **60** (Scheme 1). To vary the R^2 amide substituent, the R^3 = benzyl "shelf" group can be installed at an early stage. Accordingly, selective *N*-benzylation and a subsequent two-step process converts the ester into the corresponding methyl amide **61** in 66% yield for the three steps. At this stage, two alternate routes were utilised in parallel. Bromide **61** can be carbonylated either in the presence of 2,4,6-trichlorophenyl formate using palladium acetate and xantphos catalyst-ligand system.[71] The resultant activated ester **62** is formed in 87% yield and can be easily displaced by the desired amines in the presence of catalytic DMAP and triethylamine in THF at 45 °C to form analogues **16-17**, **19**, **21**, **25-27** and **63**. Alternatively, carbonylation under similar palladium-catalysed conditions ($Pd(OAc)_2$, dppb) but using carbon monoxide and EtOH affords the ethyl ester.[72] This transformation can be practically carried out on a small scale using a balloon of CO. However, we were able to scale this reaction using a Parr reactor vessel purged with CO to 50 psi and heated to 100 °C overnight. This approach delivered >20 g of this key intermediate. After sodium hydroxide-mediated hydrolysis, this provided carboxylic acid **64** in 75% yield over the two steps. Whilst both processes were similarly effective, employing 2,4,6-trichlorophenyl formate, which itself had to be prepared in a single step, was less atom efficient than preparing the ethyl ester. Finally, carboxylic acid **64** could be converted to the desired amides **18**, **20**, **22-24** and **65-66** using a HATU-mediated amide coupling in either DMF

or DCM. For piperidine and morpholine containing analogues **63**, **65** and **66** a subsequent Boc-deprotection step was required to afford the final free amines **28**-**30**.

For analogues where the R^3 shelf group needed to be varied, direct aminocarbonylation was utilised which meant only a single step was required after the different R^3 diversity had been installed. As such, methyl ester **60** could be converted to the corresponding methyl amide **67** in a single step with an excess of methylamine in refluxing THF in 44% yield. A variety of R^3 groups (**68**-**81**) could then be incorporated *via N*-alkylation of the pyridone using potassium carbonate and heating in either DMF or MeOH. Finally, the key aminocarbonylation step directly installs the amide using dicobalt octacarbonyl as the CO source, in the presence of palladium acetate and either Xantphos or CataCXium A as the ligand.[73] The reaction was normally conducted under microwave irradiation in the presence of DMAP, in 1,4-dioxane at 75 - 80 ^{o}C and delivers the final compounds (**33-36**, **40-44**, **46-47** and **53-54**) in low to moderate yield. Indole **57** was prepared as its *N*-tosyl derivatives **82** and the final inhibitor was obtained by deprotection with cesium carbonate in MeOH / THF at 70 ^{o}C.

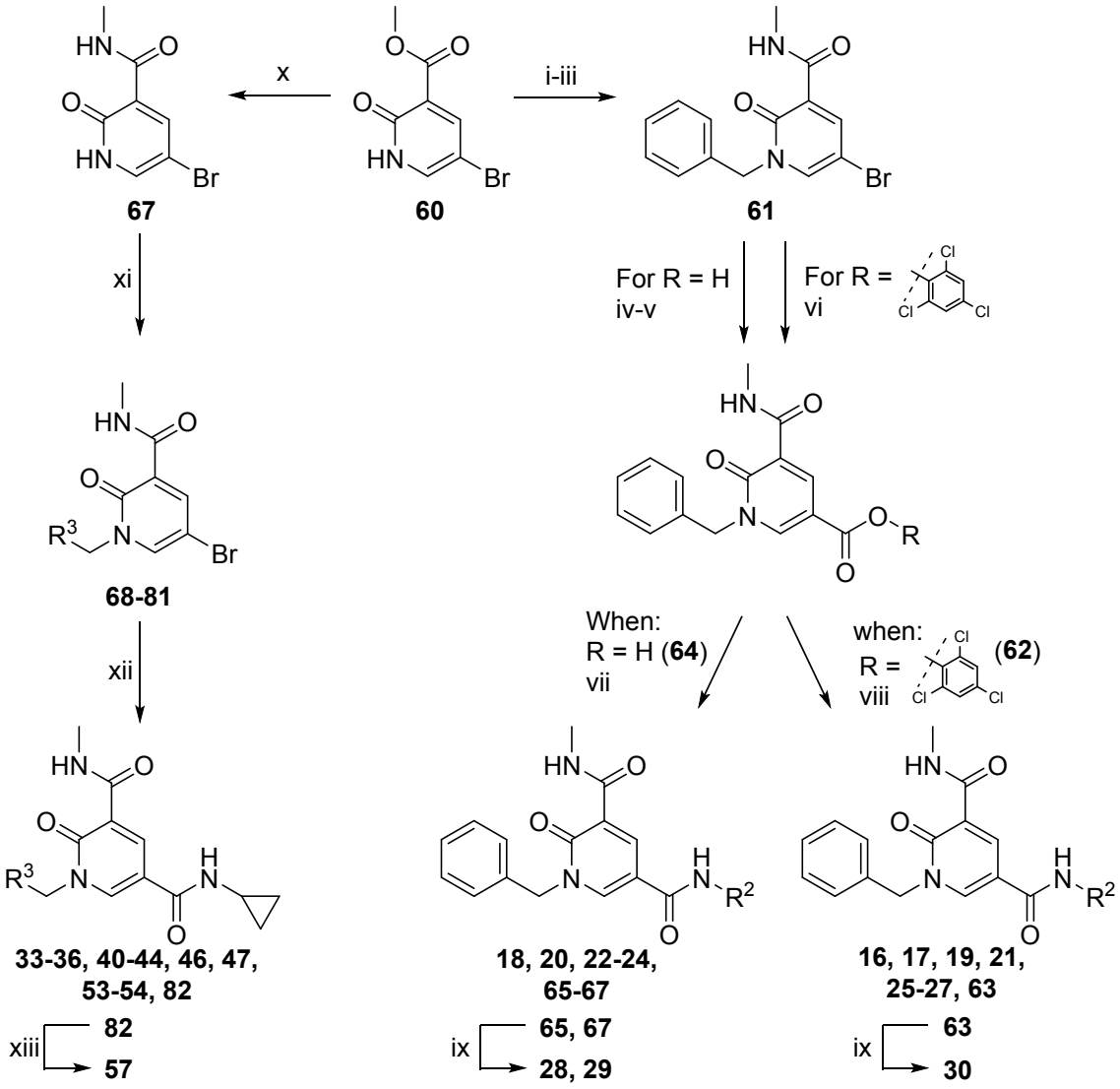

i. NaH, DMF/THF (1:1) 0 °C, 30 min, then BnBr, 0 °C to rt, 2 h (89%); ii. LiOH, THF/H_2O/MeOH (1:1:1), rt, 2 h (78%); iii. $(COCl)_2$, DMF (0.5 mol%), DCM, rt, 2 h, then $MeNH_2$ (2M in THF), Et_3N, THF, 0 °C, 1.5 h (95%); iv. $Pd(OAc)_2$ (10 mol%), dppb (10 mol%), Et_3N, EtOH, DMSO, CO, 100 °C, 50 psi, 16 h (94%); v. NaOH, MeOH/THF (1:1), rt, 2 h (80%); vi. $Pd(OAc)_2$ (5 mol%), Xantphos (10 mol%), Et_3N, toluene, 80 °C, 20 min, then 2,4,6-trichlorophenyl formate 80 °C, 2.5 h (87%); vii. R^2NH_2, HATU, DIPEA or Et_3N, DMF or DCM, rt, 2 h; viii. R^2NH_2, DMAP (0.2 eq.), Et_3N, THF, 45 °C, 3 h; ix. TFA, DCM, rt, 1 h; x. $MeNH_2$ (2M in THF), THF, reflux, 23 h (44%); xi. K_2CO_3, R^3CH_2Br, MeOH or DMF, 65 – 90 °C,; xii. $cPrNH_2$, $Co_2(CO)_8$, $Pd(OAc)_2$, xantphos or cataXium A, DMAP, 1,4-dioxane, µw 75 – 80 °C; xiii. Cs_2CO_3, MeOH/THF (1:2), 70 °C, 1 h (41%).

Scheme 1. Divergent synthetic routes for the variance of R^2 and R^3

Variations of this synthetic route were followed for additional analogues **37**-**39**, **48**-**52**, **55**-**56**, **58**-**59** as detailed in Scheme 2. The key advantage to this alternative approach was the use of pyridone *O*-alkylation as a protecting group strategy to allow preparation of advanced amides **86**-**88**, allowing for a late stage introduction of the R^3 "shelf" substituent either by Mitsunobu or alkylation chemistry.

Overall, this late stage diversification was attractive for analogue synthesis, especially where the shelf substituents required bespoke preparation. Additional late stage functional group interconversions were required to afford alcohol **48** and morpholine **49** as detailed in Scheme 2. Whilst this route was excellent for R^3 diversification it is less step efficient than the Scheme 1 route for scale up.

Finally, separate synthetic routes were utilised to prepare 6-methylpyridone **32** and benzylic-methyl derivative **31**. Their preparation is outlined in Scheme 3 and 4. 6-Methylpyridone **32** was prepared from known intermediate **94**[74] in 4 steps using similar chemistry to that already discussed. On the other hand, pyran **96** was used as a novel start point for the preparation of pyridone **31**, and allowed the commercial (*R*)-1-phenylethanamine to be used as the source of the chiral methyl group. Furthermore, selective bromination of the resultant pyridone **97** provided the functional handle to allow access to the carbonylation chemistry already discussed.

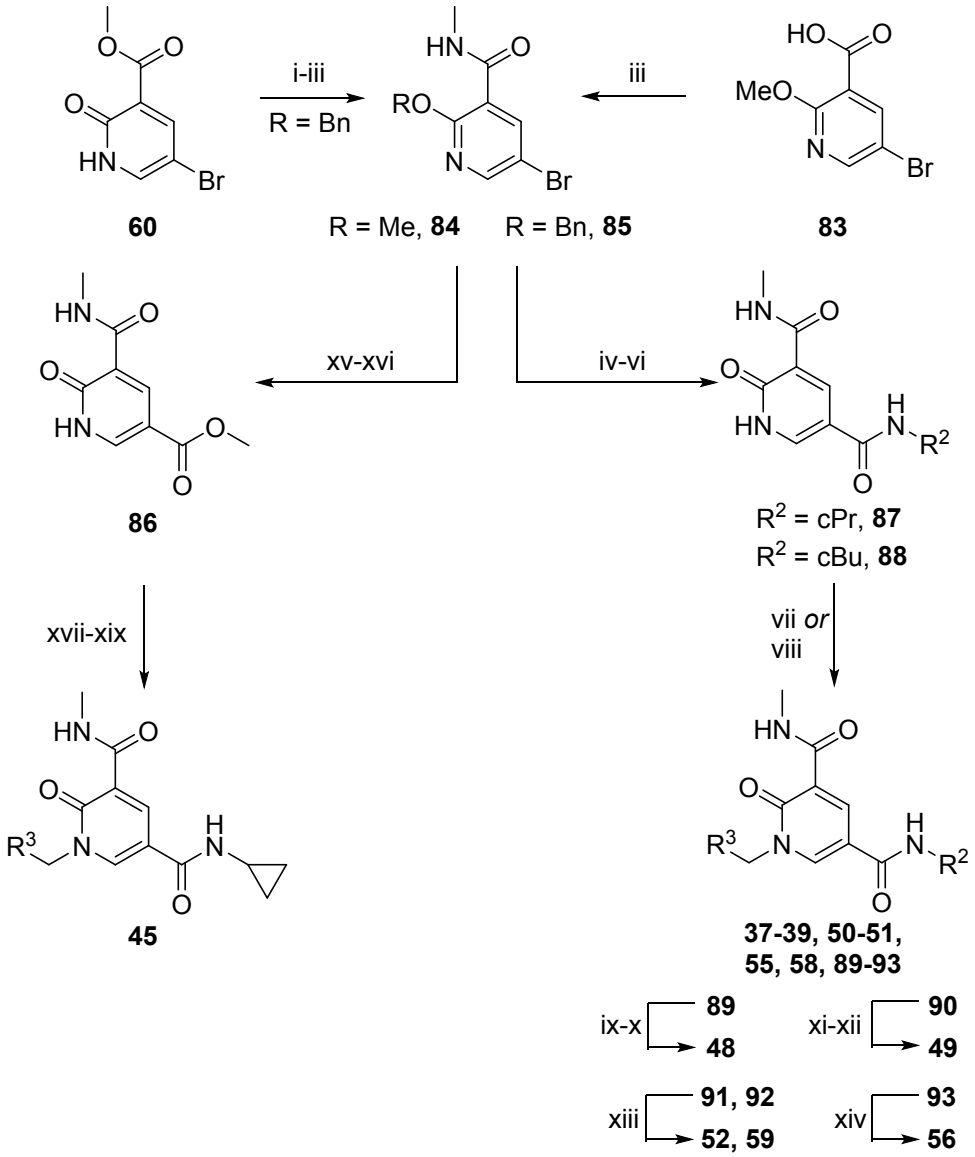

Reagents and conditions: i. BnBr, Ag_2CO_3, $CHCl_3$, reflux, 16 h (67%); ii.LiOH, THF/MeOH (1:1), rt, 2 h (94%); iii. $(COCl)_2$, DMF (0.5 mol%), DCM, rt, 2 h, then $MeNH_2$ (2M in THF), THF or 2-MeTHF, rt, 6 h (54-95%); iv. $Pd(OAc)_2$ (5 mol%), Xantphos (10 mol%), Et_3N, toluene, 80 °C, 20 min, then 2,4,6-trichlorophenyl formate 80 °C, 2-18 h (57%); v. R^2NH_2, Et_3N, DMAP (5 mol%), THF, 45 °C, 45 min – 16 h (85-86%); vi. TFA, 80 – 90 °C, 1 h (83-99%); vii. CMTP, toluene, µw 120 °C, or DIAD, PPh_3, toluene, rt, 3-24 h viii. K_2CO_3, THF or DMF, rt – 50 °C; ix. MeMgBr (3M in Et_2O), THF, -78 °C, 45 min (43%); x. chiral separation (Chiralpak AD-H); xi. DMP, DCM, 0 °C – rt, 48 h (quant.); xii. morpholine, Et_3N, DCM, rt, 45 min, then STAB, rt 24 h (25%); xiii. TFA, DCM, rt, 30-90 min (80%) or HCl, IPA, rt, 3 days (48%); xiv.Cs_2CO_3, MeOH/THF (1:2), 70 °C, 1 h (68%); xv. $Pd(OAc)_2$ (5 mol%), Xantphos (6 mol%), Et_3N, MeOH,

DMF, 60 °C, 21 h (60%); xvi. NaI, MeCN, rt, 16 h (25%); xvii. K_2CO_3, DMF, 90 °C, 1 h (67%); xviii. LiOH, 1,4-dioxane / water (1:1), rt, 30 min (90%); xix. R^2NH_2, HATU, DIPEA, DMF, rt, 7 h (quant).

Scheme 2. Alternative routes for the preparation of pyridone analogues

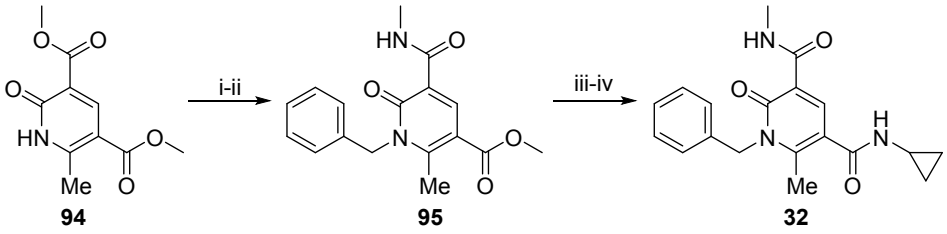

Reagents and conditions:i. K_2CO_3, BnBr, DMF, 40 °C, 4 h (35%); ii. $MeNH_2$ (2M in THF), MeOH, 50 °C, 30 min (82%); iii. LiOH, 1,4-dioxane / water (1:1), rt, 1 h 45 min (99%); ,iv. $cPrNH_2$, HATU, DIPEA, DMF, rt, 1 h (74%).

Scheme 3. Preparation of 6-methylpyridone **32**

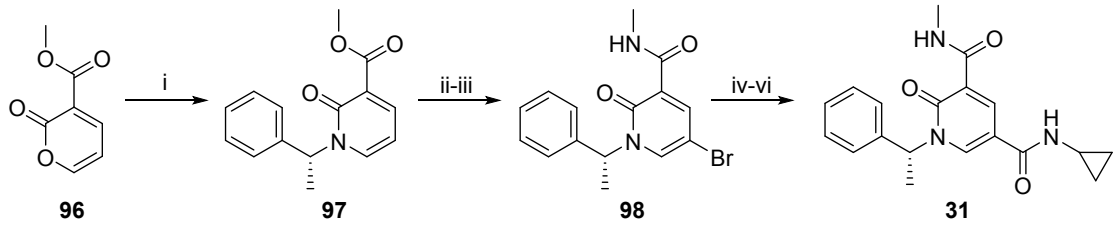

Reagents and conditions: i. (*R*)-1-phenylethanamine, DMF / THF (1:4), rt, 30 min, then EDC, DMAP (6 mol%), rt, 64 h (75%); ii. NBS, 2-MeTHF, rt, 15 min; iii. $MeNH_2$ (2M in THF), MeOH, 50 °C, 90 min (78%, 2 steps); iv. $Pd(OAc)_2$ (10 mol%), Xantphos (7 mol%), Et_3N, MeOH, DMF, 60 °C, 4 h (60%); v. NaOH, MeOH / H_2O, rt, 16 h (90%); vi. $cPrNH_2$, HATU, DIPEA, DMF, rt, 1 h (89%).

Scheme 4. Homochiral preparation of pyridone **31**

CONCLUSION

In summary, we have described the lead optimisation of a weak fragment-like hit into a range of potent pan-BD2 selective inhibitors, possessing excellent physicochemical properties and with selectivities from 200 - >1000 fold. Analogues **20** (GSK620) and **56** (GSK549) were selected for further profiling and as shown in Table 7 both compounds show agreement in their selectivity for all BET

family members (BRD2, BRD3, BRD4 and BRDT BD2 vs BD1), with indole **56** maintaining its extremely high selectivity against BD1 for the other family members. This illustrates the high sequence homology between the BD2 domains of these 4 proteins. Both **20** and **56** were evaluated using a BET surface plasmon resonance (SPR) assay.[75] Here, the same mutant protein constructs are used as for the FRET assay, but binding affinity can be assessed. Pleasingly, both compounds were similarly potent and selective as observed in the FRET assay. The selectivity of **56** was also evaluated against the wider bromodomain family using the DiscoverX BromoScan screening platform. As illustrated by Figure 6 and Supplementary Table S12, **20** is highly selective for the BET-BD2 family of proteins with >200 fold selectivity over all other bromodomains. Both **20** and **56** have also been profiled against a range of known liability targets as shown in Supplementary Table S13 and both show minimal activity against all targets tested. **20** is also Ames[76] and mouse lymphoma assay (MLA)[77-78] negative, whilst both compounds showed low levels of inhibition against indicators of hepatoxicity such as the bile salt export pump (BSEP) assay (pIC50 <3.7 for **20** and 4.3 for **56**).[79] They were also negative in the glutathione (GSH) trapping assay[80] and both showed no toxicity in the cell health evaluation of hepG2 cells against three end points. Both **20** and **56** do not have a CYP3A4 metabolism-dependant inhibition (MDI) or direct inhibition liability as tested in house and for **20** this was confirmed in an external time-dependant inhibition (TDI) assay at high concentration.[81-82] These data are particularly encouraging for the unsubstituted indole as this is often implicated in toxicities caused by reactive metabolites,[83] though at least in our *in vitro* screens, this has not been observed to date.

Table 7. Profile of Lead Compounds **20** (GSK620) and **56** (GSK549).

Compound		
	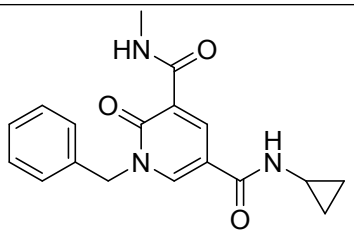 **20**	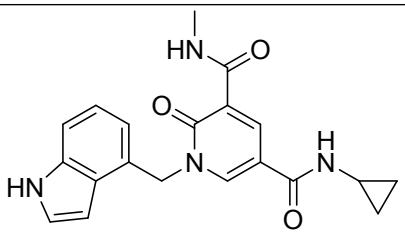 **56**

BRD4 BD2 / BD1 pIC_{50} (n)	7.1 (16) / 4.8 (14)	7.8 (8) / 4.7 (8)
BRD2 BD2 / BD1 pIC_{50} (n)	6.5 (20) / 4.6 (13[a])	7.2 (9) / <4.3 (11)
BRD3 BD2 / BD1 pIC_{50} (n)	7.1 (16) / 4.6 (6[b])	7.8 (10) / 4.7 (4[d])
BRDT BD2 / BD1 pIC_{50} (n)	6.7 (18) / 4.6 (9[c])	7.4 (12) / 4.7 (12)
BRD4 BD2 Selectivity (fold)	220	1150
BRD4 BD2 LE / LLE_{AT}	0.40 / 0.51	0.40 / 0.50
BRD4 BD2 / BD1 SPR pK_d (n)	7.3 (1) / 5.0 (1)	7.6 (1) / 5.1 (2)
LPS stim. hWB pIC_{50} (MCP-1)	6.1 (8)	6.8 (4)
CHROMlogD (pH 7.4) / clogP	3.1 / 0.1	2.9 / 0.1
CLND (µg/mL) / FaSSIF (µg/mL)	≥154 / 13-35	78 / 17-23
AMP (nm/sec)	200	178
Hepatocyte Cli (rat / hu / dog)	0.95 / <0.45 / <1.26	1.66 / <0.45 / <1.26
CYP3A4 pIC_{50} (MDI shift)	<4.4 (5) / 1.0	<4.4 (5[e]) / 1.0
Cyprotex CYP3A4 pIC_{50} / TDI shift	<3.7 / ND	-
hERG pIC_{50}	<4.3 (7)	<4.3 (8)
Ames / MLA	Negative	ND
GSH trapping / BSEP pIC_{50}	Negative / <3.7 (2)	Negative / 4.3 (2)
Cell health HepG2 pIC_{50} (nuc. morph / Mit. pot. / Mem. perm.)	<3.7 (2) / <3.7 (2) / <3.7 (2)	3.7 (1[f]) / <3.7 (2) / <3.7 (2)

[a]also tested <4.3 (n=8); [b]also tested <4.3 (n=10); [c]also tested <4.3 (n=9); [d]also tested <4.3 (n=6); [e]also tested 5.5 (n=1); [f]also tested <3.7 (n=1).

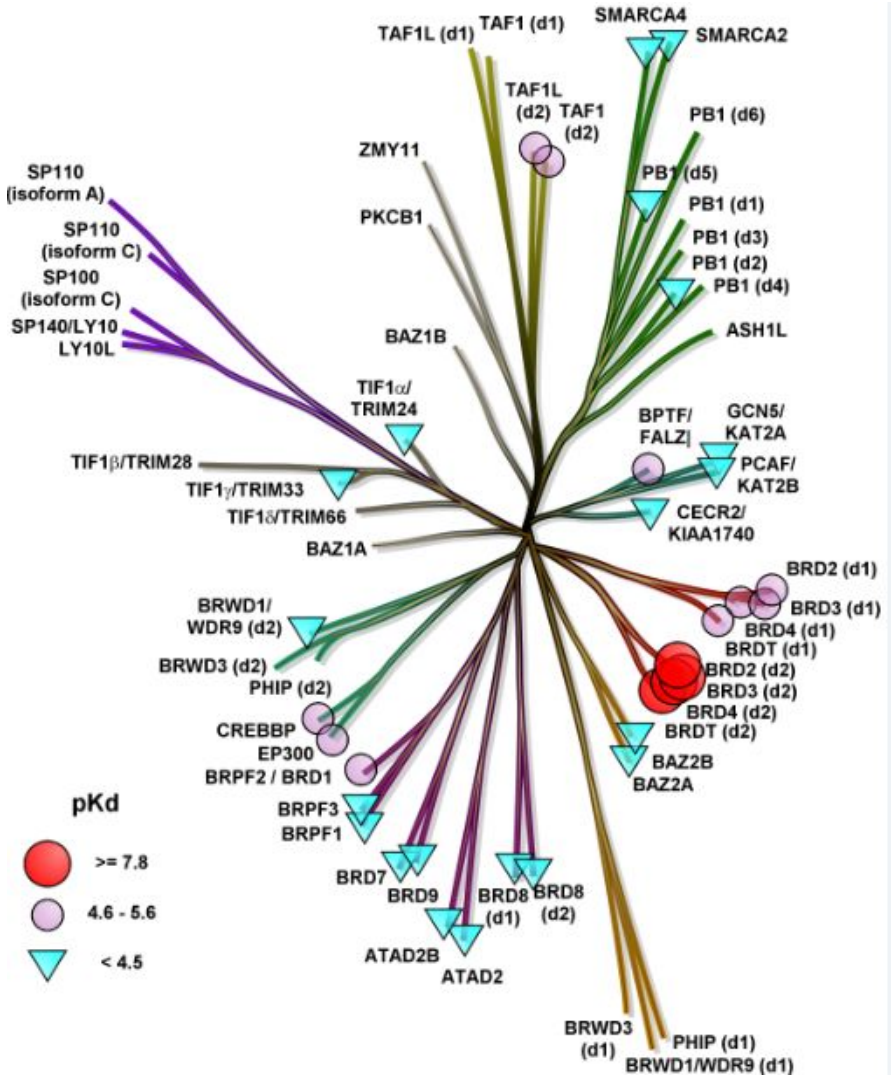

Figure 6. BromoScan profile of **20** (GSK620).

Overall, both **20** and **56** are potent and selective pan-BD2 inhibitors with excellent *in vivo* PK properties and excellent developability properties, with the exception of moderate FaSSIF solubility driven by their highly crystalline nature. Importantly, both these tools also show a biological phenotype in human whole blood as shown in Table 7. Here, human blood samples are stimulated with lipopolysaccharide (LPS) which produces a strong immune response. In this assay the monocyte chemattractant protein 1 (MCP-1 / CCL2) is measured. This is a chemokine which recruits monocytes, memory T cells, and dendritic cells to sites of inflammation.[84] Herein, we show that highly BD2 selective compounds **20** and **56** are capable of reducing the MCP-1 response in a concentration-dependant manner with (an expected) ~1 log drop off in potency relative to the biochemical BRD4

BD2 potencies observed, providing strong evidence that **20** and **56** are indeed engaging BD2 in cells. Indeed, these data in concert with the differing selectivity profiles of the two compounds and their excellent pharmacokinetics, make them excellent tools for *in vitro* and *in vivo* evaluation of the phenotype associated with pan-BD2 inhibition. A detailed comparison of the functional contribution of the BD1 and BD2 bromodomains has recently been disclosed.[53] This compared the efficacy of **20** alongside structurally differentiated BD2 inhibitor **15** (GSK046) and BD1 selective tool, **7**.[44] Highlighting the utility of **20** as an *in vivo* tool, efficacy was observed in separate models of inflammatory arthritis, psoriasis and hepatitis. Together these data demonstrate that BD2 inhibitors are effective in models of inflammatory and autoimmune disease, opening up an exciting possible new therapeutic approach against these pathologies.

General Experimental

Unless otherwise stated, all reactions were carried out under an atmosphere of nitrogen in heat or oven dried glassware and anhydrous solvent. Solvents and reagents were purchased from commercial suppliers and used as received. Reactions were monitored by thin layer chromatography (TLC) or liquid chromatography-mass spectrometry (LCMS). TLC was carried out on glass or aluminium-backed 60 silica plates coated with UV_{254} fluorescent indicator. Spots were visualized using UV light (254 or 365 nm) or alkaline $KMnO_4$ solution, followed by gentle heating. LCMS analysis was carried out on a Waters Acquity UPLC instrument equipped with a CSH C18 column (50 mm x 2.1 mm, 1.7 µm packing diameter) and Waters micromass ZQ MS using alternate-scan positive and negative electrospray. Analytes were detected as a summed UV wavelength of 210 – 350 nm. Three liquid phase methods were used: *Formic* – 40 °C, 1 mL/min flow rate. Gradient elution with the mobile phases as (A) H_2O containing 0.1% volume/volume (v/v) formic acid and (B) acetonitrile containing 0.1% (v/v) formic acid. *High pH* – 40 °C, 1 mL/min flow rate. Gradient elution with the mobile phases as (A) 10 mM aqueous ammonium bicarbonate solution, adjusted to pH 10 with 0.88 M aqueous ammonia and (B) acetonitrile. *TFA* – 40 °C, 1 mL/min flow rate. Gradient elution with the mobile phases as (A) 0.1% v/v

aqueous TFA solution and (B) 0.1% v/v TFA solution in acetonitrile. Flash column chromatography was carried out using Biotage SP4 or Isolera One apparatus with SNAP silica cartridges. Mass directed automatic purification (MDAP) was carried out using a Waters ZQ MS using alternate-scan positive and negative electrospray and a summed UV wavelength of 210 – 350 nm. Two liquid phase methods were used: *Formic* – Sunfire C18 column (100 mm x 19 mm, 5 µm packing diameter, 20 mL/min flow rate) or Sunfire C18 column (150 mm x 30 mm, 5 µm packing diameter, 40 mL/min flow rate). Gradient elution at ambient temperature with the mobile phases as (A) H_2O containing 0.1% volume/volume (v/v) formic acid and (B) acetonitrile containing 0.1% (v/v) formic acid. *High pH* – Xbridge C18 column (100 mm x 19 mm, 5 µm packing diameter, 20 mL/min flow rate) or Xbridge C18 column (150 mm x 30 mm, 5 µm packing diameter, 40 mL/min flow rate). Gradient elution at ambient temperature with the mobile phases as (A) 10 mM aqueous ammonium bicarbonate solution, adjusted to pH 10 with 0.88 M aqueous ammonia and (B) acetonitrile. NMR spectra were recorded at ambient temperature (unless otherwise stated) using standard pulse methods on any of the following spectrometers and signal frequencies: Bruker AV-400 (^{1}H = 400 MHz, ^{13}C = 101 MHz,), Bruker AV-600 (^{1}H = 600 MHz, ^{13}C = 150 MHz,) or Bruker AV4 700 MHz spectrometer (^{1}H = 700 MHz, ^{13}C = 176 MHz). Chemical shifts are referenced to trimethylsilane (TMS) or the residual solvent peak, and are reported in ppm. Coupling constants are quoted to the nearest 0.1 Hz and multiplicities are given by the following abbreviations and combinations thereof: s (singlet), δ (doublet), t (triplet), q (quartet), quin (quintet), sxt (sextet), m (multiplet), br. (broad). Liquid chromatography high resolution mass spectra (HRMS) were recorded on a Waters XEVO G2-XS Q-Tof mass spectrometer with positive electrospray ionisation mode over a scan range 100-200 AMU, with analytes separated on an Acquity UPLC CSH C18 column (100 mm x 2.1 mm, 1.7 µm packing diameter) at 50 °C. Purity of synthesized compounds was determined by LCMS analysis. All compounds for biological testing were >95% pure.

Synthetic Procedures:

1-Benzyl-N^3-methyl-2-oxo-1,2-dihydropyridine-3,5-dicarboxamide (**16**). Step 1: *Methyl 1-benzyl-5-bromo-2-oxo-1,2-dihydropyridine-3-carboxylate* (**99**). Sodium hydride (5.17 g, 60% dispersion in

mineral oil, 129 mmol) was added to a solution of methyl 5-bromo-2-oxo-1,2-dihydro-3-pyridinecarboxylate (**60**, 25 g, 108 mmol) in DMF (200 mL) and THF (200 mL) at 0 °C and the mixture was stirred for 30 min, giving a dense suspension. Benzyl bromide (14.10 mL, 119 mmol) was added and the mixture stirred for a further 2 h, allowing to warm to rt, then the resulting clear brown solution was added to water (400 mL) and extracted with EtOAc (2 x 300 mL). The combined organics were washed with water (2 x 200 mL), dried and evaporated *in vacuo* to give methyl 1-benzyl-5-bromo-2-oxo-1,2-dihydropyridine-3-carboxylate (**99**, 31 g, 96 mmol, 89% yield) as a beige solid. This material was carried through to the next step without purification. LCMS (2 min High pH): Rt = 0.98 min, [MH]+ = 322.0 & 324.1. ^{1}H NMR (400 MHz, $CHCl_3$-*d*) δ ppm 8.16 (d, J=2.9 Hz, 1 H) 7.62 (d, J=2.9 Hz, 1 H) 7.30 - 7.43 (m, 5 H) 5.15 (s, 2 H) 3.92 (s, 3 H). Step 2: *1-Benzyl-5-bromo-2-oxo-1,2-dihydropyridine-3-carboxylic acid* (**100**). Lithium hydroxide (6.91 g, 289 mmol) in water (200 mL) was added to a mixture of methyl 1-benzyl-5-bromo-2-oxo-1,2-dihydropyridine-3-carboxylate (**99**, 31 g, 96 mmol), THF (200 mL) and methanol (200 mL) and the mixture was stirred at rt for 2 h, then evaporated *in vacuo* to about half volume, giving a dense suspension. This was diluted with water (200 mL) and acidified with acetic acid to pH 5, then extracted with EtOAc (2 x 300 mL). The combined organics were dried over sodium sulphate and evaporated *in vacuo* to give an off-white solid. The product was suspended in ether (200 mL), sonicated, diluted with cyclohexane (100 mL) and collected by filtration to give 1-benzyl-5-bromo-2-oxo-1,2-dihydropyridine-3-carboxylic acid (**100**, 23 g, 74.6 mmol, 78% yield). LCMS (2 min Formic): Rt = 1.01 min, [MH]+ = 308.0 & 310.1. ^{1}H NMR (400 MHz, $CHCl_3$-*d*) δ ppm 14.02 (br. s., 1 H) 8.55 (d, J=2.7 Hz, 1 H) 7.73 (d, J=2.7 Hz, 1 H) 7.40 - 7.47 (m, 3 H) 7.31 - 7.37 (m, 2 H) 5.25 (s, 2 H). Step 3: *1-Benzyl-5-bromo-N-methyl-2-oxo-1,2-dihydropyridine-3-carboxamide* (**61**). 1-Benzyl-5-bromo-2-oxo-1,2-dihydropyridine-3-carboxylic acid (**100**, 28 g, 91 mmol) was suspended in DCM (300 mL) and oxalyl chloride (23.86 mL, 273 mmol) and DMF (0.352 mL, 4.54 mmol) were added, then the mixture was stirred for 2 h at rt. The solvent was evaporated *in vacuo* to give a brown residue, which was then dissolved in THF (300 mL) and Et_3N (12.67 mL, 91 mmol) was added. The mixture was cooled in an ice bath, then methanamine (91 mL, 2M in THF, 182 mmol) was added dropwise over 30 min and

the mixture stirred for a further 1 h at 0 °C. The solvent was evaporated *in vacuo* and the solid residue was partitioned between water (300 mL) and DCM (300 mL), the organic layer was washed with brine, dried and evaporated *in vacuo* to give 1-benzyl-5-bromo-*N*-methyl-2-oxo-1,2-dihydropyridine-3-carboxamide (**61**, 27.6 g, 86 mmol, 95% yield) as a brown solid. LCMS (2 min Formic): Rt = 0.97 min, [MH]+ = 321.0 & 323.1. ^{1}H NMR (400 MHz, $CHCl_3$-*d*) δ ppm 9.57 (br. s., 1 H) 8.60 (d, J=2.9 Hz, 1 H) 7.62 (d, J=2.9 Hz, 1 H) 7.34 - 7.48 (m, 3 H) 7.29 - 7.33 (m, 2 H) 5.20 (s, 2 H) 3.00 (d, J=4.9 Hz, 3 H). Step 4: *2,4,6-Trichlorophenyl 1-benzyl-5-(methylcarbamoyl)-6-oxo-1,6-dihydropyridine-3-carboxylate* (**62**). 1-Benzyl-5-bromo-N-methyl-2-oxo-1,2-dihydropyridine-3-carboxamide (**61**, 2 g, 6.23 mmol), Xantphos (0.360 g, 0.623 mmol), palladium acetate (0.070 g, 0.311 mmol) and Et_3N (1.302 mL, 9.34 mmol) were combined in a three necked flask equipped with a dropping funnel and a condenser with a nitrogen bubbler on the top. Toluene (30 mL) was added and the mixture was heated at 80 °C for 20 min, then a solution of 2,4,6-trichlorophenyl formate (2.106 g, 9.34 mmol) in toluene (20 mL) was added dropwise over 30 min and heating continued for 2 h. The reaction mixture was diluted with EtOAc (50 mL) and washed with water (50 mL) and brine (50 mL), dried and evaporated *in vacuo* to give an orange oil. This was dissolved in DCM (10 mL) and loaded onto a 50 g silica column, then eluted with 0-50% EtOAc/cyclohexane and the product-containing fractions evaporated *in vacuo* to give 2,4,6-trichlorophenyl 1-benzyl-5-(methylcarbamoyl)-6-oxo-1,6-dihydropyridine-3-carboxylate (**62**, 2.52 g, 5.41 mmol, 87% yield) as a beige solid. LCMS (2 min Formic): Rt=1.36min, [MH]+ = 465, 467. ^{1}H NMR (400 MHz, $CHCl_3$-*d*) δ ppm 9.32 (br. d, J=4.4 Hz, 1 H) 9.20 (d, J=2.7 Hz, 1 H) 8.58 (d, J=2.7 Hz, 1 H) 7.30 - 7.50 (m, 7 H) 5.29 (s, 2 H) 3.01 (d, J=4.9 Hz, 3 H). Step 5: *1-Benzyl-N^3-methyl-2-oxo-1,2-dihydropyridine-3,5-dicarboxamide* (**16**). Prepared from **62** (1 g, 2.15 mmol) and ammonia (21.47 mL, 10.74 mmol, 0.5M in 1,4-dioxane) using the same procedure as for compound **21**, to give 1-benzyl-N^3-methyl-2-oxo-1,2-dihydropyridine-3,5-dicarboxamide (562 mg, 1.87 mmol, 87% yield) as a white solid. LCMS (2 min High pH): Rt = 0.74 min, $[MH]^+$ = 286.3. ^{1}H NMR (400 MHz, DMSO-d_6) δ ppm 9.36 (br q, *J*=4.4 Hz, 1 H) 8.82 (d, *J*=2.5 Hz, 1 H) 8.78 (d, *J*=2.9 Hz, 1 H) 7.88 - 8.19 (m, 1 H) 7.12 - 7.57 (m, 6 H) 5.29 (s, 2 H) 2.83 (d, *J*=4.4 Hz, 3 H).

1-Benzyl-N^3,N^5-dimethyl-2-oxo-1,2-dihydropyridine-3,5-dicarboxamide (**17**). Prepared from **62** (40 mg, 0.086 mmol) and methanamine (2M in THF, 0.09 mL, 0.180 mmol) using the same procedure as for **21**, to give 1-benzyl-N^3,N^5-dimethyl-2-oxo-1,2-dihydropyridine-3,5-dicarboxamide (16 mg, 0.048 mmol, 56% yield). LCMS (2 min Formic): Rt = 0.75 min, $[MH]^+$ = 300.0. ^{1}H NMR (400 MHz, MeOH-d_4) δ ppm 8.85 (d, *J*=2.9 Hz, 1 H) 8.58 (d, *J*=2.9 Hz, 1 H) 7.26 - 7.44 (m, 5 H) 5.34 (s, 2 H) 2.97 (s, 3 H) 2.90 (s, 3 H). *Exchangeable protons not observed*.

1-Benzyl-N^5-ethyl-N^3-methyl-2-oxo-1,2-dihydropyridine-3,5-dicarboxamide (**18**): Step 1: *Ethyl 1-benzyl-5-(methylcarbamoyl)-6-oxo-1,6-dihydropyridine-3-carboxylate* (**101**). 1-Benzyl-5-bromo-*N*-methyl-2-oxo-1,2-dihydropyridine-3-carboxamide (**61**, 23 g, 71.6 mmol), DMSO (60 mL), ethanol (70 g, 1519 mmol), Et_3N (19.96 mL, 143 mmol), dppb (3.05 g, 7.16 mmol) and palladium acetate (1.608 g, 7.16 mmol) were placed in a steel Parr vessel, which was then purged with carbon monoxide by filling to 50 psi, then releasing the pressure, then refilled to 50 psi and heated overnight at 100 °C. The mixture was diluted with water (200 mL) and extracted with EtOAc (2 x 300 mL), the organic layer washed with water (2 x 300 mL), then dried and evaporated *in vacuo* and the residue was triturated with ether (200 mL) and the solid collected by filtration to give ethyl 1-benzyl-5-(methylcarbamoyl)-6-oxo-1,6-dihydropyridine-3-carboxylate (**101**, 21.2 g, 67.4 mmol, 94% yield). LCMS (2 min Formic): Rt = 0.99 min, [MH]+ = 315.2. ^{1}H NMR (400 MHz, $CHCl_3$-*d*) δ ppm 9.37 (br. s., 1 H) 9.03 (d, *J*=2.4 Hz, 1 H) 8.38 (d, *J*=2.7 Hz, 1 H) 7.34 - 7.42 (m, 3 H) 7.28 - 7.34 (m, 2 H) 5.25 (s, 2 H) 4.35 (q, *J*=7.1 Hz, 2 H) 2.99 (d, *J*=4.9 Hz, 3 H) 1.37 (t, *J*=7.2 Hz, 3 H). Step 2: *1-Benzyl-5-(methylcarbamoyl)-6-oxo-1,6-dihydropyridine-3-carboxylic acid* (**64**). Sodium hydroxide (99 mL, 199 mmol, 2M aq.) was added to a solution of ethyl 1-benzyl-5-(methylcarbamoyl)-6-oxo-1,6-dihydropyridine-3-carboxylate (**101**, 20.8 g, 66.2 mmol) in a mixture of methanol (100 mL) and THF (100 mL) and the resulting solution was stirred for 2 h at rt, then evaporated *in vacuo* to approximately 100 mL volume. The mixture was diluted with water (200 mL), then filtered to remove a dark grey solid, the filtrate was washed with MTBE (200 mL), then acidified to pH 4 with 2M HCl and the resulting suspension stirred for 2 h, then filtered and the product washed with water, then dried in the vacuum oven to give 1-benzyl-5-(methylcarbamoyl)-6-

oxo-1,6-dihydropyridine-3-carboxylic acid (**64**, 15.2 g, 53.1 mmol, 80% yield). LCMS (2 min High pH): Rt = 0.58 min, [MH]+ = 287.2. ^{1}H NMR (400 MHz, DMSO-d_6) δ ppm 13.19 (br. s., 1 H) 9.14 - 9.34 (m, 1 H) 8.88 (d, J=2.7 Hz, 1 H) 8.70 (d, J=2.7 Hz, 1 H) 7.25 - 7.42 (m, 5 H) 5.33 (s, 2 H) 2.82 (d, J=4.6 Hz, 3 H).

Step 3: *1-Benzyl-N^5-ethyl-N^3-methyl-2-oxo-1,2-dihydropyridine-3,5-dicarboxamide* (**18**). Prepared from **64** (250 mg, 0.873 mmol) and ethanamine (2M in THF, 0.873 mL, 1.747 mmol) using the same procedure as for **20**, to give 1-benzyl-N^5-ethyl-N^3-methyl-2-oxo-1,2-dihydropyridine-3,5-dicarboxamide (242 mg, 0.772 mmol, 88% yield) as a cream solid. LCMS (2 min Formic): Rt = 0.80 min, $[MH]^+$ = 314.1. ^{1}H NMR (400 MHz, DMSO-d_6) δ ppm 9.31 - 9.43 (m, 1 H) 8.82 (d, *J*=2.7 Hz, 1 H) 8.73 (d, *J*=2.7 Hz, 1 H) 8.56 (br. t, *J*=5.3, 5.3 Hz, 1 H) 7.27 - 7.40 (m, 5 H) 5.30 (s, 2 H) 3.22 - 3.28 (m, 2 H) 2.83 (d, *J*=4.9 Hz, 3 H) 1.11 (t, *J*=7.2 Hz, 3 H).

1-Benzyl-N^5-isopropyl-N^3-methyl-2-oxo-1,2-dihydropyridine-3,5-dicarboxamide (**19**). Prepared from **62** (50 mg, 0.107 mmol) and propan-2-amine (0.018 mL, 0.215 mmol), using the same procedure as for compound **21**, to give 1-benzyl-N^5-isopropyl-N^3-methyl-2-oxo-1,2-dihydropyridine-3,5-dicarboxamide (32 mg, 0.083 mmol, 77% yield) as a white solid. LCMS (2 min Formic): Rt = 0.92 min, $[MH]^+$ = 328.0. ^{1}H NMR (400 MHz, MeOH-d_4) δ ppm 9.67 - 9.94 (m, 1 H) 8.87 (d, *J*=2.4 Hz, 1 H) 8.58 (d, *J*=2.4 Hz, 1 H) 7.28 - 7.44 (m, 5 H) 5.33 (s, 2 H) 4.17 (quin, *J*=6.4 Hz, 1 H) 2.92 - 3.01 (m, 3 H) 1.25 (d, *J*=6.8 Hz, 6 H). *One exchangeable proton not observed.*

1-Benzyl-N^5-cyclopropyl-N^3-methyl-2-oxo-1,2-dihydropyridine-3,5-dicarboxamide (**20**). 1-Benzyl-5-(methylcarbamoyl)-6-oxo-1,6-dihydropyridine-3-carboxylic acid (**64**, 5.5 g, 19.21 mmol) was suspended in DCM (100 mL) and Et_3N (3.21 mL, 23.05 mmol), HATU (9.50 g, 24.98 mmol) and cyclopropylamine (1.625 mL, 23.05 mmol) were added, then the mixture was stirred for 2 h at rt. The mixture was washed with water (100 mL), 0.5 M HCl (100 mL) and saturated sodium bicarbonate solution (100 mL) and the organic layer was dried and evaporated *in vacuo* to give a pale yellow solid. The solid was suspended in ether (20 mL) and sonicated, then filtered and the solid dried in the vacuum oven to give 1-benzyl-N^5-cyclopropyl-N^3-methyl-2-oxo-1,2-dihydropyridine-3,5-dicarboxamide (5.25 g, 16.14 mmol, 84 % yield) as a colourless solid. The product was combined with

another batch, prepared by a similar method (2.4 g), the combined material was dissolved by refluxing in ethanol (200 mL) for 20 min, then Silicycle thiourea palladium scavenging resin (10 g) was added and the mixture heated for a further 30 min. The mixture was filtered into a Buchner flask and allowed to cool to rt over 1 h, then cooled in an ice bath for 1 h and the resulting solid collected by filtration and dried in the vacuum oven to give 1-benzyl-*N*^{5}-cyclopropyl-*N*^{3}-methyl-2-oxo-1,2-dihydropyridine-3,5-dicarboxamide (6.76 g, 20.78 mmol, 66% yield) as a colourless solid. LCMS (2 min high pH): Rt = 0.84 min, $[MH]^+$= 326.3. HRMS ($C_{18}H_{19}N_3O_3$): $[M+H]^+$ calculated 326.1499, found 326.1499. ^{1}H NMR (400 MHz, DMSO-d_6) δ ppm 9.35 (d, *J*=4.9 Hz, 1 H) 8.80 (d, *J*=2.7 Hz, 1 H) 8.72 (d, *J*=2.7 Hz, 1 H) 8.54 (d, *J*=3.9 Hz, 1 H) 7.25 - 7.42 (m, 5 H) 5.29 (s, 2 H) 2.75 - 2.89 (m, 4 H) 0.65 - 0.72 (m, 2 H) 0.53 - 0.59 (m, 2 H). ^{13}C NMR (151 MHz, DMSO-d_6) δ ppm 163.9, 163.1, 161.1, 144.0, 140.8, 136.2, 128.6 (2C), 127.7, 127.7 (2C), 119.3, 113.5, 52.8, 25.8, 22.9, 5.5 (2C).

1-Benzyl-N^5*-cyclobutyl-N*^{3}*-methyl-2-oxo-1,2-dihydropyridine-3,5-dicarboxamide* (**21**). 2,4,6-Trichlorophenyl 1-benzyl-5-(methylcarbamoyl)-6-oxo-1,6-dihydropyridine-3-carboxylate (**62**, 401 mg, 0.861 mmol), cyclobutanamine (0.15 mL, 1.757 mmol), DMAP (23 mg, 0.188 mmol), triethylamine (0.48 mL, 3.44 mmol) and THF (8 mL) were stirred at 45 °C under N_2 for 3 h. The reaction mixture was concentrated to give 600 mg of an off white solid which was purified by chromatography on SiO_2 (Biotage SNAP 50 g cartridge, eluting with 0-100% ethylacetate/cyclohexane). The desired fractions were concentrated to give 1-benzyl-*N*^{5}-cyclobutyl-*N*^{3}-methyl-2-oxo-1,2-dihydropyridine-3,5-dicarboxamide (295 mg, 0.782 mmol, 91% yield) as an off white solid. LCMS (2 min Formic): Rt=0.91 min, $[MH]^+$ = 340.0. ^{1}H NMR (400 MHz, MeOH-d_4) δ ppm 8.88 (d, *J*=2.9 Hz, 1 H) 8.59 (d, *J*=2.9 Hz, 1 H) 7.29 - 7.43 (m, 5 H) 5.33 (s, 2 H) 4.46 (quin, *J*=8.3 Hz, 1 H) 2.97 (s, 3 H) 2.22 - 2.47 (m, 2 H) 1.95 - 2.22 (m, 2 H) 1.62 - 1.91 (m, 2 H). *Exchangeable protons not observed.*

1-Benzyl-N^3*-methyl-2-oxo-N*^{5}*-(tetrahydro-2H-pyran-4-yl)-1,2-dihydropyridine-3,5-dicarboxamide* (**22**). Prepared from **64** (49.5 mg, 0.173 mmol) and tetrahydro-2*H*-pyran-4-amine, hydrochloride (50.2 mg, 0.365 mmol) using the same procedure as for **20**, to give 1-benzyl-*N*^{3}-methyl-2-oxo-*N*^{5}-(tetrahydro-2*H*-pyran-4-yl)-1,2-dihydropyridine-3,5-dicarboxamide (58.8 mg, 0.159 mmol, 92% yield). LCMS (2 min

formic): Rt = 0.81 min, $[MH]^+$ = 370.3. ^{1}H NMR (400 MHz, DMSO-d_6) δ ppm 9.32 - 9.42 (m, 1 H) 8.85 (d, *J*=2.7 Hz, 1 H) 8.75 (d, *J*=2.7 Hz, 1 H) 8.43 (d, *J*=7.6 Hz, 1 H) 7.26 - 7.40 (m, 5 H) 5.30 (s, 2 H) 3.92 - 4.05 (m, 1 H) 3.87 (br. dd, *J*=11.9, 2.1 Hz, 2 H) 3.37 (td, *J*=11.7, 1.8 Hz, 2 H) 2.83 (d, *J*=4.9 Hz, 3 H) 1.75 (br. dd, *J*=12.5, 2.2 Hz, 2 H) 1.56 (qd, *J*=12.0, 4.4 Hz, 2 H).

1-Benzyl-N^5-(2-methoxyethyl)-N^3-methyl-2-oxo-1,2-dihydropyridine-3,5-dicarboxamide (**23**). Prepared from **64** (50 mg, 0.175 mmol) and 2-methoxyethanamine (0.015 mL, 0.175 mmol) using the same procedure as **20**, to give the title compound (46 mg, 0.135 mmol, 77%). LCMS (2 min formic): Rt = 0.78 min, $[MH]^+$ = 344.3. ^{1}H NMR (400 MHz, MeOH-d_4) δ ppm 8.86 (d, *J*=2.7 Hz, 1 H) 8.58 (d, *J*=2.7 Hz, 1 H) 7.29 - 7.40 (m, 5 H) 5.33 (s, 2 H) 3.51 - 3.56 (m, 4 H) 3.37 (s, 3 H) 2.96 (s, 3 H). *Exchangeable protons not observed.*

1-Benzyl-N^5-(2-hydroxyethyl)-N^3-methyl-2-oxo-1,2-dihydropyridine-3,5-dicarboxamide (**24**). Prepared from **64** (154.3 mg, 0.539 mmol) and ethanolamine (0.065 mL, 1.078 mmol) using the same procedure as **20**, to give 1-benzyl-*N^5*-(2-hydroxyethyl)-*N^3*-methyl-2-oxo-1,2-dihydropyridine-3,5-dicarboxamide (175 mg, 0.531 mmol, 99% yield). LCMS (2 min formic): Rt = 0.69 min, $[MH]^+$ = 330.1. ^{1}H NMR (400 MHz, DMSO-d_6) δ ppm 9.37 (br. q, *J*=4.4, 4.4, 4.4 Hz, 1 H) 8.83 (d, *J*=2.7 Hz, 1 H) 8.79 (d, *J*=2.7 Hz, 1 H) 8.56 (br. t, *J*=5.4, 5.4 Hz, 1 H) 7.27 - 7.40 (m, 5 H) 5.30 (s, 2 H) 4.71 (t, *J*=5.6 Hz, 1 H) 3.50 (q, *J*=5.9 Hz, 2 H) 3.26 - 3.34 (obs. q, *J*=5.6 Hz, 2 H) 2.83 (d, *J*=4.9 Hz, 3 H).

1-Benzyl-N^5-isobutyl-N^3-methyl-2-oxo-1,2-dihydropyridine-3,5-dicarboxamide (**25**). Prepared from **62** (52 mg, 0.112 mmol) and 2-methylpropan-1-amine (0.02 mL, 0.201 mmol), using the same procedure as for compound **21**, to give 1-benzyl-*N^5*-isobutyl-*N^3*-methyl-2-oxo-1,2-dihydropyridine-3,5-dicarboxamide (36 mg, 0.095 mmol, 85% yield). LCMS (2 min Formic): Rt = 0.98 min, $[MH]^+$ = 342.0. ^{1}H NMR (400 MHz, MeOH-d_4) δ ppm 8.88 (d, *J*=2.4 Hz, 1 H) 8.58 (d, *J*=2.9 Hz, 1 H) 7.28 - 7.45 (m, 5 H) 5.34 (s, 2 H) 3.17 (d, *J*=6.8 Hz, 2 H) 2.97 (s, 3 H) 1.91 (dquin, *J*=13.4, 6.8, 6.8, 6.8, 6.8 Hz, 1 H) 0.96 (d, *J*=6.4 Hz, 6 H). *Exchangeable protons not observed.*

1-Benzyl-N^5-isopentyl-N^3-methyl-2-oxo-1,2-dihydropyridine-3,5-dicarboxamide (**26**)**.** Prepared from **62** (50 mg, 0.107 mmol) and 3-methylbutan-1-amine (18.72 mg, 0.215 mmol) using the same procedure

as for compound **21**, to give the title compound (6 mg, 16%). LCMS (2 min Formic): Rt = 1.04 min, $[MH]^+$ = 356.3. ^{1}H NMR (400 MHz, MeOH-d_4) δ ppm 8.85 (d, *J*=2.4 Hz, 1 H) 8.56 (d, *J*=2.4 Hz, 1 H) 7.28 - 7.42 (m, 5 H) 5.33 (s, 2 H) 3.35 - 3.42 (m, 2 H) 2.97 (s, 3 H) 1.59 - 1.74 (m, 1 H) 1.45 - 1.55 (m, 2 H) 0.97 (d, *J*=6.4 Hz, 6 H). *Exchangeable protons not observed.*

1-Benzyl-N^3-methyl-2-oxo-N^5-(2-(tetrahydro-2H-pyran-4-yl)ethyl)-1,2-dihydropyridine-3,5-dicarboxamide (**27**)**.** Prepared from **62** (61 mg, 0.131 mmol) and 2-(tetrahydro-2*H*-pyran-4-yl)ethanamine (33.8 mg, 0.262 mmol), using the same procedure as for compound **21**, to give 1-benzyl-*N*^{3}-methyl-2-oxo-*N*^{5}-(2-(tetrahydro-2*H*-pyran-4-yl)ethyl)-1,2-dihydropyridine-3,5-dicarboxamide (9 mg, 0.020 mmol, 16% yield) as a white solid. LCMS (2 min Formic): Rt=0.90 min, $[MH]^+$ = 398.1. ^{1}H NMR (400 MHz, MeOH-d_4) δ ppm 8.86 (d, *J*=2.4 Hz, 1 H) 8.57 (d, *J*=2.9 Hz, 1 H) 7.28 - 7.44 (m, 5 H) 5.34 (s, 2 H) 3.88 - 3.98 (m, 2 H) 3.36 - 3.47 (m, 4 H) 2.97 (s, 3 H) 1.52 - 1.76 (m, 6 H) 1.22 - 1.40 (m, 2 H). *Exchangeable protons not observed.*

1-Benzyl-N^3-methyl-2-oxo-N^5-(2-(piperidin-3-yl)ethyl)-1,2-dihydropyridine-3,5-dicarboxamide, hydrochloride (**28**)*: Step 1.* tert-Butyl 3-(2-(1-benzyl-5-(methylcarbamoyl)-6-oxo-1,6-dihydropyridine-3-carboxamido)ethyl)piperidine-1-carboxylate ***(65)*:** Prepared from **64** (101 mg, 0.353 mmol), and *tert*-butyl 3-(2-aminoethyl)piperidine-1-carboxylate (174 mg, 0.762 mmol) using the same procedure as for **20**, to give *tert*-butyl 3-(2-(1-benzyl-5-(methylcarbamoyl)-6-oxo-1,6-dihydropyridine-3-carboxamido)ethyl)piperidine-1-carboxylate (175 mg, 0.282 mmol, 80% yield) as a colourless oil. LCMS (2 min formic):Rt = 1.18 min, $[MH]^+$ = 397.2. ^{1}H NMR (400 MHz, MeOH-d_4) δ ppm 8.45 (d, *J*=2.7 Hz, 1 H) 8.21 (d, *J*=2.7 Hz, 1 H) 7.27 - 7.41 (m, 5 H) 5.23 - 5.37 (ABq, *J*=14.4 Hz, 2 H) 2.97 - 3.11 (m, 3 H) 2.94 (s, 3 H) 2.69 - 2.84 (m, 2 H) 1.87 - 1.99 (m, 1 H) 1.66 - 1.80 (m, 1 H) 1.19 - 1.65 (m, 14 H).

Step 2: *1-Benzyl-N^3-methyl-2-oxo-N^5-(2-(piperidin-3-yl)ethyl)-1,2-dihydropyridine-3,5-dicarboxamide, hydrochloride (***28**)**.** *tert*-Butyl 3-(2-(1-benzyl-5-(methylcarbamoyl)-6-oxo-1,6-dihydropyridine-3-carboxamido)ethyl)piperidine-1-carboxylate (**65**, 146 mg, 0.294 mmol) and TFA (1 mL, 12.98 mmol) were stirred at rt in DCM (4 mL) for 1 h. The reaction mixture was concentrated and loaded onto a 2 g SCX cartridge (pre-conditioned with MeOH) and eluted with MeOH (40 mL) followed by 2M NH_3 in

MeOH (40 mL). The methanolic ammonia fractions containing product were combined and concentrated to give 112 mg of a colourless oil. The reaction was purified by MDAP (High pH). Fractions containing the desired product were concentrated to give 1-benzyl-N^3-methyl-2-oxo-N^5-(2-(piperidin-3-yl)ethyl)-1,2-dihydropyridine-3,5-dicarboxamide (93 mg, 0.211 mmol, 72% yield). The yellow oil was dissolved in 1 mL MeOH and 1M HCl in diethyl ether (0.23 mL, 0.230 mmol) was added and the solvent removed to afford 1-benzyl-N^3-methyl-2-oxo-N^5-(2-(piperidin-3-yl)ethyl)-1,2-dihydropyridine-3,5-dicarboxamide, hydrochloride (97 mg, 0.202 mmol, 69% yield) as a white solid. LCMS (2 min formic): Rt = 0.54 min, $[MH]^+$ = 397.2. ^{1}H NMR (400 MHz, DMSO-d_6) δ ppm 9.39 (br q, *J*=4.7 Hz, 1 H) 8.45 (d, *J*=2.4 Hz, 1 H) 8.34 (d, *J*=2.4 Hz, 1 H) 7.71 - 7.91 (m, 3 H) 7.29 - 7.42 (m, 5 H) 5.25 - 5.34 (ABq, *J*=14.2 Hz, 2 H) 3.90 (br s, 2 H) 2.95 - 3.12 (m, 1 H) 2.74 - 2.90 (m, 6 H) 1.78 - 1.88 (m, 1 H) 1.54 - 1.73 (m, 2 H) 1.36 - 1.54 (m, 3 H) 1.15 - 1.32 (m, 1 H).

1-Benzyl-N^3-methyl-2-oxo-N^5-(3-(piperidin-3-yl)propyl)-1,2-dihydropyridine-3,5-dicarboxamide hydrochloride (**29**): Step 1: *tert-Butyl 3-(3-(1-benzyl-5-(methylcarbamoyl)-6-oxo-1,6-dihydropyridine-3-carboxamido)propyl)piperidine-1-carboxylate* (**66**)**.** Prepared from **64** (123 mg, 0.430 mmol) and *tert*-butyl 3-(3-aminopropyl)piperidine-1-carboxylate (125 mg, 0.516 mmol) using the same procedure as for **20**, to give *tert*-butyl 3-(3-(1-benzyl-5-(methylcarbamoyl)-6-oxo-1,6-dihydropyridine-3-carboxamido)propyl)piperidine-1-carboxylate (188 mg, 0.331 mmol, 77% yield) as a white solid. LCMS (2 min Formic): Rt = 1.20 min, $[MH]^+$ = 511.2. ^{1}H NMR (400 MHz, $CHCl_3$-*d*) δ ppm 9.54 (br d, *J*=4.9 Hz, 1 H) 8.75 (d, *J*=2.9 Hz, 1 H) 8.47 (d, *J*=2.9 Hz, 1 H) 7.32 - 7.41 (m, 5 H) 6.36 (br s, 1 H) 5.27 (s, 2 H) 3.87 - 4.03 (m, 2 H) 3.36 - 3.49 (m, 2 H) 3.00 (d, *J*=4.9 Hz, 3 H) 2.74 - 2.86 (m, 2 H) 2.39 - 2.59 (m, 1 H) 1.76 - 1.92 (m, 1 H) 1.62 - 1.69 (m, 3 H) 1.41 - 1.53 (m, 9 H) 1.18 - 1.36 (m, 3 H) 1.04 - 1.17 (m, 1 H). Step 2: *1-Benzyl-N^3-methyl-2-oxo-N^5-(3-(piperidin-3-yl)propyl)-1,2-dihydropyridine-3,5-dicarboxamide hydrochloride* (**29**)**.** Prepared from **66** (177 mg, 0.347 mmol) using the same deprotection conditions as for **28**, to give 1-benzyl-N^3-methyl-2-oxo-N^5-(3-(piperidin-3-yl)propyl)-1,2-dihydropyridine-3,5-dicarboxamide, hydrochloride (40 mg, 0.081 mmol, 23% yield) as a white solid. LCMS (2 min Formic): Rt = 0.57 min, $[MH]^+$ = 411.2. ^{1}H NMR (400 MHz, DMSO-d_6) δ ppm 9.38 (q, *J*=4.9 Hz, 1 H) 8.78 - 8.86

(m, 2 H) 8.60 (br t, *J*=5.1 Hz, 1 H) 7.28 - 7.40 (m, 5 H) 5.31 (s, 2 H) 3.19 - 3.25 (m, 3 H) 2.92 - 3.08 (m, 3 H) 2.83 (d, *J*=4.9 Hz, 3 H) 2.52 - 2.62 (m, 1 H) 2.19 - 2.39 (m, 1 H) 1.69 - 1.84 (m, 1 H) 1.58 - 1.70 (m, 1 H) 1.34 - 1.58 (m, 4 H) 1.13 - 1.31 (m, 2 H) 0.95 - 1.06 (m, 1 H).

*(+/-)-1-Benzyl-N^3-methyl-N^5-(3-(morpholin-2-yl)propyl)-2-oxo-1,2-dihydropyridine-3,5-dicarboxamide (**30**):* Step 1: *(+/-)-tert-Butyl 2-(3-(1-benzyl-5-(methylcarbamoyl)-6-oxo-1,6-dihydropyridine-3-carboxamido)propyl)morpholine-4-carboxylate* (**63**)**:** Prepared from **62** (25.7 mg, 0.055 mmol) and *tert*-butyl 2-(3-aminopropyl)morpholine-4-carboxylate (18 mg, 0.037 mmol) using the same procedure as for compound **21**, to give *tert*-butyl 2-(3-(1-benzyl-5-(methylcarbamoyl)-6-oxo-1,6-dihydropyridine-3-carboxamido)propyl)morpholine-4-carboxylate (8 mg, 0.012 mmol, 34% yield) as a colourless oil. LCMS (2 min Formic): Rt = 1.07 min, [MH]+ = 513.5. Step 2: *(+/-)-1-Benzyl-N^3-methyl-N^5-(3-(morpholin-2-yl)propyl)-2-oxo-1,2-dihydropyridine-3,5-dicarboxamide* (**30**)**.** *tert*-Butyl 2-(3-(1-benzyl-5-(methylcarbamoyl)-6-oxo-1,6-dihydropyridine-3-carboxamido)propyl)morpholine-4-carboxylate (**63**, 11 mg, 0.017 mmol) and TFA (0.1 mL, 1.298 mmol) were stirred at rt in dichloromethane (0.4 mL) for 30 min. The reaction mixture was then concentrated and loaded onto a 500 mg SCX cartridge (pre-conditioned with MeOH) and eluted with MeOH (4 CV's) followed by 2M NH_3 in MeOH (4 CV's). The ammonia fractions containing product were combined and concentrated to give 15 mg of a colourless oil. This oil was purified by MDAP (High pH). The appropriate fractions were concentrated to give (+/-)-1-benzyl-*N^3*-methyl-*N^5*-(3-(morpholin-2-yl)propyl)-2-oxo-1,2-dihydropyridine-3,5-dicarboxamide (2 mg, 4.36 µmol, 25% yield) as a white solid. LCMS (2 min Formic): Rt = 0.54 min, [MH]+ = 413.5. ^{1}H NMR (400 MHz, MeOH-d_4) δ ppm 9.79 (br s, 1 H) 8.85 (d, *J*=2.9 Hz, 1 H) 8.45 - 8.62 (m, 2 H) 7.26 - 7.44 (m, 5 H) 5.34 (s, 2 H) 4.04 (dd, *J*=12.7, 3.4 Hz, 1 H) 3.75 (td, *J*=12.5, 2.4 Hz, 1 H) 3.62 - 3.71 (m, 1 H) 3.34 - 3.44 (m, 2 H) 3.12 - 3.25 (m, 2 H) 3.00 - 3.12 (m, 1 H) 2.97 (s, 3 H) 2.79 (dd, *J*=12.2, 11.2 Hz, 1 H) 1.62 - 1.86 (m, 2 H) 1.51 - 1.61 (m, 2 H). *One exchangeable proton not observed.*

(R)-N^5-Cyclopropyl-N^3-methyl-2-oxo-1-(1-phenylethyl)-1,2-dihydropyridine-3,5-dicarboxamide (**31**)**:** Step 1: *(R)-Methyl 2-oxo-1-(1-phenylethyl)-1,2-dihydropyridine-3-carboxylate* (***97***)**.** (*R*)-1-

Phenylethanamine (8.93 mL, 70.2 mmol) was added to a stirred solution of methyl 2-oxo-2*H*-pyran-3-carboxylate (**96**, 10.3 g, 66.8 mmol, commercially available from, for example, Sigma-Aldrich) in a mixture of dry DMF (43 mL) and dry THF (173 mL). The resulting dark red solution was stirred for 30 min, under N_2. EDC (16.66 g, 87 mmol) and DMAP (0.506 g, 4.14 mmol) were added and the resulting suspension stirred over the weekend. The reaction mixture was evaporated *in vacuo* to a brown slurry. The residue was partitioned between EtOAc and water and the aqueous layer removed. The organic layer was washed (3x 2 M aq. HCl, 1x brine), dried over $MgSO_4$ and filtered through silica eluting with EtOAc. The filtrate was evaporated *in vacuo* to give the product as a brown oil (12.94 g). LCMS (2 min TFA): Rt = 0.84 min, $[MH]^+$ = 258.1. ^{1}H NMR (400 MHz, DMSO-d_6) δ ppm 7.97 - 8.01 (m, 1 H) 7.94 (dd, *J*=6.8, 2.4 Hz, 1 H) 7.25 - 7.41 (m, 5 H) 6.34 (t, *J*=6.8 Hz, 1 H) 6.20 (q, *J*=7.2 Hz, 1 H) 3.74 (s, 3 H) 1.71 (d, *J*=7.3 Hz, 3 H). Step 2*: (R)-Methyl 5-bromo-2-oxo-1-(1-phenylethyl)-1,2-dihydropyridine-3-carboxylate* (**131**). NBS (10.74 g, 60.4 mmol) was added in one portion to a dark brown solution of (*R*)-methyl 2-oxo-1-(1-phenylethyl)-1,2-dihydropyridine-3-carboxylate (**97**, 12.94 g, 50.3 mmol) in 2-MeTHF (150 mL). The initial suspension became a light brown solution and was stirred for 15 min whereupon it was a dark brown solution. The reaction mixture was washed [3x sat. aq. $NaHCO_3$ (40 mL), 1x aq. 10% sodium thiosulfate (20 mL), 1x brine (10 mL)], dried over $MgSO_4$ and evaporated *in vacuo* to a black oil. The residue was dissolved in toluene (40 mL), filtered through celite, washing with toluene (80 mL) and evaporated *in vacuo* to give the product (19.62 g, 81% yield, 70% purity) as a black oil which was used without further purification. LCMS (2 min TFA): Rt = 1.02 min, $[MH]^+$ = 336.0 & 337.9. Step 3*: (R)-5-Bromo-N-methyl-2-oxo-1-(1-phenylethyl)-1,2-dihydropyridine-3-carboxamide* (**98**). Methylamine solution (74 mL, 40% aq., 855 mmol) was added to a solution of (*R*)-methyl 5-bromo-2-oxo-1-(1-phenylethyl)-1,2-dihydropyridine-3-carboxylate (**131**, 19.2 g, 40.0 mmol) in methanol (133 mL). The resulting solution was heated to 50 °C with a balloon fitted to the top of a condenser. The reaction mixture was stirred for 90 min. The reaction mixture was evaporated *in vacuo* to a black gum that was suspended in EtOAc. The suspension was filtered through silica eluting with EtOAc and the filtrate evaporated to give the product (13.1 g, 83% yield, 85% purity) as a brown

gum. LCMS (2 min TFA): Rt = 1.01 min, $[MH]^+$ = 335.1 & 337.1. ^{1}H NMR (400 MHz, DMSO-d_6) δ ppm 9.45 (br d, *J*=4.4 Hz, 1 H) 8.22 - 8.32 (m, 2 H) 7.25 - 7.47 (m, 5 H) 6.20 (q, *J*=7.2 Hz, 1 H) 2.83 (d, *J*=4.9 Hz, 3 H) 1.79 (d, *J*=6.8 Hz, 3 H). Step 4: *(R)-Methyl 5-(methylcarbamoyl)-6-oxo-1-(1-phenylethyl)-1,6-dihydropyridine-3-carboxylate* (**132**). Xantphos (1.65 g, 2.85 mmol) and palladium(II) acetate (0.877 g, 3.91 mmol) were added to a solution of (*R*)-5-bromo-N-methyl-2-oxo-1-(1-phenylethyl)-1,2-dihydropyridine-3-carboxamide (**98**, 13.1 g, 39.1 mmol), triethylamine (16.34 mL, 117 mmol) and methanol (15.81 mL, 391 mmol) in DMF (220 mL). Carbon monoxide was sparged through the mixture until a brown suspension formed. The reaction was held under a balloon of carbon monoxide and heated to 60 °C for 4 h. The reaction mixture was cooled to rt and sparged with N_2 to remove any residual carbon monoxide. The reaction mixture was filtered through celite, rinsing with EtOAc and the filtrate evaporated *in vacuo* to a black slurry. The residue was partitioned between EtOAc (350 mL) and water (100 mL). The aqueous layer was removed, the organic layer washed (2x water [50 mL], 1x brine [50 mL]), dried over $MgSO_4$ and evaporated *in vacuo* to a black gum. The gum was dissolved in toluene (60 mL) and loaded on to a Biotage 340 g silica column. The column was eluted with cyclohexane:EtOAc (20 -> 66%). The product containing fractions were evaporated to give the product (7.43 g, 58% yield) as a brown gum. LCMS (2 min TFA): Rt = 0.94 min, $[MH]^+$ = 315.2. ^{1}H NMR (400 MHz, DMSO-d_6) δ ppm 9.18 - 9.31 (m, 1 H) 8.68 (d, *J*=2.4 Hz, 1 H) 8.46 (d, *J*=2.4 Hz, 1 H) 7.28 - 7.46 (m, 5 H) 6.21 (q, *J*=7.3 Hz, 1 H) 3.81 (s, 3 H) 2.84 (d, *J*=4.9 Hz, 3 H) 1.81 (d, *J*=6.8 Hz, 3 H). Step 5: *(R)-5-(Methylcarbamoyl)-6-oxo-1-(1-phenylethyl)-1,6-dihydropyridine-3-carboxylic acid* (**133**). Sodium hydroxide (1.891 g, 47.3 mmol) was added to a solution of (*R*)-methyl 5-(methylcarbamoyl)-6-oxo-1-(1-phenylethyl)-1,6-dihydropyridine-3-carboxylate (**132**, 7.43 g, 23.64 mmol) in methanol (70 mL). Water was added to the stirred suspension and the resulting solution stirred overnight. The reaction mixture was evaporated *in vacuo* to a pale brown solid and acidified with 2M aq. HCl (100 mL). Acetone (10 mL) was added and the suspension stirred for 15 min and filtered. The filtercake was washed [water:acetone (1:1, 20 mL), acetone (20 mL)] and dried *in vacuo* to give the product (6.40 g, 86% yield) as a beige solid. LCMS (2 min TFA): Rt = 0.82 min, $[MH]^+$ = 301.0. ^{1}H NMR (400 MHz, DMSO-

d_6) δ ppm 13.21 (br s, 1 H) 9.29 (br d, *J*=4.9 Hz, 1 H) 8.68 (d, *J*=2.4 Hz, 1 H) 8.40 (d, *J*=2.4 Hz, 1 H) 7.23 - 7.52 (m, 5 H) 6.22 (q, *J*=7.2 Hz, 1 H) 2.84 (d, *J*=4.9 Hz, 3 H) 1.80 (d, *J*=7.3 Hz, 3 H). Step 6: *(R)-N^5-Cyclopropyl-N^3-methyl-2-oxo-1-(1-phenylethyl)-1,2-dihydropyridine-3,5-dicarboxamide* (**31**). HATU (95 mg, 0.250 mmol) was added to a solution of (*R*)-5-(methylcarbamoyl)-6-oxo-1-(1-phenylethyl)-1,6-dihydropyridine-3-carboxylic acid (**133**, 50 mg, 0.166 mmol) and DIPEA (0.058 mL, 0.333 mmol) in DMF (0.5 mL). The solution was stirred for 5 min and cyclopropylamine (0.014 mL, 0.200 mmol) added. The resulting solution was stirred for 1 h. The reaction mixture was purified by MDAP (Formic). The product containing fraction was azeotroped *in vacuo* to dryness with EtOH to give a white solid (50 mg, 84% yield). LCMS (2 min TFA): Rt = 0.85 min, $[MH]^+$ = 340.1**.** ^{1}H NMR (400 MHz, DMSO-d_6) δ ppm 9.39 (q, *J*=4.4 Hz, 1 H) 8.80 (d, *J*=2.4 Hz, 1 H) 8.59 (d, *J*=3.4 Hz, 1 H) 8.41 (d, *J*=2.4 Hz, 1 H) 7.35 - 7.44 (m, 2 H) 7.29 - 7.35 (m, 3 H) 6.23 (q, *J*=7.3 Hz, 1 H) 2.73 - 2.87 (m, 4 H) 1.80 (d, *J*=7.3 Hz, 3 H) 0.65 - 0.73 (m, 2 H) 0.51 - 0.58 (m, 2 H). Chiral HPLC (25 cm Chiralcel OJ, col.no. OJOOCE-IF013, eluent: 5% EtOH/heptane, flow rate = 1 mL/min, detection wavelength = 215 nm, RT, sample dissolved in EtOH/heptane): Rt = 12.8 min, *er* = 100 : 0. (Enantiomer, Rt = 17.8 min). **1-***Benzyl-N^5-cyclopropyl-N^3,6-dimethyl-2-oxo-1,2-dihydropyridine-3,5-dicarboxamide* (**32**)**:** Step 1: *Methyl 2-((dimethylamino)methylene)-3-oxobutanoate* (**128**).[85] A solution of methyl 3-oxobutanoate (4640 µL, 43.0 mmol) and DMF-DMA (6050 µL, 45.2 mmol) was heated to 80 °C for 3 h after which TLC (80 % ethyl acetate/cyclohexane) indicated reaction completion. The reaction mixture was evaporated *in vacuo*, and azeotroped with toluene 3 times to remove any residual DMF-DMA. The residual red oil was left to stand overnight, after which time it solidified to give methyl 2-((dimethylamino)methylene)-3-oxobutanoate (5761 mg, 30.3 mmol, 70% yield) as a single unknown geometric isomer (E/Z). LCMS (2 min Formic): Rt = 0.50 min, $[MH]^+$ = 172.1. Step 2: *Dimethyl 6-methyl-2-oxo-1,2-dihydropyridine-3,5-dicarboxylate* (**94**).[74] A mixture of methyl 2-((dimethylamino)methylene)-3-oxobutanoate (**128**, 4600 mg, 26.9 mmol) and methyl 2-cyanoacetate (2371 µl, 26.9 mmol) was stirred for 5 h at 40 °C, then cooled to rt and left to stand over a weekend. The solid reaction mixture was suspended in diethyl ether (50 mL) by sonication and filtered. The filter

cake was washed with diethyl ether (3 x 15 mL) and dried *in vacuo* to yield the desired product dimethyl 6-methyl-2-oxo-1,2-dihydropyridine-3,5-dicarboxylate (5480 mg, 21.90 mmol, 82% yield) as an orange solid. LCMS (2 min Formic): Rt = 0.58 min, $[MH]^+$ = 226.2. Step 3: *Dimethyl 1-benzyl-6-methyl-2-oxo-1,2-dihydropyridine-3,5-dicarboxylate* (**129**). To a stirred solution of dimethyl 6-methyl-2-oxo-1,2-dihydropyridine-3,5-dicarboxylate (**94**, 2000 mg, 8.88 mmol) in DMF (40 mL) was added potassium carbonate (3682 mg, 26.6 mmol) and (bromomethyl)benzene (1.056 mL, 8.88 mmol) and the reaction was heated to 40 °C for 4 h. The reaction mixture was then poured onto water (400 mL) and extracted with ethyl acetate (3 x 100 mL). The combined organics were washed with brine (3 x 50 mL), dried through a hydrophobic frit and evaporated *in vacuo* to yield an orange solid (2.35 g). The residue was loaded in dichloromethane onto a 50 g SNAP cartridge and purified *via* Biotage SP4 flash chromatography, eluting from 17-87% ethyl acetate / cyclohexane. The relevant fractions were combined and evaporated *in vacuo* to yield the desired product - dimethyl 1-benzyl-6-methyl-2-oxo-1,2-dihydropyridine-3,5-dicarboxylate (1034 mg, 3.12 mmol, 35% yield) as an orange solid. LCMS (2 min Formic): Rt = 0.97 min, $[MH]^+$ = 316.1. ^{1}H NMR (400 MHz, $CHCl_3$-*d*) δ ppm 8.78 (s, 1 H) 7.25 - 7.38 (obs. m, 3 H) 7.13 - 7.20 (m, 2 H) 5.50 (br s, 2 H) 3.94 (s, 3 H) 3.87 (s, 3 H) 2.81 (s, 3 H). Step 4: *Methyl 1-benzyl-2-methyl-5-(methylcarbamoyl)-6-oxo-1,6-dihydropyridine-3-carboxylate* (**95**). Methanamine (2M in THF, 7.9 mL, 15.80 mmol) was added to a solution of dimethyl 1-benzyl-6-methyl-2-oxo-1,2-dihydropyridine-3,5-dicarboxylate (**129**, 500 mg, 1.586 mmol) in methanol (5.8 mL) and the resulting solution was heated to 50 °C for 30 min then left to stand at rt overnight. The reaction mixture was evaporated *in vacuo* to yield the crude product as a yellow solid (525 mg). The residue was loaded in dichloromethane onto a 25 g SNAP cartridge and purified *via* Biotage SP4 flash chromatography, eluting from 0 - 50% (3:1 ethyl acetate:ethanol) / cyclohexane. The relevant fractions were combined and evaporated *in vacuo* to yield the desired product methyl 1-benzyl-2-methyl-5-(methylcarbamoyl)-6-oxo-1,6-dihydropyridine-3-carboxylate (430 mg, 1.300 mmol, 82% yield) as a white solid. LCMS (2 min Formic): Rt = 0.95 min, $[MH]^+$ = 315.1. ^{1}H NMR (600 MHz, DMSO-d_6) δ ppm 9.25 (q, *J*=4.3 Hz, 1 H) 8.78 (s, 1 H) 7.32 - 7.37 (m, 2 H) 7.26 - 7.31 (m, 1 H) 7.13 (d, *J*=7.3 Hz, 2 H) 5.51 (br s, 2 H) 3.82 (s, 3 H)

2.83 (d, *J*=4.8 Hz, 3 H) 2.73 (s, 3 H). Step 5: *1-Benzyl-2-methyl-5-(methylcarbamoyl)-6-oxo-1,6-dihydropyridine-3-carboxylic acid* (**130**). Methyl 1-benzyl-2-methyl-5-(methylcarbamoyl)-6-oxo-1,6-dihydropyridine-3-carboxylate (**95**, 420 mg, 1.336 mmol) was suspended in 1,4-dioxane (3.4 mL). Water (3.4 mL) was added, followed by lithium hydroxide (64.0 mg, 2.67 mmol) and the reaction mixture stirred at rt for 1 h 45 min. The reaction mixture was neutralized with 2M HCl and evaporated *in vacuo* to yield 1-benzyl-2-methyl-5-(methylcarbamoyl)-6-oxo-1,6-dihydropyridine-3-carboxylic acid (613 mg, 1.327 mmol, 99% yield) as a white solid which was used crude in the subsequent reaction. LCMS (2 min Formic): Rt = 0.83 min, $[MH]^+$ = 301.1. ^{1}H NMR (400 MHz, DMSO-d_6) δ ppm 12.19 - 14.36 (m, 1 H) 9.28 (q, *J*=4.7 Hz, 1 H) 8.80 (s, 1 H) 7.31 - 7.38 (m, 2 H) 7.24 - 7.31 (m, 1 H) 7.10 - 7.16 (m, 2 H) 5.51 (s, 2 H) 2.83 (d, *J*=4.9 Hz, 3 H) 2.75 (s, 3 H). Step 6: *1-Benzyl-N^5-cyclopropyl-N^3,6-dimethyl-2-oxo-1,2-dihydropyridine-3,5-dicarboxamide* (**32**). To a solution of 1-benzyl-2-methyl-5-(methylcarbamoyl)-6-oxo-1,6-dihydropyridine-3-carboxylic acid (**130**, 120 mg, 0.240 mmol) and HATU (164 mg, 0.432 mmol) in DMF (2.4 mL) was added DIPEA (84 µL, 0.480 mmol) and cyclopropanamine (19.9 µL, 0.287 mmol). The reaction mixture was stirred for 1 h. The reaction mixture was then poured onto water (30 mL) and extracted with ethyl acetate (3 x 10 mL). The ethyl acetate portions were washed with brine (2 x 10 mL) and evaporated *in vacuo* to yield the crude product (162 mg) as a red gum. The residue was loaded in dichloromethane and purified *via* Biotage SP4 flash chromatography, eluting from 12-62% (3:1 ethyl acetate:ethanol) / cyclohexane. The relevant fractions were combined and evaporated *in vacuo*. The residue was taken up in ethyl acetate (30 mL) and washed with water (2 x 30 mL) and brine (10 mL). The organic layer was dried through a hydrophobic frit and evaporated *in vacuo* to yield the desired product, 1-benzyl-N^5-cyclopropyl-N^3,6-dimethyl-2-oxo-1,2-dihydropyridine-3,5-dicarboxamide (63 mg, 0.176 mmol, 74% yield) as an off white solid. LCMS (2 min Formic): Rt = 0.80 min, $[MH]^+$ = 340.2. ^{1}H NMR (400 MHz, DMSO-d_6) δ ppm 9.35 - 9.49 (m, 1 H) 8.52 (d, *J*=3.9 Hz, 1 H) 8.29 (s, 1 H) 7.32 - 7.40 (m, 2 H) 7.25 - 7.32 (m, 1 H) 7.10 - 7.17 (m, 2 H) 5.47 (s, 2 H) 2.75 - 2.87 (m, 4 H) 2.47 (s, 3 H) 0.65 - 0.72 (m, 2 H) 0.49 - 0.55 (m, 2 H).

1-(Cyclohexylmethyl)-N^5-cyclopropyl-N^3-methyl-2-oxo-1,2-dihydropyridine-3,5-dicarboxamide (**33**):: Step 1: *5-Bromo-N-methyl-2-oxo-1,2-dihydropyridine-3-carboxamide* (**67**): Methyl 5-bromo-2-oxo-1,2-dihydropyridine-3-carboxylate (**60**, 2 g, 8.62 mmol) and methylamine (13 mL, 26.0 mmol, 2M in THF) were refluxed under N_2. After 4 h a white precipitate had formed. THF (15 mL) was added and the solution was refluxed for 1 h. Further methylamine (13 mL, 26.0 mmol, 2M in THF) was added and the reaction refluxed for 2 h. Further methylamine (22 mL, 44.0 mmol, 2M in THF) was added and the reaction refluxed overnight. The solution was concentrated to give a yellow solid. This was transferred to 2 x 20 mL microwave vials with methylamine (15 mL, 30.0 mmol, 2M in THF) and THF (15 mL) and both were heated at 80 °C for 1 h. The suspension from the first microwave vial was concentrated, and triturated from diethyl ether to give 5-bromo-*N*-methyl-2-oxo-1,2-dihydropyridine-3-carboxamide (**67**, 880 mg, 38% yield, 85% purity). The suspension from the second microwave vial was concentrated and triturated from diethyl ether to give further 5-bromo-*N*-methyl-2-oxo-1,2-dihydropyridine-3-carboxamide (**67**, 880 mg, 40% yield, 90% purity). LCMS (2 min Formic): Rt = 0.50 min, [MH]+ = 231.0, 233.0. ^{1}H NMR (400 MHz, MeOH-d_4) δ ppm 8.38 (d, *J*=2.9 Hz, 1 H) 7.87 (d, *J*=2.9 Hz, 1 H) 2.95 (s, 3 H). *Exchangeable protons not observed.* Step 2: *5-Bromo-1-(cyclohexylmethyl)-N-methyl-2-oxo-1,2-dihydropyridine-3-carboxamide* (**69**). Prepared from **67** (103.4 mg, 0.448 mmol) and (bromomethyl)cyclohexane (0.156 mL, 1.119 mmol) using the same procedure as for **68**, to give 5-bromo-1-(cyclohexylmethyl)-*N*-methyl-2-oxo-1,2-dihydropyridine-3-carboxamide (83.4 mg, 0.255 mmol, 57% yield) as a white solid. LCMS (2 min Formic): Rt = 1.16 min, [MH]$^+$ = 327.1, 329.1. ^{1}H NMR (400 MHz, $CHCl_3$-*d*) δ ppm 9.61 (br s, 1 H) 8.59 (d, *J*=2.9 Hz, 1 H) 7.54 (d, *J*=2.9 Hz, 1 H) 3.83 (d, *J*=7.3 Hz, 2 H) 2.99 (d, *J*=4.9 Hz, 3 H) 1.66 - 1.91 (m, 6 H) 1.14 - 1.33 (m, 3 H) 0.96 - 1.09 (m, 2 H). Step 3: *1-(Cyclohexylmethyl)-N^5-cyclopropyl-N^3-methyl-2-oxo-1,2-dihydropyridine-3,5-dicarboxamide* (**33**). Prepared from **69** (30.2 mg, 0.092 mmol) and cyclopropylamine (0.020 mL, 0.277 mmol), using the same procedure as for **35**, to give 1-(cyclohexylmethyl)-*N^5*-cyclopropyl-*N^3*-methyl-2-oxo-1,2-dihydropyridine-3,5-dicarboxamide (7.4 mg, 0.022 mmol, 24% yield) as a cream solid. LCMS (2 min Formic): Rt = 0.97 min, [MH]$^+$ = 332.3. ^{1}H NMR (400 MHz, $CHCl_3$-*d*) δ ppm 9.67 (br d, *J*=4.4 Hz, 1 H) 8.83

(d, *J*=2.9 Hz, 1 H) 8.35 (d, *J*=2.9 Hz, 1 H) 6.95 (br s, 1 H) 3.93 (d, *J*=7.3 Hz, 2 H) 3.00 (d, *J*=5.4 Hz, 3 H) 2.82 - 2.96 (m, 1 H) 1.64 - 1.92 (m, 6 H) 1.13 - 1.30 (m, 3 H) 0.98 - 1.13 (m, 2 H) 0.82 - 0.95 (m, 2 H) 0.59 - 0.73 (m, 2 H).

(+/-)-N^5-Cyclopropyl-N^3-methyl-2-oxo-1-((tetrahydro-2H-pyran-2-yl)methyl)-1,2-dihydropyridine-3,5-dicarboxamide (**34**). Step 1: *(+/-)-5-Bromo-N-methyl-2-oxo-1-((tetrahydro-2H-pyran-2-yl)methyl)-1,2-dihydropyridine-3-carboxamide* (**70**). Prepared from **67** (99.8 mg, 0.432 mmol) and (±)-2-(bromomethyl)tetrahydro-2*H*-pyran (0.138 mL, 1.080 mmol) using the same procedure as for **68**, to give (±)-5-bromo-*N*-methyl-2-oxo-1-((tetrahydro-2*H*-pyran-2-yl)methyl)-1,2-dihydropyridine-3-carboxamide (45.3 mg, 0.138 mmol, 32% yield) as a white solid. LCMS (2 min Formic): Rt = 0.92 min, $[MH]^+$ = 329.1, 331.1. ^{1}H NMR (400 MHz, $CHCl_3$-*d*) δ ppm 9.56 (br s, 1 H) 8.59 (d, *J*=2.9 Hz, 1 H) 7.72 (d, *J*=2.9 Hz, 1 H) 4.36 - 4.43 (m, 1 H) 3.94 - 4.00 (m, 1 H) 3.56 - 3.64 (m, 2 H) 3.29 - 3.40 (m, 1 H) 2.99 (d, *J*=4.9 Hz, 3 H) 1.85 - 1.95 (m, 1 H) 1.73 (br d, *J*=12.2 Hz, 1 H) 1.49 - 1.64 (m, 3 H) 1.23 - 1.37 (m, 1 H). Step 2: *(+/-)-N^5-Cyclopropyl-N^3-methyl-2-oxo-1-((tetrahydro-2H-pyran-2-yl)methyl)-1,2-dihydropyridine-3,5-dicarboxamide* (**34**). Prepared from **70** (45.3 mg, 0.138 mmol) and cyclopropylamine (0.029 mL, 0.413 mmol) using the same procedure as for **35**, to give (±)-N^5-cyclopropyl-N^3-methyl-2-oxo-1-((tetrahydro-2*H*-pyran-2-yl)methyl)-1,2-dihydropyridine-3,5-dicarboxamide (3.7 mg, 0.011 mmol, 8% yield) as a yellow solid. LCMS (2 min High pH): Rt = 0.78 min, $[MH]^+$ = 334.2. ^{1}H NMR (400 MHz, $CHCl_3$-*d*) δ ppm 9.56 (br d, *J*=4.4 Hz, 1 H) 8.76 (d, *J*=2.9 Hz, 1 H) 8.44 (d, *J*=2.9 Hz, 1 H) 6.69 (br s, 1 H) 4.39 (dd, *J*=13.2, 2.4 Hz, 1 H) 3.91 - 3.98 (m, 1 H) 3.76 (dd, *J*=13.2, 8.8 Hz, 1 H) 3.63 (ddt, *J*=11.0, 8.7, 2.4, 2.4 Hz, 1 H) 3.26 - 3.36 (m, 1 H) 3.00 (d, *J*=4.9 Hz, 3 H) 2.83 - 2.97 (m, 1 H) 1.85 - 1.96 (m, 1 H) 1.72 (br d, *J*=12.7 Hz, 1 H) 1.46 - 1.67 (m, 3 H) 1.24 - 1.46 (m, 1 H) 0.81 - 0.94 (m, 2 H) 0.57 - 0.71 (m, 2 H).

(+/-)-N^5-Cyclopropyl-N^3-methyl-2-oxo-1-((tetrahydro-2H-pyran-3-yl)methyl)-1,2-dihydropyridine-3,5-dicarboxamide (**35**): Step 1: *(+/-)-5-Bromo-N-methyl-2-oxo-1-((tetrahydro-2H-pyran-3-yl)methyl)-1,2-dihydropyridine-3-carboxamide* (**68**). 5-Bromo-N-methyl-2-oxo-1,2-dihydropyridine-3-carboxamide (**67**, 102.8 mg, 0.445 mmol), (±)-3-(bromomethyl)tetrahydro-2*H*-pyran (197.6 mg, 1.104 mmol) and

potassium carbonate (134.5 mg, 0.973 mmol) were stirred in methanol (2 mL) and the mixture was heated at 60 °C for 8 days. The reaction mixture was then sealed and left to stand at room temperature for 2.75 days before stirring at 60 °C was resumed for 3 days. Over this time the solvent level was maintained at 2 mL by the addition of further methanol. After allowing to cool to rt, the mixture was partitioned between water (5 mL) and ethyl acetate (5 mL). The aqueous phase was extracted with further ethyl acetate (2 x 5 mL) and the combined organic phases were dried by filtering through a hydrophobic frit. The solvent was evaporated under a stream of nitrogen and the residue was dissolved in a mixture of DMSO/methanol (1:1, 2 mL) and directly purified by MDAP (formic). The required fractions were concentrated *in vacuo* to give (±)-5-bromo-N-methyl-2-oxo-1-((tetrahydro-2H-pyran-3-yl)methyl)-1,2-dihydropyridine-3-carboxamide (71.2 mg, 0.216 mmol, 49% yield) as a cream solid. A small amount of the O-alkylated regioisomer: (±)-5-bromo-N-methyl-2-((tetrahydro-2H-pyran-3-yl)methoxy)nicotinamide (7.2 mg, 0.022 mmol, 5% yield) was also isolated. LCMS (2 min Formic): Rt = 0.77 min, $[MH]^+$ = 329.1, 331.1. ^{1}H NMR (400 MHz, DMSO-d_6) δ ppm 9.47 (br d, *J*=4.9 Hz, 1 H) 8.35 (d, *J*=2.9 Hz, 1 H) 8.28 (d, *J*=2.9 Hz, 1 H) 3.87 - 3.96 (m, 2 H) 3.63 - 3.73 (m, 2 H) 3.31 - 3.39 (m, 1 H) 3.17 (dd, *J*=11.2, 9.3 Hz, 1 H) 2.83 (d, *J*=4.9 Hz, 3 H) 1.99 - 2.09 (m, 1 H) 1.58 - 1.69 (m, 2 H) 1.37 - 1.49 (m, 1 H) 1.21 - 1.31 (m, 1 H). Step 2: *(+/-)-N^5-Cyclopropyl-N^3-methyl-2-oxo-1-((tetrahydro-2H-pyran-3-yl)methyl)-1,2-dihydropyridine-3,5-dicarboxamide* (**35**)**.** A microwave vial was charged with (±)-5-bromo-N-methyl-2-oxo-1-((tetrahydro-2*H*-pyran-3-yl)methyl)-1,2-dihydropyridine-3-carboxamide (**68**, 66.8 mg, 0.203 mmol), cobalt octacarbonyl (17.8 mg, 0.052 mmol), palladium (II) acetate (3.6 mg, 0.016 mmol), xantphos (6.1 mg, 10.54 µmol) and DMAP (52.8 mg, 0.432 mmol). 1,4-Dioxane (2 mL) was added followed by cyclopropylamine (0.043 mL, 0.609 mmol), the vial was sealed and the reaction mixture was heated in a microwave reactor at 75 °C for 30 min. The mixture was diluted with ethyl acetate (5 mL) and filtered using a Celite cartridge (2.5 g) which was eluted with further ethyl acetate (3 x 5 mL). The combined organic fractions were concentrated *in vacuo* to give a brown residue which was dissolved in DMSO/methanol (1:1, 2 mL) and directly purified by MDAP (formic). The required fractions were combined and concentrated *in vacuo* to give the desired product

as a pale brown solid, (±)-N^5-cyclopropyl-N^3-methyl-2-oxo-1-((tetrahydro-2*H*-pyran-3-yl)methyl)-1,2-dihydropyridine-3,5-dicarboxamide (18.1 mg, 0.054 mmol, 27% yield). LCMS (2 min High pH): Rt = 0.69 min, $[MH]^+$ = 334.2. ^{1}H NMR (400 MHz, DMSO-d_6) δ ppm 9.41 (br d, *J*=4.4 Hz, 1 H) 8.77 (d, *J*=2.9 Hz, 1 H) 8.51 (d, *J*=2.9 Hz, 2 H) 3.88 - 4.08 (m, 2 H) 3.59 - 3.77 (m, 2 H) 3.29 - 3.42 (m, 1 H) 3.19 (dd, *J*=11.0, 9.0 Hz, 1 H) 2.84 (d, *J*=4.9 Hz, 3 H) 1.99 - 2.11 (m, 1 H) 1.58 - 1.70 (m, 2 H) 1.36 - 1.50 (m, 1 H) 1.23 - 1.35 (m, 1 H) 0.66 - 0.73 (m, 2 H) 0.54 - 0.60 (m, 2 H).

N^5-Cyclopropyl-N^3-methyl-2-oxo-1-((tetrahydro-2H-pyran-4-yl)methyl)-1,2-dihydropyridine-3,5-dicarboxamide (**36**): Step 1: 5-Bromo-*N*-methyl-2-oxo-1-((tetrahydro-2*H*-pyran-4-yl)methyl)-1,2-dihydropyridine-3-carboxamide (**71**). Prepared from **67** (99.2 mg, 0.429 mmol) and 4-(bromomethyl)tetrahydro-2*H*-pyran (194.4 mg, 1.086 mmol) using the same procedure as for **68**, to give 5-bromo-*N*-methyl-2-oxo-1-((tetrahydro-2*H*-pyran-4-yl)methyl)-1,2-dihydropyridine-3-carboxamide (70.4 mg, 0.214 mmol, 50% yield) as a white solid. LCMS (2 min Formic): Rt = 0.73 min, $[MH]^+$ = 329.1 & 331.1. ^{1}H NMR (400 MHz, DMSO-d_6) δ ppm 9.49 (br d, *J*=4.9 Hz, 1 H) 8.37 (d, *J*=2.9 Hz, 1 H) 8.29 (d, *J*=2.9 Hz, 1 H) 3.92 (d, *J*=7.3 Hz, 2 H) 3.84 (dd, *J*=11.5, 2.7 Hz, 2 H) 3.23 (td, *J*=11.6, 2.2 Hz, 2 H) 2.83 (d, *J*=4.9 Hz, 3 H) 1.98 - 2.14 (m, 1 H) 1.42 (br dd, *J*=12.7, 2.0 Hz, 2 H) 1.27 (qd, *J*=12.2, 4.4 Hz, 2 H). *Step 2: N^5-Cyclopropyl-N^3-methyl-2-oxo-1-((tetrahydro-2H-pyran-4-yl)methyl)-1,2-dihydropyridine-3,5-dicarboxamide* (**36**). Prepared from **71** (65.2 mg, 0.198 mmol) and cyclopropylamine (0.028 mL, 0.396 mmol) using the same procedure as for **35**, to give N^5-cyclopropyl-N^3-methyl-2-oxo-1-((tetrahydro-2*H*-pyran-4-yl)methyl)-1,2-dihydropyridine-3,5-dicarboxamide (13.8 mg, 0.041 mmol, 21% yield) as a cream coloured solid. LCMS (2 min Formic): Rt = 0.63 min, $[MH]^+$ = 334.1. ^{1}H NMR (400 MHz, DMSO-d_6) δ ppm 9.44 (br d, *J*=4.9 Hz, 1 H) 8.78 (d, *J*=2.4 Hz, 1 H) 8.46 - 8.56 (m, 2 H) 3.99 (d, *J*=7.3 Hz, 2 H) 3.84 (br dd, *J*=11.5, 2.7 Hz, 2 H) 3.23 (td, *J*=11.5, 2.0 Hz, 2 H) 2.80 - 2.87 (m, 4 H) 1.98 - 2.13 (m, 1 H) 1.37 - 1.51 (m, 2 H) 1.22 - 1.37 (m, 2 H) 0.63 - 0.73 (m, 2 H) 0.52 - 0.63 (m, 2 H).

Compounds **37**-**39**: Step 1: *Methyl 2-(benzyloxy)-5-bromonicotinate* (**110**). Methyl 5-bromo-2-oxo-1,2-dihydropyridine-3-carboxylate (**60**, 5 g, 21.55 mmol, commercially available from, for example, Sigma-

Aldrich) was dissolved in chloroform (100 mL), then silver carbonate (11.88 g, 43.1 mmol) and benzyl bromide (3.33 mL, 28.0 mmol) were added and the mixture heated at reflux overnight. The mixture was filtered and the filtrate evaporated *in vacuo* to give a pale yellow liquid. This was dissolved in DCM (5 mL) and loaded onto a 50 g silica column, then eluted with 0-50% EtOAc/cyclohexane and the product-containing fractions evaporated *in vacuo* to give methyl 2-(benzyloxy)-5-bromonicotinate (4.65 g, 14.43 mmol, 67% yield) as a colourless solid. LCMS (2 min High pH): Rt = 1.37 min, [MH]+ = 322.1, 324.1. ^{1}H NMR (400 MHz, $CHCl_3$-d) δ ppm 8.35 (d, J=2.7 Hz, 1 H) 8.29 (d, J=2.4 Hz, 1 H) 7.51 (d, J=7.6 Hz, 2 H) 7.38 (t, J=7.5 Hz, 2 H) 7.28 - 7.34 (m, 1 H) 5.51 (s, 2 H) 3.93 (s, 3 H). Step 2: *2-(Benzyloxy)-5-bromonicotinic acid* (**111**). Methyl 2-(benzyloxy)-5-bromonicotinate (**110**, 4.6 g, 14.28 mmol) was dissolved in THF (50 mL) and methanol (50 mL), then LiOH (1.368 g, 57.1 mmol) in water (50 mL) was added and the mixture stirred for 2 h at rt. The solvent was evaporated *in vacuo* and the residue was suspended in water (100 mL) and acidified with 2M HCl to pH 4, then extracted with 10% MeOH/DCM (3 x 100 mL, poor solubility) and the organic layer washed with water, dried and evaporated *in vacuo* to give 2-(benzyloxy)-5-bromonicotinic acid (4.15 g, 13.47 mmol, 94% yield) as a colourless solid. LCMS (2 min High pH): Rt = 0.68 min, [MH]+ = 308.2, 310.0. ^{1}H NMR (400 MHz, DMSO-d_6) δ ppm 8.43 (d, J=2.4 Hz, 1 H) 8.18 (d, J=2.7 Hz, 1 H) 7.47 (d, J=7.1 Hz, 2 H) 7.37 (t, J=7.3 Hz, 2 H) 7.27 - 7.33 (m, 1 H) 5.43 (s, 2 H). Step 3: *2-(Benzyloxy)-5-bromo-N-methylnicotinamide* (**85**). 2-(Benzyloxy)-5-bromonicotinic acid (**111**, 4.2 g, 13.63 mmol) was suspended in DCM (50 mL) and oxalyl chloride (2.386 mL, 27.3 mmol) was added, followed by DMF (0.053 mL, 0.682 mmol) and the reaction mixture was stirred for 2 h at rt, then evaporated *in vacuo*. The residue was dissolved in THF (50 mL), then methanamine (13.63 mL, 2M in THF, 27.3 mmol) was added and the resulting suspension stirred for 2 h at rt, then evaporated *in vacuo*. The residue was dissolved in THF (50 mL) and methanamine (13.63 mL, 2M in THF, 27.3 mmol) was added, then the resulting mixture stirred for 2 h, then evaporated *in vacuo*. The residue was partitioned between EtOAc (100 mL) and water (100 mL), the aq. layer was extracted with further EtOAc (100 mL) and the combined organics washed with brine, dried and evaporated *in vacuo* to give a yellow gummy solid. This was dissolved in a mixture of DCM (20 mL) and

methanol (5 mL) with difficulty, then loaded onto a 50 g silica column, which was then sucked dry using a vacuum line. The column was eluted with 0-100% EtOAc/cyclohexane to give 2-(benzyloxy)-5-bromo-N-methylnicotinamide (2.35 g, 7.32 mmol, 54% yield). LCMS (2 min High pH): Rt = 1.19 min, [MH]+ = 321.1, 323.1. ^{1}H NMR (400 MHz, $CHCl_3$-*d*) δ ppm 8.65 (d, J=2.4 Hz, 1 H) 8.31 (d, J=2.4 Hz, 1 H) 7.87 (br. s., 1 H) 7.33 - 7.48 (m, 5 H) 5.53 (s, 2 H) 2.94 (d, J=4.9 Hz, 3 H). Step 4: *2,4,6-Trichlorophenyl 6-(benzyloxy)-5-(methylcarbamoyl)nicotinate* (**116**). Prepared from **85** (2 g, 6.23 mmol) and 2,4,6-trichlorophenyl formate (2.106 g, 9.34 mmol) using the same procedure as for **62**, to give 2,4,6-trichlorophenyl 6-(benzyloxy)-5-(methylcarbamoyl)nicotinate (1.65 g, 3.54 mmol, 56.9 % yield). LCMS (2 min High pH): Rt = 1.52 min, [MH]+ = 465.3. ^{1}H NMR (400 MHz, $CHCl_3$-*d*) δ ppm 9.31 (d, J=2.4 Hz, 1 H) 9.10 (d, J=2.4 Hz, 1 H) 7.80 (d, J=3.7 Hz, 1 H) 7.38 - 7.53 (m, 7 H) 5.68 (s, 2 H) 2.98 (d, J=4.6 Hz, 3 H). Step 5: *2-(Benzyloxy)-N^5-cyclobutyl-N^3-methylpyridine-3,5-dicarboxamide* (**118**). Prepared from **116** (1.65 g, 3.54 mmol) and cyclobutanamine (0.605 mL, 7.09 mmol) using the same procedure as for **21**, to give 2-(benzyloxy)-N^5-cyclobutyl-N^3-methylpyridine-3,5-dicarboxamide (1.025 g, 3.02 mmol, 85% yield) as a white solid. LCMS (2 min Formic): Rt = 1.01 min, $[MH]^+$ = 340.0. ^{1}H NMR (400 MHz, DMSO-d_6) δ ppm 8.77 (d, *J*=7.8 Hz, 1 H) 8.70 (d, *J*=2.4 Hz, 1 H) 8.51 (d, *J*=2.4 Hz, 1 H) 8.33 (br d, *J*=4.4 Hz, 1 H) 7.46 - 7.51 (m, 2 H) 7.36 - 7.42 (m, 2 H) 7.29 - 7.35 (m, 1 H) 5.56 (s, 2 H) 4.41 (sxt, *J*=8.1 Hz, 1 H) 2.81 (d, *J*=4.9 Hz, 3 H) 2.15 - 2.28 (m, 2 H) 2.00 - 2.14 (m, 2 H) 1.61 - 1.75 (m, 2 H).

Step 6: Standard Procedure for the alkylation of N^5-cyclobutyl-N^3-methyl-2-oxo-1,2-dihydropyridine-3,5-dicarboxamide**.** A stock solution of N^5-cyclobutyl-N^3-methyl-2-oxo-1,2-dihydropyridine-3,5-dicarboxamide (**88**, 475 mg) in DMSO (11.4 mL) was made up. 0.6 mL of this solution was added separately to each of 2-(bromomethyl)pyridine, 3-(bromomethyl)pyridine and 4-(chloromethyl)pyridine, (0.301 mmol). Potassium carbonate (41.6 mg, 0.301 mmol) was added to each of the reaction vessels and the reactions left stirring overnight. The samples were then filtered before purification. The samples were dissolved in DMSO (0.8 mL) and purified by high pH MDAP. The solvent was dried under a stream of nitrogen to give the required products: *N^5-Cyclobutyl-N^3-methyl-2-oxo-1-(pyridin-2-ylmethyl)-1,2-dihydropyridine-3,5-dicarboxamide* (**37**): (13 mg, 34% yield). LCMS (2 min

Formic): Rt = 0.71 min, $[MH]^+$ = 341.0. ^{1}H NMR (600 MHz, DMSO-d_6) δ ppm 9.30 (br d, *J*=4.9 Hz, 1 H) 8.87 (d, *J*=2.6 Hz, 1 H) 8.70 - 8.81 (m, 2 H) 8.47 (d, *J*=4.5 Hz, 1 H) 7.79 (td, *J*=7.7, 1.5 Hz, 1 H) 7.37 (d, *J*=7.9 Hz, 1 H) 7.30 (dd, *J*=6.8, 5.3 Hz, 1 H) 5.39 (s, 2 H) 4.40 (sxt, *J*=7.9 Hz, 1 H) 2.80 (d, *J*=4.9 Hz, 3 H) 2.16 - 2.27 (m, 2 H) 2.00 - 2.13 (m, 2 H) 1.61 - 1.74 (m, 2 H). *N^5-Cyclobutyl-N^3-methyl-2-oxo-1-(pyridin-3-ylmethyl)-1,2-dihydropyridine-3,5-dicarboxamide* (**38**): (12 mg, 32% yield). LCMS (2 min Formic): Rt = 0.51 min, $[MH]^+$ = 341.0. ^{1}H NMR (600 MHz, DMSO-d_6) δ ppm 9.31 (br d, *J*=4.5 Hz, 1 H) 8.83 (d, *J*=1.9 Hz, 2 H) 8.76 (br d, *J*=7.2 Hz, 1 H) 8.63 (s, 1 H) 8.51 (d, *J*=4.2 Hz, 1 H) 7.74 (br d, *J*=7.9 Hz, 1 H) 7.38 (dd, *J*=7.7, 4.7 Hz, 1 H) 5.32 (s, 2 H) 4.39 (sxt, *J*=8.2 Hz, 1 H) 2.82 (d, *J*=4.9 Hz, 3 H) 2.13 - 2.28 (m, 2 H) 2.02 - 2.10 (m, 2 H) 1.62 - 1.74 (m, 2 H). *N^5-Cyclobutyl-N^3-methyl-2-oxo-1-(pyridin-4-ylmethyl)-1,2-dihydropyridine-3,5-dicarboxamide* (**39**): (15 mg, 39% yield). LCMS (2 min Formic): Rt = 0.46 min, $[MH]^+$ = 341.0. ^{1}H NMR (600 MHz, DMSO-d_6) δ ppm 9.28 (br d, *J*=4.5 Hz, 1 H) 8.87 (d, *J*=2.6 Hz, 1 H) 8.71 - 8.81 (m, 2 H) 8.53 (d, *J*=6.0 Hz, 2 H) 7.22 (d, *J*=6.0 Hz, 2 H) 5.33 (s, 2 H) 4.39 (sxt, *J*=8.2 Hz, 1 H) 2.81 (d, *J*=4.9 Hz, 3 H) 2.21 (dtd, *J*=10.8, 8.0, 8.0, 2.6 Hz, 2 H) 2.00 - 2.12 (m, 2 H) 1.61 - 1.75 (m, 2 H).

N^5-Cyclopropyl-1-(2-fluorobenzyl)-N^3-methyl-2-oxo-1,2-dihydropyridine-3,5-dicarboxamide (**40**): Step 1: *5-Bromo-1-(2-fluorobenzyl)-N-methyl-2-oxo-1,2-dihydropyridine-3-carboxamide* (**72**). Prepared from **67** (500 mg, 2.164 mmol) and 1-(bromomethyl)-2-fluorobenzene (0.392 mL, 3.25 mmol) using the same procedure as for **68**, to give the title compound (536.3 mg, 73%) as a pale yellow solid. LCMS (2 min Formic): Rt = 0.98 min, $[MH]^+$ = 338.9 & 340.9. ^{1}H NMR (400 MHz, $CHCl_3$-*d*) δ ppm 9.51 (br s, 1 H) 8.58 (d, *J*=2.9 Hz, 1 H) 7.74 (dd, *J*=2.9, 1.0 Hz, 1 H) 7.44 (td, *J*=7.5, 1.7 Hz, 1 H) 7.37 (tdd, *J*=7.8, 7.8, 5.7, 1.7 Hz, 1 H) 7.11 - 7.21 (m, 2 H) 5.22 (s, 2 H) 2.99 (d, *J*=4.9 Hz, 3 H). *Step 2: N^5-Cyclopropyl-1-(2-fluorobenzyl)-N^3-methyl-2-oxo-1,2-dihydropyridine-3,5-dicarboxamide* (**40**). Prepared from **72** (150 mg, 0.442 mmol) and cyclopropanamine (0.061 mL, 0.885 mmol) using the same procedure as for **35**, to give *N^5*-cyclopropyl-1-(2-fluorobenzyl)-*N^3*-methyl-2-oxo-1,2-dihydropyridine-3,5-dicarboxamide (59.6 mg, 0.174 mmol, 39% yield) as a pale yellow solid. LCMS (2 min Formic): Rt = 0.82 min, $[MH]^+$ = 344.1. ^{1}H NMR (400 MHz, DMSO-d_6) δ ppm 9.29 (q, *J*=4.4 Hz, 1 H) 8.82 (d, *J*=2.9 Hz, 1 H) 8.70 (d, *J*=2.0

Hz, 1 H) 8.57 (br d, *J*=4.4 Hz, 1 H) 7.32 - 7.43 (m, 1 H) 7.16 - 7.26 (m, 3 H) 5.34 (s, 2 H) 2.78 - 2.88 (m, 4 H) 0.67 - 0.73 (m, 2 H) 0.54 - 0.61 (m, 2 H).

N^5-Cyclopropyl-1-(3-fluorobenzyl)-N^3-methyl-2-oxo-1,2-dihydropyridine-3,5-dicarboxamide (**41**): Step 1: *5-Bromo-1-(3-fluorobenzyl)-N-methyl-2-oxo-1,2-dihydropyridine-3-carboxamide* (**73**). Prepared from **67** (150 mg, 0.649 mmol) and 1-(bromomethyl)-3-fluorobenzene (116 µL, 0.946 mmol) using the same procedure as for **68** to give 5-bromo-1-(3-fluorobenzyl)-*N*-methyl-2-oxo-1,2-dihydropyridine-3-carboxamide (135 mg, 0.398 mmol, 61% yield) as a white solid. LCMS (2 min Formic): Rt = 0.96 min, $[MH]^+$ = 338.9, 340.9. ^{1}H NMR (400 MHz, $CHCl_3$-*d*) δ ppm 9.51 (br s, 1 H) 8.61 (d, *J*=2.9 Hz, 1 H) 7.63 (d, *J*=2.9 Hz, 1 H) 7.38 (td, *J*=7.8, 5.9 Hz, 1 H) 7.01 - 7.10 (m, 3 H) 5.18 (s, 2 H) 3.00 (d, *J*=4.9 Hz, 3 H). *Step 2: N^5-Cyclopropyl-1-(3-fluorobenzyl)-N^3-methyl-2-oxo-1,2-dihydropyridine-3,5-dicarboxamide* (**41**). Prepared from **73** (122 mg, 0.360 mmol) and cyclopropylamine (50.7 µL, 0.719 mmol) using the same procedure as for **35**, to give N^5-cyclopropyl-1-(3-fluorobenzyl)-N^3-methyl-2-oxo-1,2-dihydropyridine-3,5-dicarboxamide (38 mg, 0.105 mmol, 29% yield) as a white solid. LCMS (2 min Formic): Rt = 0.84 min, $[MH]^+$ = 344.1. ^{1}H NMR (400 MHz, $CHCl_3$-*d*) δ ppm 9.50 (br s, 1 H) 8.74 (d, *J*=2.4 Hz, 1 H) 8.47 (d, *J*=2.9 Hz, 1 H) 7.31 - 7.40 (m, 1 H) 7.02 - 7.12 (m, 3 H) 6.63 (br s, 1 H) 5.25 (s, 2 H) 3.00 (d, *J*=4.9 Hz, 3 H) 2.85 - 2.94 (m, 1 H) 0.85 - 0.92 (m, 2 H) 0.61 - 0.67 (m, 2 H).

N^5-Cyclopropyl-1-(4-fluorobenzyl)-N^3-methyl-2-oxo-1,2-dihydropyridine-3,5-dicarboxamide (**42**): Step 1: *5-Bromo-1-(4-fluorobenzyl)-N-methyl-2-oxo-1,2-dihydropyridine-3-carboxamide* (**74**). Prepared from **67** (150 mg, 0.649 mmol) and 1-(bromomethyl)-4-fluorobenzene (118 µL, 0.947 mmol). using the same procedure as for **68**, to give 5-bromo-1-(4-fluorobenzyl)-*N*-methyl-2-oxo-1,2-dihydropyridine-3-carboxamide (127 mg, 0.374 mmol, 58% yield) as a white solid. LCMS (2 min Formic): Rt = 0.96 min, $[MH]^+$ = 339.0, 341.0. ^{1}H NMR (400 MHz, $CHCl_3$-*d*) δ ppm 9.53 (br s, 1 H) 8.60 (d, *J*=2.9 Hz, 1 H) 7.62 (d, *J*=2.9 Hz, 1 H) 7.29 - 7.34 (m, 2 H) 7.05 - 7.13 (m, 2 H) 5.16 (s, 2 H) 3.00 (d, *J*=4.9 Hz, 3 H). *Step 2: N^5-Cyclopropyl-1-(4-fluorobenzyl)-N^3-methyl-2-oxo-1,2-dihydropyridine-3,5-dicarboxamide* (**42**): Prepared from **74** (123 mg, 0.363 mmol) and cyclopropylamine (51.1 µL, 0.725 mmol) using the same procedure as for **35**, to give N^5-cyclopropyl-1-(4-fluorobenzyl)-N^3-methyl-2-

oxo-1,2-dihydropyridine-3,5-dicarboxamide (47 mg, 0.130 mmol, 36% yield) as a white solid. LCMS (2 min Formic): Rt = 0.85 min, $[MH]^+$ = 344.2. ^{1}H NMR (400 MHz, $CHCl_3$-*d*) δ ppm 9.52 (br d, *J*=4.4 Hz, 1 H) 8.76 (d, *J*=2.9 Hz, 1 H) 8.49 (d, *J*=2.9 Hz, 1 H) 7.32 - 7.37 (m, 2 H) 7.04 - 7.10 (m, 2 H) 6.74 (br s, 1 H) 5.23 (s, 2 H) 2.99 (d, *J*=5.4 Hz, 3 H) 2.85 - 2.92 (m, 1 H) 0.83 - 0.92 (m, 2 H) 0.60 - 0.67 (m, 2 H).

N^5-Cyclopropyl-N^3-methyl-1-(3-methylbenzyl)-2-oxo-1,2-dihydropyridine-3,5-dicarboxamide (**43**): Step 1: *5-Bromo-N-methyl-1-(3-methylbenzyl)-2-oxo-1,2-dihydropyridine-3-carboxamide* (**75**). Prepared from **67** (300 mg, 1.298 mmol) and 1-(bromomethyl)-3-methylbenzene (0.263 mL, 1.948 mmol) using the same procedure as for **68**, to give 5-bromo-*N*-methyl-1-(3-methylbenzyl)-2-oxo-1,2-dihydropyridine-3-carboxamide (205.8 mg, 0.614 mmol, 47% yield) as a white solid. LCMS (2 min Formic): Rt = 1.05 min, $[MH]^+$ = 335.0 & 337.0. ^{1}H NMR (400 MHz, $CHCl_3$-*d*) δ ppm 9.58 (br s, 1 H) 8.59 (d, *J*=2.9 Hz, 1 H) 7.61 (d, *J*=2.9 Hz, 1 H) 7.27 - 7.32 (obs. m, 1 H) 7.19 (d, *J*=7.8 Hz, 1 H) 7.08 - 7.11 (m, 2 H) 5.16 (s, 2 H) 3.00 (d, *J*=4.9 Hz, 3 H) 2.38 (s, 3 H). *Step 2: N^5-Cyclopropyl-N^3-methyl-1-(3-methylbenzyl)-2-oxo-1,2-dihydropyridine-3,5-dicarboxamide* (**43**). Prepared from **75** (100 mg, 0.298 mmol) and cyclopropanamine (0.041 mL, 0.597 mmol) using the same procedure as for **35**, to give *N^5*-cyclopropyl-*N^3*-methyl-1-(3-methylbenzyl)-2-oxo-1,2-dihydropyridine-3,5-dicarboxamide (52.7 mg, 0.155 mmol, 52% yield) as a yellow solid. LCMS (2 min Formic): Rt = 0.90 min, $[MH]^+$ = 340.1. ^{1}H NMR (400 MHz, $CHCl_3$-*d*) δ ppm 9.55 (br d, *J*=1.5 Hz, 1 H) 8.69 (br t, *J*=2.9 Hz, 1 H) 8.46 (d, *J*=2.4 Hz, 1 H) 7.24 - 7.30 (obs. m, 1 H) 7.10 - 7.19 (m, 3 H) 6.46 (br d, *J*=10.8 Hz, 1 H) 5.22 (s, 2 H) 3.00 (d, *J*=4.9 Hz, 3 H) 2.85 - 2.93 (m, 1 H) 2.36 (s, 3 H) 0.85 - 0.92 (m, 2 H) 0.61 - 0.67 (m, 2 H).

N^5-Cyclopropyl-N^3-methyl-1-(4-methylbenzyl)-2-oxo-1,2-dihydropyridine-3,5-dicarboxamide (**44**): Step 1: *5-Bromo-N-methyl-1-(4-methylbenzyl)-2-oxo-1,2-dihydropyridine-3-carboxamide* (**76**). Prepared from **67** (136 mg, 0.589 mmol) and 1-(bromomethyl)-4-methylbenzene (327 mg, 1.766 mmol) using the same procedure as for **68**, to give 5-bromo-*N*-methyl-1-(4-methylbenzyl)-2-oxo-1,2-dihydropyridine-3-carboxamide (120 mg, 0.358 mmol, 61% yield) as a white solid. LCMS (2 min Formic): Rt = 1.04 min, $[MH]^+$ = 335.0, 337.0. ^{1}H NMR (400 MHz, $CHCl_3$-*d*) δ ppm 9.58 (br d, *J*=1.5 Hz, 1 H) 8.58 (d, *J*=2.9 Hz, 1 H) 7.60 (d, *J*=2.9 Hz, 1 H) 7.21 (app. s, 4 H) 5.15 (s, 2 H) 3.00 (d, *J*=4.9 Hz, 3 H)

2.38 (s, 3 H). *Step 2: N^5-Cyclopropyl-N^3-methyl-1-(4-methylbenzyl)-2-oxo-1,2-dihydropyridine-3,5-dicarboxamide* (**44**). Prepared from **76** (120 mg, 0.358 mmol) and cyclopropylamine (50.5 µL, 0.716 mmol) using the same procedure as for **35**, to give N^5-cyclopropyl-N^3-methyl-1-(4-methylbenzyl)-2-oxo-1,2-dihydropyridine-3,5-dicarboxamide (51 mg, 0.150 mmol, 42% yield) as a white solid. LCMS (2 min Formic): Rt = 0.90 min, $[MH]^+$ = 340.1. ^{1}H NMR (400 MHz, $CHCl_3$-*d*) δ ppm 9.56 (br d, *J*=4.4 Hz, 1 H) 8.73 (d, *J*=2.4 Hz, 1 H) 8.47 (d, *J*=2.9 Hz, 1 H) 7.15 - 7.26 (m, 4 H) 6.66 (br s, 1 H) 5.22 (s, 2 H) 2.99 (d, *J*=4.9 Hz, 3 H) 2.84 - 2.92 (m, 1 H) 2.35 (s, 3 H) 0.83 - 0.91 (m, 2 H) 0.60 - 0.65 (m, 2 H).

N^5-Cyclopropyl-1-(3-methoxybenzyl)-N^3-methyl-2-oxo-1,2-dihydropyridine-3,5-dicarboxamide (**45**): Step 1: *5-Bromo-2-methoxynicotinoyl chloride* (**112**). 5-Bromo-2-methoxynicotinic acid (**83**, 15 g, 64.6 mmol, commercially available from, for example Apollo Scientific) was suspended in DCM (100 mL) and then oxalyl chloride (16.98 mL, 194 mmol) was added, followed by DMF (5.01 mL, 64.6 mmol) and the mixture was stirred for 18 h at rt. The solvent was evaporated *in vacuo* and the residue was redissolved in DCM (100 mL) and evaporated to dryness to give 5-bromo-2-methoxynicotinoyl chloride (16.33 g, 65.2 mmol, quant.) which was used in the next step immediately. ^{1}H NMR (400 MHz, $CHCl_3$-*d*) δ ppm 8.49 (d, J=2.7 Hz, 1 H) 8.44 (d, J=2.4 Hz, 1 H) 4.06 (s, 3 H). Step 2: *5-Bromo-2-methoxy-N-methylnicotinamide* (**84**). 5-Bromo-2-methoxynicotinoyl chloride (**112**, 16 g, 63.9 mmol) was dissolved in 2-methyltetrahydrofuran (100 mL) and Et_3N (8.90 mL, 63.9 mmol) was added, followed by methanamine (31.9 mL, 2M in THF, 63.9 mmol) and the mixture was stirred for 3 h at rt, then added to water (200 mL) and extracted with EtOAc (200 mL). The organic layer was washed with brine (200 mL), dried and evaporated *in vacuo* to give 5-bromo-2-methoxy-*N*-methylnicotinamide (14.8 g, 60.4 mmol, 95% yield) as a pale yellow solid. LCMS (2 min High pH): Rt = 0.83 min, [MH]+ = 245.1, 247.1. ^{1}H NMR (400 MHz, $CHCl_3$-*d*) δ ppm 8.62 (d, J=2.4 Hz, 1 H) 8.29 (d, J=2.4 Hz, 1 H) 7.80 (br. s., 1 H) 4.09 (s, 3 H) 3.02 (d, J=4.9 Hz, 3 H). Step 3: *Methyl 6-methoxy-5-(methylcarbamoyl)nicotinate* (**113**). Carbon monoxide was gently bubbled through a mixture of 5-bromo-2-methoxy-*N*-methylnicotinamide (**84**, 10.6 g, 43.3 mmol), xantphos (1.502 g, 2.60 mmol), triethylamine (12.06 mL, 87 mmol), palladium(II) acetate (0.486 g, 2.163 mmol) and methanol (17.50 mL, 433 mmol) in DMF (150 mL) until a

yellow/green suspension resulted. The suspension was held under a balloon of carbon monoxide and heated to 60 °C for 5 h. LCMS showed significant SM, so the reaction was left overnight (16 h). The reaction mixture was then allowed to cool to rt. The solution was diluted with water (300 mL) and extracted with EtOAc (3 x 300 mL), and the combined organics back extracted with brine (3 x 100 mL). The combined organics were then dried (Na2SO4) and evaporated *in vacuo* to a brown solid. The residue was dissolved in DCM, loaded on to a 340 g Biotage silica SNAP column and eluted with 20 -> 80% EtOAc/cyclohexane. The product containing fractions were evaporated *in vacuo* to a yellow solid - methyl 6-methoxy-5-(methylcarbamoyl)nicotinate (4 g, 17.84 mmol, 41% yield). As the yield was lower than expected, the retained aqueous layer was analysed by LCMS and found to contain further product. This was therefore further extracted with DCM (3 x 100 mL), the combined organics were dried (Na_2SO_4) and concentrated *in vacuo* (for a prolonged period to remove DMF). The aqueous layer was re-analysed by LCMS and found to no longer contain product. The crude product from the organic phase, a yellow solid was taken up in DCM and added to a SNAP silica cartridge (100 g) and eluted with 20 -> 80% EtOAc/cyclohexane The product containing fractions were evaporated *in vacuo* to a yellow solid - methyl 6-methoxy-5-(methylcarbamoyl)nicotinate (1.9 g, 8.47 mmol, 20% yield). LCMS (2 min Formic): Rt = 0.67 min, [MH]+ = 225.1. ^{1}H NMR (400 MHz, DMSO-d_6) δ ppm 8.82 (d, J=2.2 Hz, 1 H) 8.55 (d, J=2.4 Hz, 1 H) 8.30 (br. d, J=3.9 Hz, 1 H) 4.05 (s, 3 H) 3.87 (s, 3 H) 2.82 (d, J=4.6 Hz, 3 H). Step 4: *Methyl 5-(methylcarbamoyl)-6-oxo-1,6-dihydropyridine-3-carboxylate* (**86**). Sodium iodide (4.88 g, 32.6 mmol) was added to a solution of methyl 6-methoxy-5-(methylcarbamoyl)nicotinate (**113**, 3.65 g, 16.28 mmol) in acetonitrile (100 mL) and this solution was stirred for 10 min. TMS-Cl (10.40 mL, 81 mmol) was added dropwise, and the reaction mixture was stirred at rt for 1 h. The reaction was quenched with water (100 mL) and the mixture was extracted five times with a mix of DCM/MeOH and the combined organic phase was dried over a hydrophobic frit and evaporated under vacuum. The crude material was dissolved in DCM and loaded onto a 100 g SNAP silica cartridge and eluted with 0-100% ethanol in EtOAc. The appropriate fractions were evaporated under vacuum, and the desired product was obtained - methyl 5-(methylcarbamoyl)-6-oxo-1,6-dihydropyridine-3-carboxylate

(1.5 g, 7.14 mmol, 44% yield). LCMS (2 min Formic): Rt = 0.47 min, [MH]+ = 211.1. ^{1}H NMR (400 MHz, DMSO-d_6) δ ppm 10.25 (br. s, 1 H) 9.55 (br. d, J=4.4 Hz, 1 H) 8.63 (d, J=2.7 Hz, 1 H) 8.32 (d, J=2.7 Hz, 1 H) 3.80 (s, 3 H) 2.82 (d, J=4.9 Hz, 3 H). Step 5: *Methyl 1-(3-methoxybenzyl)-5-(methylcarbamoyl)-6-oxo-1,6-dihydropyridine-3-carboxylate* (**114**). Methyl 5-(methylcarbamoyl)-6-oxo-1,6-dihydropyridine-3-carboxylate (**86**, 580 mg, 2.76 mmol), 1-(bromomethyl)-3-methoxybenzene (0.580 mL, 4.14 mmol), potassium carbonate (770 mg, 5.57 mmol) and DMF (5 mL) were stirred at 90 °C for 1 h. This was washed with LiCl (20 mL), partitioned between EtOAc (40 mL) and water (40 mL), the aqueous phase was extracted with EtOAc (2 x 40 mL), dried over a hydrophobic frit and concentrated to give a colourless oil. This was purified by chromatography on SiO_2 (Biotage SNAP 100 g cartridge, eluting with 0-100% EtOAc/cyclohexane). The appropriate fractions were concentrated to give methyl 1-(3-methoxybenzyl)-5-(methylcarbamoyl)-6-oxo-1,6-dihydropyridine-3-carboxylate (683 mg, 1.861 mmol, 67% yield) as a white solid. LCMS (2 min Formic): Rt = 0.91 min, [MH]+ = 331.0. ^{1}H NMR (400 MHz, DMSO-d_6) δ ppm 9.22 (br. d, J=4.6 Hz, 1 H) 8.93 (d, J=2.7 Hz, 1 H) 8.70 (d, J=2.7 Hz, 1 H) 7.27 (t, J=7.9 Hz, 1 H) 6.92 (m, J=1.7 Hz, 1 H) 6.84 - 6.90 (m, 2 H) 5.30 (s, 2 H) 3.84 (s, 3 H) 3.73 (s, 3 H) 2.83 (s, 3 H). Step 6: *1-(3-Methoxybenzyl)-5-(methylcarbamoyl)-6-oxo-1,6-dihydropyridine-3-carboxylic acid* (**115**). Methyl 1-(3-methoxybenzyl)-5-(methylcarbamoyl)-6-oxo-1,6-dihydropyridine-3-carboxylate (**114**, 670 mg, 2.028 mmol), lithium hydroxide (146 mg, 6.08 mmol), 1,4-dioxane (3 mL) and water (3 mL) were stirred at rt for 30 min. Acetic acid (1 mL, 17.47 mmol) was added and the solution was partitioned between EtOAc (20 mL) and water (20 mL), the aqueous phase was extracted with EtOAc (2 x 20 mL), dried over a hydrophobic frit and concentrated to give 1-(3-methoxybenzyl)-5-(methylcarbamoyl)-6-oxo-1,6-dihydropyridine-3-carboxylic acid (641 mg, 1.824 mmol, 90% yield) as a white solid. LCMS (2 min Formic): Rt = 0.81 min, [MH]+ = 317.0. ^{1}H NMR (400 MHz, DMSO-d_6) δ ppm 13.09 (br. s, 1 H) 9.26 (br. q, J=4.4, 4.4, 4.4 Hz, 1 H) 8.84 (d, J=2.7 Hz, 1 H) 8.70 (d, J=2.4 Hz, 1 H) 7.27 (t, J=7.9 Hz, 1 H) 6.91 - 6.94 (m, 1 H) 6.84 - 6.90 (m, 2 H) 5.29 (s, 2 H) 3.73 (s, 3 H) 2.82 (d, J=4.9 Hz, 3 H). *Step 7: N^5-Cyclopropyl-1-(3-methoxybenzyl)-N^3-methyl-2-oxo-1,2-dihydropyridine-3,5-dicarboxamide* (**45**). Prepared from **115** (70 mg, 0.221 mmol) using the same procedure as for **20**, to

give N^5-cyclopropyl-1-(3-methoxybenzyl)-N^3-methyl-2-oxo-1,2-dihydropyridine-3,5-dicarboxamide (97 mg, 0.232 mmol, 100 % yield) as a colourless oil. LCMS (2 min Formic): Rt=0.84 min, $[MH]^+$ = 356.2. ^{1}H NMR (400 MHz, MeOH-d_4) δ ppm 8.83 (d, *J*=2.4 Hz, 1 H) 8.55 (d, *J*=2.9 Hz, 1 H) 7.27 (t, *J*=7.8 Hz, 1 H) 6.87 - 6.94 (m, 3 H) 5.28 (s, 2 H) 3.79 (s, 3 H) 2.96 (s, 3 H) 2.78 - 2.86 (m, 1 H) 0.76 - 0.84 (m, 2 H) 0.60 - 0.66 (m, 2 H).

N^5-Cyclopropyl-1-(4-methoxybenzyl)-N^3-methyl-2-oxo-1,2-dihydropyridine-3,5-dicarboxamide (**46**): Step 1: *5-Bromo-1-(4-methoxybenzyl)-N-methyl-2-oxo-1,2-dihydropyridine-3-carboxamide* (**77**). Prepared from **67** (205 mg, 0.887 mmol) and 1-(bromomethyl)-4-methoxybenzene (274 mg, 1.363 mmol), using the same procedure as for **68**, to give 5-bromo-1-(4-methoxybenzyl)-*N*-methyl-2-oxo-1,2-dihydropyridine-3-carboxamide (85 mg, 0.218 mmol, 25% yield) as a white solid. LCMS (2 min Formic): Rt=0.97 min, $[MH]^+$ = 351, 353. ^{1}H NMR (400 MHz, MeOH-d_4) δ ppm 8.42 (d, *J*=2.9 Hz, 1 H) 8.19 (d, *J*=2.9 Hz, 1 H) 7.31 - 7.37 (m, 2 H) 6.90 - 6.95 (m, 2 H) 5.18 (s, 2 H) 3.79 (s, 3 H) 2.95 (s, 3 H). *Exchangeable proton not observed*. Step 2: *N^5-Cyclopropyl-1-(4-methoxybenzyl)-N^3-methyl-2-oxo-1,2-dihydropyridine-3,5-dicarboxamide* (**46**). Prepared from **77** (100 mg, 0.285 mmol) and cyclopropanamine (0.04 mL, 0.577 mmol) using the same procedure as for **35**, to give *N^5*-cyclopropyl-1-(4-methoxybenzyl)-*N^3*-methyl-2-oxo-1,2-dihydropyridine-3,5-dicarboxamide (37 mg, 0.094 mmol, 33% yield) as a white solid. LCMS (2 min Formic): Rt=0.82 min, $[MH]^+$ = 356.1. ^{1}H NMR (400 MHz, MeOH-d_4) δ ppm 9.80 (br d, *J*=3.9 Hz, 1 H) 8.81 (d, *J*=2.4 Hz, 1 H) 8.54 (d, *J*=2.4 Hz, 1 H) 7.32 - 7.36 (m, 2 H) 6.90 - 6.94 (m, 2 H) 5.24 (s, 2 H) 3.79 (s, 3 H) 2.96 (d, *J*=4.9 Hz, 3 H) 2.82 (tt, *J*=7.5, 3.8 Hz, 1 H) 0.76 - 0.84 (m, 2 H) 0.59 - 0.68 (m, 2 H). *One exchangeable proton not observed*.

1-(3-Cyanobenzyl)-N^5-cyclopropyl-N^3-methyl-2-oxo-1,2-dihydropyridine-3,5-dicarboxamide (**47**): Step 1: *5-Bromo-1-(3-cyanobenzyl)-N-methyl-2-oxo-1,2-dihydropyridine-3-carboxamide* (**78**). Prepared from **67** (155 mg, 0.671 mmol) and 3-(bromomethyl)benzonitrile (200 mg, 1.020 mmol) using the same procedure as for **68**, to give 5-bromo-1-(3-cyanobenzyl)-*N*-methyl-2-oxo-1,2-dihydropyridine-3-carboxamide (182 mg, 0.473 mmol, 71% yield) as a white solid. LCMS (2 min formic):Rt = 0.88 min, $[MH]^+$ = 346.0, 348.0. ^{1}H NMR (400 MHz, MeOH-d_4) δ ppm 8.46 (d, *J*=2.9 Hz, 1 H) 8.35 (d, *J*=2.9 Hz, 1

H) 7.80 (s, 1 H) 7.68 - 7.72 (m, 2 H) 7.52 - 7.60 (m, 1 H) 5.29 (s, 2 H) 2.95 (s, 3 H). *Exchangeable proton not observed*. Step 2: *1-(3-Cyanobenzyl)-N^5-cyclopropyl-N^3-methyl-2-oxo-1,2-dihydropyridine-3,5-dicarboxamide* (**47**). Prepared from **78** (92 mg, 0.266 mmol) and cyclopropanamine (0.04 mL, 0.577 mmol), using the same procedure as for **35**, to give 1-(3-cyanobenzyl)-N^5-cyclopropyl-N^3-methyl-2-oxo-1,2-dihydropyridine-3,5-dicarboxamide (13 mg, 0.033 mmol, 13% yield) as a white solid. LCMS (2 min formic): Rt = 0.76 min, $[MH]^+$ = 351.1. ^{1}H NMR (400 MHz, MeOH-d_4) δ ppm 8.84 (d, *J*=2.4 Hz, 1 H) 8.64 (d, *J*=2.9 Hz, 1 H) 7.82 (s, 1 H) 7.69 - 7.73 (m, 2 H) 7.54 - 7.58 (m, 1 H) 5.36 (s, 2 H) 2.94 - 2.97 (m, 3 H) 2.84 (tt, *J*=7.5, 3.8 Hz, 1 H) 0.78 - 0.85 (m, 2 H) 0.62 - 0.68 (m, 2 H). *Exchangeable protons partially evident: 9.70 (br. s, 0.65 H) and 8.45 (br. s, 0.49 H).*

(R)-N^5-Cyclopropyl-1-(3-(1-hydroxyethyl)benzyl)-N^3-methyl-2-oxo-1,2-dihydropyridine-3,5-dicarboxamide* (**48**): Step 1: *2-(Benzyloxy)-N^5-cyclopropyl-N^3-methylpyridine-3,5-dicarboxamide* (**117**). Prepared from **116** (771 mg, 1.656 mmol) and cyclopropanamine (327 mg, 5.73 mmol), using the same procedure as for **21**, to give 2-(benzyloxy)-N^5-cyclopropyl-N^3-methylpyridine-3,5-dicarboxamide (485.2 mg, 1.417 mmol, 86% yield) as a cream solid. LCMS (2 min Formic): Rt = 0.90 min, [MH]+ = 326.3. ^{1}H NMR (400 MHz, $CHCl_3$-*d*) δ ppm 8.88 (d, J=2.7 Hz, 1 H) 8.72 (d, J=2.4 Hz, 1 H) 7.88 (br. s., 1 H) 7.32 - 7.50 (m, 5 H) 6.40 (br. s., 1 H) 5.62 (s, 2 H) 2.87 - 2.99 (m, 4 H) 0.82 - 0.95 (m, 2 H) 0.57 - 0.70 (m, 2 H). *Step 2: N^5-Cyclopropyl-N^3-methyl-2-oxo-1,2-dihydropyridine-3,5-dicarboxamide* (**87**). 2-(Benzyloxy)-N^5-cyclopropyl-N^3-methylpyridine-3,5-dicarboxamide (**117**, 485 mg, 1.491 mmol) was taken up in TFA (5 mL, 64.9 mmol) and heated to 90 °C for 3 h and the reaction was concentrated *in vacuo*. The residue was stirred in Et_2O (20 mL) for 30 min and then left to stand over the weekend. The resulting precipitate was collected by filtration to give N^5-cyclopropyl-N^3-methyl-2-oxo-1,2-dihydropyridine-3,5-dicarboxamide (364.9 mg, 1.474 mmol, 99% yield) as a cream solid. LCMS (2 min Formic): Rt = 0.45 min, [MH]+ = 236.2. ^{1}H NMR (400 MHz, DMSO-d_6) δ ppm 12.79 (br. s., 1 H) 9.41 (d, J=4.9 Hz, 1 H) 8.76 (d, J=2.7 Hz, 1 H) 8.44 (d, J=3.7 Hz, 1 H) 8.19 (d, J=2.7 Hz, 1 H) 2.76 - 2.87 (m, 4 H) 0.64 - 0.71 (m, 2 H) 0.51 - 0.57 (m, 2 H). *Step 3: N^5-Cyclopropyl-1-(3-formylbenzyl)-N^3-methyl-2-oxo-1,2-dihydropyridine-3,5-dicarboxamide* (**89**). Prepared from **87** (300 mg, 1.275 mmol) and 3-

(bromomethyl)benzaldehyde (381 mg, 1.913 mmol) using the same procedure as for **93**, to give N^5-cyclopropyl-1-(3-formylbenzyl)-N^3-methyl-2-oxo-1,2-dihydropyridine-3,5-dicarboxamide (369 mg, 0.992 mmol, 78% yield). LCMS (2 min Formic): Rt = 0.73 min, $[MH]^+$ = 354.1. ^{1}H NMR (400 MHz, DMSO-d_6) δ ppm 10.00 (s, 1 H) 9.32 (q, *J*=4.4 Hz, 1 H) 8.82 (s, 2 H) 8.59 (d, *J*=3.9 Hz, 1 H) 7.82 - 7.88 (m, 2 H) 7.66 - 7.70 (m, 1 H) 7.61 (t, *J*=7.8 Hz, 1 H) 5.39 (s, 2 H) 2.77 - 2.88 (m, 4 H) 0.66 - 0.74 (m, 2 H) 0.53 - 0.60 (m, 2 H). Step 4: *(R*)-N^5-Cyclopropyl-1-(3-(1-hydroxyethyl)benzyl)-N^3-methyl-2-oxo-1,2-dihydropyridine-3,5-dicarboxamide* (**48**). To a solution of N^5-cyclopropyl-1-(3-formylbenzyl)-N^3-methyl-2-oxo-1,2-dihydropyridine-3,5-dicarboxamide (**89**, 183 mg, 0.518 mmol) in THF (10 mL) at -78 °C was added drop-wise a solution of methylmagnesium bromide (3M in diethyl ether, 0.690 mL, 2.071 mmol). The reaction was stirred at -78 °C for 45 min. The reaction was quenched with methanol while still at -78 °C. The solution was warmed to ambient temperature and concentrated *in vacuo*. The residue was suspended in ethyl acetate (50 mL) and washed with water (50 mL). Some insoluble solid remained in the aqueous layer. The aqueous layer was back extracted with ethyl acetate (2 x 20 mL) and the combined organics were washed with brine (10 mL), dried through a hydrophobic frit and evaporated *in vacuo* to yield the crude product as a yellow glass (202 mg). The solid was loaded in the minimum volume of dichloromethane onto a SNAP cartridge (10 g) and purified *via* Biotage SP4 flash chromatography, eluting from 15-75 % (3:1 ethyl acetate:ethanol)/cyclohexane. The relevant fractions were combined and evaporated *in vacuo* to yield a pale yellow gum (145 mg). The sample was dissolved in MeOH:DMSO (2 x 1 mL, 1:1) and purified by MDAP (High pH). The relevant fractions were combined and evaporated *in vacuo* to yield the desired product - N^5-cyclopropyl-1-(3-(1-hydroxyethyl)benzyl)-N^3-methyl-2-oxo-1,2-dihydropyridine-3,5-dicarboxamide (62 mg, 0.156 mmol, 30% yield) as a yellow solid. This product was combined with a second batch of the product prepared in an analogous manner, by sonicating together in diethyl ether and evaporating *in vacuo* to yield - N^5-cyclopropyl-1-(3-(1-hydroxyethyl)benzyl)-N^3-methyl-2-oxo-1,2-dihydropyridine-3,5-dicarboxamide (86.4 mg, 0.222 mmol, 43% yield) as a pale yellow solid. The enantiomers were separated by chiral HPLC: The sample was dissolved in EtOH (2 mL). Injection: 1 mL of the solution was injected onto the

column (Column: 30 mm x 25 cm Chiralpak AD-H (5 µm, Lot No ADH12143-01) which was eluted with 25% EtOH (+0.2% isopropylamine)/heptane (+0.2% isopropylamine), flow rate = 25 mL/min, detection wavelength, 215 nm, 4. Ref 550, 100. Total number of injections = 4. Fractions from 22-25.5 min were bulked and labelled peak 1. Fractions from 25.5-28.5 min were bulked and labelled mix. Fractions from 28.5-35 min were bulked and labelled peak 2. The bulked mix fractions were concentrated *in vacuo* and reprocessed using the prep method above. The bulked pure fractions were concentrated *in vacuo* and then transferred to a weighed flask. Peak 1 was the desired product and was dried *in vacuo* to afford – (*R**)-N^5-cyclopropyl-1-(3-(1-hydroxyethyl)benzyl)-N^3-methyl-2-oxo-1,2-dihydropyridine-3,5-dicarboxamide (36 mg, 0.097 mmol, 19% yield). LCMS (2 min Formic): Rt = 0.71 min, [MH]+ = 370.2. ^{1}H NMR (400 MHz, DMSO-d_6) δ ppm 9.37 (q, *J*=4.4 Hz, 1 H) 8.81 (d, *J*=2.9 Hz, 1 H) 8.71 (d, *J*=2.9 Hz, 1 H) 8.55 (d, *J*=4.4 Hz, 1 H) 7.25 - 7.33 (m, 3 H) 7.14 (dt, *J*=6.8, 2.0 Hz, 1 H) 5.29 (s, 2 H) 5.15 (d, *J*=3.9 Hz, 1 H) 4.63 - 4.78 (m, 1 H) 2.78 - 2.87 (m, 3 H) 1.30 (d, *J*=6.8 Hz, 4 H) 0.65 - 0.74 (m, 2 H) 0.53 - 0.60 (m, 2 H).

N^5-Cyclopropyl-N^3-methyl-1-(3-(2-morpholinoethyl)benzyl)-2-oxo-1,2-dihydropyridine-3,5-dicarboxamide (**49**): Step 1: *2-(3-(Bromomethyl)phenyl)ethanol* (**119**): Borane tetrahydrofuran complex (1M in THF, 4.37 mL, 4.37 mmol) was added dropwise to a THF (20 mL) solution of 2-(3-(bromomethyl)phenyl)acetic acid (500 mg, 2.18 mmol, commercially available from, for example, Fluorochem) at 0 °C. The mixture was allowed to warm to rt and stirred for 2 h. Excess reagent was quenched by the slow addition of MeOH at 0 °C. The reaction mixture was concentrated *in vacuo*, loaded in DCM and purified by Biotage Isolera flash chromatography, using a SNAP 25 g silica cartridge and eluting with a gradient of 0-100% EtOAc / cyclohexane to give after concentration *in vacuo* 2-(3-(bromomethyl)phenyl)ethanol (440 mg, 2.05 mmol, 94% yield) as a brown residue. LCMS (2 min Formic): Rt = 0.87 min, $[MH]^+$ = 216. ^{1}H NMR (400 MHz, DMSO-d_6) δ ppm 7.25 - 7.32 (m, 3 H) 7.13 - 7.21 (m, 1 H) 4.50 - 4.75 (m, 3 H) 3.61 (t, *J*=6.8 Hz, 2 H) 2.72 (t, *J*=7.1 Hz, 2 H). *Step 2: N^5-Cyclopropyl-1-(3-(2-hydroxyethyl)benzyl)-N^3-methyl-2-oxo-1,2-dihydropyridine-3,5-dicarboxamide* (**90**). 2-(3-(Bromomethyl)phenyl)ethanol (**119**, 247 mg, 1.15 mmol) was added to a solution of N^5-cyclopropyl-

N^3-methyl-2-oxo-1,2-dihydropyridine-3,5-dicarboxamide (**87**, 270 mg, 1.15 mmol) and potassium carbonate (317 mg, 2.30 mmol) in THF (15 mL). The reaction mixture was left to stir at rt for 2 h. The reaction mixture was heated to 50 °C and left to stir under N_2 overnight. The reaction mixture was then concentrated *in vacuo* and separated between DCM and water. The organic solution was concentrated *in vacuo*, loaded in DCM and purified by Biotage Isolera flash chromatography using a SNAP 25 g silica cartridge and eluting with a gradient of 0-10% EtOH / EtOAc to give, after concentration *in vacuo* - *N*^{5}-cyclopropyl-1-(3-(2-hydroxyethyl)benzyl)-*N*^{3}-methyl-2-oxo-1,2-dihydropyridine-3,5-dicarboxamide (310 mg, 0.08 mmol, 23% yield) as a white solid. LCMS (2 min Formic): Rt = 0.69 min, $[MH]^+$ = 370. ^{1}H NMR (400 MHz, DMSO-d_6) δ ppm 9.37 (q, *J*=4.7 Hz, 1 H) 8.80 (d, *J*=2.9 Hz, 1 H) 8.70 (d, *J*=2.4 Hz, 1 H) 8.54 (d, *J*=3.9 Hz, 1 H) 7.26 (t, *J*=7.3 Hz, 1 H) 7.14 - 7.20 (m, 2 H) 7.10 (br d, *J*=7.8 Hz, 1 H) 5.26 (s, 2 H) 4.60 (t, *J*=5.4 Hz, 1 H) 3.58 (td, *J*=7.1, 5.4 Hz, 2 H) 2.83 (d, *J*=4.9 Hz, 4 H) 2.70 (t, *J*=7.1 Hz, 2 H) 0.65 - 0.73 (m, 2 H) 0.54 - 0.60 (m, 2 H). *Step 3: N*^{5}*-Cyclopropyl-N*^{3}*-methyl-2-oxo-1-(3-(2-oxoethyl)benzyl)-1,2-dihydropyridine-3,5-dicarboxamide* (**120**). Dess-Martin periodinane (149 mg, 0.35 mmol) was added to a solution of *N*^{5}-cyclopropyl-1-(3-(2-hydroxyethyl)benzyl)-*N*^{3}-methyl-2-oxo-1,2-dihydropyridine-3,5-dicarboxamide (**90**, 100 mg, 0.27 mmol) in DCM (2.5 mL) at 0 °C. The reaction mixture was allowed to warm to rt and stirred for 48 h. The reaction was quenched with water and extracted with DCM. The organic layer was passed through a hydrophobic frit and concentrated *in vacuo* to give *N*^{5}-cyclopropyl-*N*^{3}-methyl-2-oxo-1-(3-(2-oxoethyl)benzyl)-1,2-dihydropyridine-3,5-dicarboxamide (100 mg, 0.27 mmol, quant.) as a white solid, which was used crude in the next step. LCMS (2 min Formic): Rt = 0.70 min, [MH]+ = 368. *Step 4: N*^{5}*-Cyclopropyl-N*^{3}*-methyl-1-(3-(2-morpholinoethyl)benzyl)-2-oxo-1,2-dihydropyridine-3,5-dicarboxamide* (**49**). A mixture of *N*^{5}-cyclopropyl-*N*^{3}-methyl-2-oxo-1-(3-(2-oxoethyl)benzyl)-1,2-dihydropyridine-3,5-dicarboxamide (**120**, 100 mg, 0.27 mmol), morpholine (0.047 mL, 0.54 mmol) and triethylamine (0.152 mL, 1.09 mmol) in DCM (3 mL) were stirred at rt for 45 min. Sodium triacetoxyborohydride (231 mg, 1.09 mmol) was added and the reaction was stirred at rt for 24 h. The reaction mixture was then left to stand for 9 days. Sat. $NaHCO_3$ (aq, 40 mL) was added and the mixture stirred at rt for 15 min. The

organic phase was separated. The aqueous phase was extracted with DCM. The combined organics were passed through a hydrophobic frit and concentrated *in vacuo*. The resulting compound was then purified by MDAP (High pH). The appropriate fractions were combined and evaporated to give N^5-cyclopropyl-N^3-methyl-1-(3-(2-morpholinoethyl)benzyl)-2-oxo-1,2-dihydropyridine-3,5-dicarboxamide (30 mg, 0.07 mmol, 25% yield). LCMS (2 min Formic): Rt = 0.44 min, [MH]+ = 439.4. ^{1}H NMR (400 MHz, DMSO-d_6) δ ppm 9.37 (q, *J*=4.4 Hz, 1 H) 8.80 (d, *J*=2.4 Hz, 1 H) 8.70 (d, *J*=2.4 Hz, 1 H) 8.55 (d, *J*=3.9 Hz, 1 H) 7.26 (t, *J*=7.7 Hz, 1 H) 7.14 - 7.22 (m, 2 H) 7.11 (d, *J*=7.3 Hz, 1 H) 5.26 (s, 2 H) 3.50 - 3.58 (m, 4 H) 2.77 - 2.87 (m, 4 H) 2.67 - 2.76 (m, 2 H) 2.44 - 2.51 (obs. m, 2 H) 2.34 - 2.43 (m, 4 H) 0.65 - 0.74 (m, 2 H) 0.52 - 0.60 (m, 2 H).

N^5-Cyclobutyl-N^3-methyl-1-(3-(methylamino)benzyl)-2-oxo-1,2-dihydropyridine-3,5-dicarboxamide (**50**): Step 1: *N^5-Cyclobutyl-N^3-methyl-2-oxo-1,2-dihydropyridine-3,5-dicarboxamide* (**88**). Prepared from **118** (1.18 g, 3.48 mmol) using the same procedure as for **87**, to give N^5-cyclobutyl-N^3-methyl-2-oxo-1,2-dihydropyridine-3,5-dicarboxamide (718 mg, 2.88 mmol, 83% yield) as a white solid. LCMS (2 min Formic): Rt = 0.55 min, $[MH]^+$ = 250.0. ^{1}H NMR (400 MHz, DMSO-d_6) δ ppm 12.91 (br s, 1 H) 9.53 (br s, 1 H) 8.90 (br s, 1 H) 8.74 (br s, 1 H) 8.34 (br s, 1 H) 4.39 - 4.53 (m, 1 H) 2.95 (br d, *J*=2.5 Hz, 4 H) 2.29 (br s, 2 H) 2.07 - 2.21 (m, 2 H) 1.78 (br s, 2 H). Step 2: *N^5-Cyclobutyl-N^3-methyl-1-(3-(methylamino)benzyl)-2-oxo-1,2-dihydropyridine-3,5-dicarboxamide* (**50**). N^5-Cyclobutyl-N^3-methyl-2-oxo-1,2-dihydropyridine-3,5-dicarboxamide (**88**, 25 mg, 0.100 mmol), (3-(methylamino)phenyl)methanol (20.64 mg, 0.150 mmol) and 2-(tributylphosphoranylidene)acetonitrile (0.083 mL, 0.316 mmol) were combined in toluene (0.75 mL) and the reaction mixture heated in a 5 mL microwave vial at 120 °C for 30 min. The reaction mixture was poured onto water (10 mL) and extracted with ethyl acetate (3 x 8 mL). The combined ethyl acetate layers were washed with brine (10 mL), dried through a hydrophobic frit and evaporated *in vacuo* to yield the crude product (170 mg). The residue was dissolved in MeOH/DMSO (1:1, 2 x 1 mL and purified by MDAP (High pH) The solvent was dried under a stream of nitrogen to leave a white powder. The fractions were combined in dichloromethane, evaporated *in vacuo*, sonicated with

diethyl ether and evaporated once more to yield the product - *N*^{5}-cyclobutyl-*N*^{3}-methyl-1-(3-(methylamino)benzyl)-2-oxo-1,2-dihydropyridine-3,5-dicarboxamide (17 mg, 0.046 mmol, 46% yield) as an off white solid. LCMS (2 min Formic): Rt = 0.72 min, $[MH]^+$ = 369.1. ^{1}H NMR (400 MHz, $CHCl_3$-*d*) δ ppm 9.59 (br d, *J*=3.4 Hz, 1 H) 8.73 (d, *J*=2.9 Hz, 1 H) 8.44 (d, *J*=2.9 Hz, 1 H) 7.18 (t, *J*=7.8 Hz, 1 H) 6.62 (d, *J*=7.3 Hz, 1 H) 6.57 (ddd, *J*=8.1, 2.5, 1.0 Hz, 1 H) 6.52 (t, *J*=2.0 Hz, 1 H) 6.42 (br d, *J*=7.3 Hz, 1 H) 5.17 (s, 2 H) 4.54 (sxt, *J*=8.1 Hz, 1 H) 3.74 - 3.92 (m, 1 H) 3.01 (d, *J*=4.9 Hz, 3 H) 2.83 (s, 3 H) 2.34 - 2.47 (m, 2 H) 1.90 - 2.06 (m, 2 H) 1.71 - 1.87 (m, 2 H).

1-((1H-Benzo[d]imidazol-6-yl)methyl)-N^5*-cyclopropyl-N*^{3}*-methyl-2-oxo-1,2-dihydropyridine-3,5-dicarboxamide* (**51**): Step 1: *6-(Bromomethyl)-1H-benzo[d]imidazole* (**121**). 1*H*-Benzo[d]imidazol-6-yl)methanol (205 mg, 1.384 mmol, commercially available from, for example, Fluorochem) and HBr (3.4 mL, 48% in water, 28.2 mmol) were heated at 80 °C for 30 min. The pH of the solution was adjusted to pH 9 with sodium bicarbonate solution and extracted with EtOAc (2 x 20 mL). The combined organic layers were dried over a hydrophobic frit and concentrated to give 6-(bromomethyl)-1*H*-benzo[d]imidazole (90 mg, 0.341 mmol, 25% yield) as a colourless oil. ^{1}H NMR (400 MHz, MeOH-d_4) δ ppm 8.26 (s, 1 H) 7.65 (s, 1 H) 7.61 (d, *J*=8.3 Hz, 1 H) 7.32 (dd, *J*=8.3, 1.5 Hz, 1 H) 5.66 - 5.66 (m, 1 H) 4.74 (s, 2 H). *Exchangeable proton not observed*. Step 2: *1-((1H-Benzo[d]imidazol-6-yl)methyl)-N*^{5}*-cyclopropyl-N*^{3}*-methyl-2-oxo-1,2-dihydropyridine-3,5-dicarboxamide* (**51**). Prepared from **87** (60 mg, 0.255 mmol) and 6-(bromomethyl)-1*H*-benzo[d]imidazole (**121**, 88 mg, 0.417 mmol), using the same procedure as for **93**, to give 1-((1*H*-benzo[d]imidazol-6-yl)methyl)-*N*^{5}-cyclopropyl-*N*^{3}-methyl-2-oxo-1,2-dihydropyridine-3,5-dicarboxamide (7 mg, 0.017 mmol, 7% yield) as a white solid. LCMS (2 min Formic): Rt = 0.40 min, [MH]+ = 366.2. ^{1}H NMR (400 MHz, MeOH-d_4) δ ppm 9.81 (br d, *J*=4.4 Hz, 1 H) 8.83 (d, *J*=2.9 Hz, 1 H) 8.60 (d, *J*=2.9 Hz, 1 H) 8.36 - 8.36 (m, 1 H) 8.22 (br s, 1 H) 7.69 (s, 1 H) 7.63 (d, *J*=8.3 Hz, 1 H) 7.36 (d, *J*=8.3 Hz, 1 H) 5.45 (s, 2 H) 2.97 (d, *J*=4.9 Hz, 3 H) 2.81 (tt, *J*=7.4, 3.9 Hz, 1 H) 0.76 - 0.84 (m, 2 H) 0.58 - 0.66 (m, 2 H). *One exchangeable proton not observed*.

N^5-Cyclopropyl-N^3-methyl-1-((2-methyl-1H-benzo[d]imidazol-4-yl)methyl)-2-oxo-1,2-dihydropyridine-3,5-dicarboxamide (**52**): Step 1: *Methyl 2-methyl-1H-benzo[d]imidazole-7-carboxylate* (**122**). To 2-methyl-1*H*-benzo[d]imidazole-7-carboxylic acid (500 mg, 2.84 mmol, commercially available from, for example Fluorochem) in methanol (30 mL), sulfuric acid (2.84 mL, 53.3 mmol) was added and the reaction stirred at 65 °C for 4 h. The reaction was then left to sit at rt for 3 days. The reaction mixture was basified with aqueous ammonia at 65 °C. The reaction mixture was extracted with DCM and concentrated under vacuum to give the title compound (410 mg, 2.156 mmol, 76% yield) as a yellow solid. LCMS (2 min Formic): Rt = 0.35 min, $[MH]^+$ = 191.2. ^{1}H NMR (400 MHz, DMSO-d_6) δ ppm 12.19 (br s, 1 H) 7.79 (d, *J*=8.3 Hz, 1 H) 7.75 (d, *J*=8.3 Hz, 1 H) 7.23 (t, *J*=7.8 Hz, 1 H) 3.95 (s, 3 H) 2.56 (s, 3 H). Step 2: *(2-Methyl-1H-benzo[d]imidazol-7-yl)methanol* (**123**). Lithium borohydride (85 mg, 3.88 mmol) and methanol (4 mL, 99 mmol) were dissolved in THF (20 mL). Then, methyl 2-methyl-1*H*-benzo[d]imidazole-7-carboxylate (**122**, 410 mg, 2.156 mmol) in THF (5 mL) was added to the mixture. The reaction was then stirred overnight at 50 °C under an inert atmosphere. The reaction mixture was quenched with water and 2M hydrochloric acid. The reaction mixture was then partitioned between water (50 mL) and ethyl acetate (50 mL). The aqueous layer was then extracted with ethyl acetate (2 x 50 mL). The combined organic layers were passed through a hydrophobic frit and the solvent was removed under vacuum to give mainly unreacted SM. DIBAL-H (1.812 mL, 25% in toluene, 2.69 mmol) was added dropwise to the crude recovered sample (500 mg) in a solution of anhydrous DCM (20 mL) cooled to 0 °C. The reaction was allowed to stir at 0 °C for 1 h. Further DIBAL-H (1.812 mL, 25% in toluene, 2.69 mmol) was added to the solution and the reaction mixture was allowed to stir overnight. Methanol (4 mL, 99 mmol) was added slowly to the solution, followed by Rochelle's salt solution (40 mL) and the mixture allowed to stir for 40 min. The organic layer was separated and the aqueous layer extracted with DCM (2 x 20 mL).The combined organics were washed with water (40 mL) followed by brine (40 mL). The organic layer was passed through a hydrophobic frit and concentrated under vacuum to give the title compound (250 mg, 1.541 mmol, 72% yield) as a white solid which was used crude in the next reaction. LCMS (2 min High pH): Rt = 0.48 min, $[MH]^+$ = 163.1. *Step 3: tert-Butyl 7-*

(hydroxymethyl)-2-methyl-1H-benzo[d]imidazole-1-carboxylate (**124**). To a solution of (2-methyl-1*H*-benzo[d]imidazol-7-yl)methanol (**123**, 250 mg, 1.541 mmol) in acetonitrile (11 mL) and water (2.75 mL) was added Boc_2O (0.501 mL, 2.158 mmol) and sodium bicarbonate (259 mg, 3.08 mmol). The mixture was stirred overnight at rt. The reaction mixture was diluted with ethyl acetate (70 mL) and washed with 10% aqueous citric acid (3 x 25 mL). The aqueous layer was extracted with ethyl acetate (3 x 25 mL). The combined ethyl acetate portions were washed with water (25 mL) and brine (25 mL) before drying through a hydrophobic frit and evaporating *in vacuo* to yield the crude product. The product was loaded in dichloromethane onto a SNAP cartridge (25 g) and purified *via* Biotage SP4 flash chromatography eluting from 0-100% ethyl acetate/cyclohexane. The relevant fractions were evaporated *in vacuo* to yield the title compound (128 mg, 0.488 mmol, 32% yield) as a white solid. LCMS (2 min Formic): Rt = 0.90 min, $[MH]^+$ = 263.1. ^{1}H NMR (400 MHz, DMSO-d_6) δ ppm 7.76 (dd, *J*=8.1, 1.2 Hz, 1 H) 7.34 - 7.40 (m, 1 H) 7.31 (t, *J*=7.8 Hz, 1 H) 5.12 - 5.19 (m, 1 H) 4.88 (d, *J*=5.4 Hz, 2 H) 2.73 (s, 3 H) 1.67 (s, 9 H). *Step 4: tert-Butyl 7-((5-(cyclopropylcarbamoyl)-3-(methylcarbamoyl)-2-oxopyridin-1(2H)-yl)methyl)-2-methyl-1H-benzo[d]imidazole-1-carboxylate* (**91**). DIAD (0.087 mL, 0.446 mmol) was added to a suspension of N^5-cyclopropyl-N^3-methyl-2-oxo-1,2-dihydropyridine-3,5-dicarboxamide (**87**, 50 mg, 0.213 mmol), *tert*-butyl 4-(hydroxymethyl)-2-methyl-1*H*-benzo[d]imidazole-1-carboxylate (**124**, 66.9 mg, 0.255 mmol) and triphenylphosphine (117 mg, 0.446 mmol) in toluene (2 mL). The reaction was stirred at rt under N_2 overnight. Further DIAD (0.087 mL, 0.446 mmol) and triphenylphosphine (117 mg, 0.446 mmol) were added and the reaction stirred for 3 h. The reaction was concentrated, loaded in DCM and purified by chromatography on SiO_2 (Biotage SNAP 10 g cartridge, eluting with 0-100% EtOAc/cyclohexane). The appropriate fractions were concentrated to give the crude product. This was purified further by MDAP (High pH). The appropriate fractions were combined to give the title compound (14 mg, 0.029 mmol, 14% yield). LCMS (2 min Formic): Rt = 1.07 min, $[MH]^+$ = 480.2. ^{1}H NMR (400 MHz, MeOH-d_4) δ ppm 8.80 (d, *J*=2.4 Hz, 1 H) 8.73 (d, *J*=2.4 Hz, 1 H) 7.95 (d, *J*=7.8 Hz, 1 H) 7.34 (t, *J*=7.8 Hz, 1 H) 7.23 (d, *J*=7.3 Hz, 1 H) 5.66 (s, 2 H) 2.94 - 2.97 (m, 3 H) 2.84 (s, 3 H) 2.76 - 2.83 (m, 1 H) 1.73 (s, 9 H). *Exchangeable protons not observed*. *Step*

5: N^5-Cyclopropyl-N^3-methyl-1-((2-methyl-1H-benzo[d]imidazol-4-yl)methyl)-2-oxo-1,2-dihydropyridine-3,5-dicarboxamide (**52**). *tert*-Butyl 7-((5-(cyclopropylcarbamoyl)-3-(methylcarbamoyl)-2-oxopyridin-1(2*H*)-yl)methyl)-2-methyl-1*H*-benzo[d]imidazole-1-carboxylate (**91**, 10 mg, 0.021 mmol) was dissolved in HCl in IPA (0.634 µL, 0.021 mmol) and allowed to stir at rt over 3 days. The reaction mixture was concentrated under vacuum, dissolved in methanol and loaded onto a pre-conditioned SCX column (1 g). Methanol (10 mL) was then passed through the column followed by 2M methanolic ammonia. The methanolic ammonia fractions were combined and concentrated under vacuum to give the title compound (3.7 mg, 9.75 µmol, 47% yield). LCMS (2 min Formic): Rt = 0.42 min, $[MH]^+$ = 380.2. ^{1}H NMR (400 MHz, MeOH-d_4) δ ppm 8.82 (d, *J*=2.9 Hz, 1 H) 8.62 (d, *J*=2.9 Hz, 1 H) 7.46 (br d, *J*=8.3 Hz, 1 H) 7.19 (t, *J*=7.6 Hz, 1 H) 7.09 (d, *J*=7.3 Hz, 1 H) 5.61 (s, 2 H) 2.96 (s, 3 H) 2.79 (tt, *J*=7.2, 3.8 Hz, 1 H) 2.63 (s, 3 H) 0.74 - 0.83 (m, 2 H) 0.58 - 0.65 (m, 2 H). *Exchangeable protons not observed*.

1-((1H-Indazol-4-yl)methyl)-N^5-cyclopropyl-N^3-methyl-2-oxo-1,2-dihydropyridine-3,5-dicarboxamide (**53**): Step 1: *4-(Bromomethyl)-1H-indazole, hydrobromide* (**105**). 1*H*-Indazol-4-yl)methanol (202 mg, 1.363 mmol, commercially available from, for example, Apollo Scientific) and HBr (3.3 mL, 48% in water, 27.4 mmol) were heated at 80 °C for 2 h. The resulting suspension was allowed to cool to rt, filtered under vacuum, washed with cold water and dried in a vacuum oven to give 4-(bromomethyl)-1*H*-indazole, hydrobromide (**105**, 213 mg, 0.657 mmol, 48% yield) as an off white solid. LCMS (2 min Formic): Rt=0.85 min, $[MH]^+$ = 211, 213. ^{1}H NMR (400 MHz, MeOH-d_4) δ ppm 8.43 (d, *J*=1.0 Hz, 1 H) 7.59 (d, *J*=8.3 Hz, 1 H) 7.44 (dd, *J*=8.3, 6.8 Hz, 1 H) 7.28 (d, *J*=7.3 Hz, 1 H) 4.95 (s, 2 H). Step 2: *1-((1H-Indazol-4-yl)methyl)-5-bromo-N-methyl-2-oxo-1,2-dihydropyridine-3-carboxamide* (**79**). Prepared from **67** (130 mg, 0.563 mmol), 4-(bromomethyl)-1*H*-indazole, hydrobromide (**105**, 214 mg, 0.731 mmol), using the same procedure as for **68**, to give 1-((1*H*-indazol-4-yl)methyl)-5-bromo-*N*-methyl-2-oxo-1,2-dihydropyridine-3-carboxamide (234 mg, 0.453 mmol, 81% yield) as a colourless oil which was used crude in the subsequent step. LCMS (2 min Formic): 74% purity, Rt=0.78 min, $[MH]^+$ = 361, 363. ^{1}H NMR (400 MHz, MeOH-d_4) δ ppm 8.42 (d, *J*=2.9 Hz, 1 H) 8.19 (d, *J*=1.0 Hz, 1 H) 8.17 (d, *J*=2.9 Hz, 1

H) 7.53 (d, *J*=8.3 Hz, 1 H) 7.36 (dd, *J*=8.3, 6.8 Hz, 1 H) 7.01 - 7.06 (m, 1 H) 5.57 (s, 2 H) 2.94 (s, 3 H). *Exchangeable protons not observed. Step 3: 1-((1H-Indazol-4-yl)methyl)-N^5-cyclopropyl-N^3-methyl-2-oxo-1,2-dihydropyridine-3,5-dicarboxamide* (**53**). Prepared from **79** (140 mg, 0.388 mmol) and cyclopropanamine (0.05 mL, 0.722 mmol), using the same procedure as for **35**, to give 1-((1*H*-indazol-4-yl)methyl)-*N*^{5}-cyclopropyl-*N*^{3}-methyl-2-oxo-1,2-dihydropyridine-3,5-dicarboxamide (10 mg, 0.025 mmol, 6% yield) as a white solid. LCMS (2 min Formic): Rt=0.67 min, $[MH]^+$ = 366.1. ^{1}H NMR (400 MHz, MeOH-d_4) δ ppm 8.85 (d, *J*=2.9 Hz, 1 H) 8.57 (d, *J*=2.4 Hz, 1 H) 8.53 (br s, 1 H) 8.19 (s, 1 H) 7.56 (d, *J*=8.8 Hz, 1 H) 7.40 (dd, *J*=8.1, 7.1 Hz, 1 H) 7.07 (d, *J*=7.3 Hz, 1 H) 5.69 (s, 2 H) 2.97 (s, 3 H) 2.77 - 2.83 (m, 1 H) 0.75 - 0.81 (m, 2 H) 0.58 - 0.63 (m, 2 H). *Two exchangeable protons not observed*.

1-((1H-Indazol-7-yl)methyl)-N^5-cyclopropyl-N^3-methyl-2-oxo-1,2-dihydropyridine-3,5-dicarboxamide (**54**): Step 1: *7-(Bromomethyl)-1H-indazole, hydrobromide* (**106**). (1*H*-Indazol-7-yl)methanol (250 mg, 1.687 mmol, commercially available from, for example Fluorochem) and HBr (4 mL, 48% in water, 33.2 mmol) were heated at 80 °C for 1 h. The suspension was allowed to cool to rt, filtered under vacuum, washed with cold water and dried in a vacuum oven to give 7-(bromomethyl)-1*H*-indazole, hydrobromide (**106**, 449 mg, 1.307 mmol, 77% yield) as a white solid. LCMS (2 min Formic): Rt=0.84 min, $[MH]^+$ = 211, 213. ^{1}H NMR (400 MHz, DMSO-d_6) δ ppm 8.15 (s, 1 H) 7.77 (dd, *J*=7.8, 1.0 Hz, 1 H) 7.45 (d, *J*=7.8 Hz, 1 H) 7.11 (dd, *J*=8.1, 7.1 Hz, 1 H) 5.05 (s, 2 H). *Exchangeable proton not observed*.

Step 2: *1-((1H-Indazol-7-yl)methyl)-5-bromo-N-methyl-2-oxo-1,2-dihydropyridine-3-carboxamide* (**80**). Prepared from **67** (312 mg, 1.350 mmol), 7-(bromomethyl)-1*H*-indazole, hydrobromide (**106**, 415 mg, 1.421 mmol), using the same procedure as for **68**, to give 1-((1*H*-indazol-7-yl)methyl)-5-bromo-N-methyl-2-oxo-1,2-dihydropyridine-3-carboxamide (396 mg, 0.877 mmol, 65% yield) as an off white solid. LCMS (2 min Formic): Rt=0.86 min, $[MH]^+$ = 361, 363. ^{1}H NMR (400 MHz, MeOH-d_4) δ ppm 8.48 (d, *J*=2.9 Hz, 1 H) 8.29 (d, *J*=2.4 Hz, 1 H) 8.12 (s, 1 H) 7.81 (d, *J*=8.3 Hz, 1 H) 7.34 (d, *J*=7.3 Hz, 1 H) 7.13 - 7.23 (m, 1 H) 5.57 (s, 2 H) 2.97 (s, 3 H). *Exchangeable protons not observed*. Step 3: *1-((1H-Indazol-7-yl)methyl)-N^5-cyclopropyl-N^3-methyl-2-oxo-1,2-dihydropyridine-3,5-dicarboxamide* (**54**). Prepared from **80** (204 mg, 0.565 mmol) and cyclopropanamine (0.08 mL, 1.155 mmol), using the same

procedure as for **35**, to give 1-((1*H*-indazol-7-yl)methyl)-N^5-cyclopropyl-N^3-methyl-2-oxo-1,2-dihydropyridine-3,5-dicarboxamide (38 mg, 0.094 mmol, 17% yield) as a white solid. LCMS (2 min Formic): Rt = 0.75 min, $[MH]^+$ = 366.1. ^{1}H NMR (400 MHz, MeOH-d_4) δ ppm 9.75 (br s, 1 H) 8.86 (d, *J*=2.9 Hz, 1 H) 8.62 (d, *J*=2.4 Hz, 1 H) 8.13 (s, 1 H) 7.80 (d, *J*=8.3 Hz, 1 H) 7.33 (d, *J*=7.3 Hz, 1 H) 7.17 (t, *J*=7.6 Hz, 1 H) 5.63 (s, 2 H) 2.98 (d, *J*=4.9 Hz, 3 H) 2.74 - 2.85 (m, 1 H) 0.71 - 0.83 (m, 2 H) 0.53 - 0.65 (m, 2 H). *Two exchangeable protons not observed*.

1-(Benzofuran-4-ylmethyl)-N^5-cyclopropyl-N^3-methyl-2-oxo-1,2-dihydropyridine-3,5-dicarboxamide (**55**): Step 1: *4-(Bromomethyl)benzofuran* (**125**). Benzofuran-4-ylmethanol (35 mg, 0.236 mmol) was dissolved in diethyl ether (1 mL) and DCM (1 mL) at 0 °C under N_2. PBr_3 (0.04 mL, 0.424 mmol) was added dropwise and the reaction was stirred at rt under N_2. After 30 min, TLC (eluting with 50:50 EtOAc:water) showed complete conversion to a non polar product. The solution was quenched with water (10 mL) and extracted with diethyl ether (3 x 20 mL), dried over a hydrophobic frit and concentrated to give 4-(bromomethyl)benzofuran (41 mg, 0.117 mmol, 49% yield) as a white solid. LCMS (2 min Formic): Rt = 1.15 min, product does not ionise at correct $[MH]^+$. ^{1}H NMR (400 MHz, $CHCl_3$-*d*) δ ppm 7.73 (d, *J*=2.4 Hz, 1 H) 7.47 - 7.54 (m, 1 H) 7.27 - 7.29 (obs. m, 2 H) 6.98 (dd, *J*=2.4, 1.0 Hz, 1 H) 4.77 (s, 2 H). Step 2: *1-(Benzofuran-4-ylmethyl)-N^5-cyclopropyl-N^3-methyl-2-oxo-1,2-dihydropyridine-3,5-dicarboxamide* (**55**). Prepared from **87** (44 mg, 0.187 mmol) and 4-(bromomethyl)benzofuran (**105**, 45 mg, 0.213 mmol) using the same procedure as for **93**, to give 1-(benzofuran-4-ylmethyl)-N^5-cyclopropyl-N^3-methyl-2-oxo-1,2-dihydropyridine-3,5-dicarboxamide (13 mg, 0.032 mmol, 17% yield) as a colourless oil. LCMS (2 min Formic): Rt = 0.88 min, [MH]+ = 366.1. ^{1}H NMR (400 MHz, MeOH-d_4) δ ppm 8.83 (d, *J*=2.4 Hz, 1 H) 8.53 (d, *J*=2.9 Hz, 1 H) 7.81 (d, *J*=2.4 Hz, 1 H) 7.52 (d, *J*=8.3 Hz, 1 H) 7.32 (t, *J*=7.8 Hz, 1 H) 7.19 (d, *J*=7.3 Hz, 1 H) 7.01 (d, *J*=2.0 Hz, 1 H) 5.59 (s, 2 H) 2.97 (s, 3 H) 2.80 (tt, *J*=7.2, 3.8 Hz, 1 H) 0.74 - 0.84 (m, 2 H) 0.56 - 0.65 (m, 2 H). *Exchangeable protons not observed*.

1-((1H-Indol-4-yl)methyl)-N^5-cyclopropyl-N^3-methyl-2-oxo-1,2-dihydropyridine-3,5-dicarboxamide (**56**): Step 1: *Methyl 1-tosyl-1H-indole-4-carboxylate* (**102**). Methyl 1*H*-indole-4-carboxylate (750 mg,

4.28 mmol, commercially available from, for example, Sigma-Aldrich) was dissolved in DMF (13.591 mL) at 0 °C. Sodium hydride (205 mg, 5.14 mmol, 60% dispersion in mineral oil) was added in portions. The reaction was stirred at 0 °C for 10 min before warming to rt and stirring for 30 min. Tosyl-Cl (979 mg, 5.14 mmol) was added and the reaction mixture was stirred at rt for 10 min. The reaction was cooled to 0 °C and quenched by the dropwise addition of water (3.86 mL, 214 mmol), before pouring onto saturated aqueous lithium chloride (140 mL). The product was extracted with ethyl acetate (3 x 30 mL) and the combined organic portions were dried through a hydrophobic frit and evaporated *in vacuo* to yield the crude product (2056 mg). The residue was dry loaded onto a 50 g SNAP silica cartridge and purified *via* Biotage SP4 flash chromatography, eluting from 0-25% ethyl acetate/cyclohexane. The relevant fractions were combined and evaporated *in vacuo* to yield the pure product - methyl 1-tosyl-1*H*-indole-4-carboxylate (**102**, 1039 mg, 3.15 mmol, 74% yield) as a white solid. LCMS (2 min Formic): Rt = 1.30 min, [MH]+ = 330.0. ^{1}H NMR (400 MHz, $CHCl_3$-*d*) δ ppm 8.23 (dt, *J*=8.3, 1.0 Hz, 1 H) 7.99 (dd, *J*=7.8, 1.0 Hz, 1 H) 7.74 - 7.80 (m, 2 H) 7.71 (d, *J*=3.4 Hz, 1 H) 7.33 - 7.42 (m, 2 H) 7.24 (d, *J*=7.8 Hz, 2 H) 3.97 (s, 3 H) 2.36 (s, 3 H). Step 2: *(1-Tosyl-1H-indol-4-yl)methanol* (**103**). A solution of methyl 1-tosyl-1*H*-indole-4-carboxylate (**102**, 1016 mg, 3.08 mmol) in DCM (30 mL) was cooled to -78 °C and DIBAL-H (1M in toluene, 13.57 mL, 13.57 mmol) was added dropwise over 1 h. The reaction mixture was stirred for a further 1.5 h, followed by a further 40 min. The reaction was quenched with methanol (0.125 mL, 3.08 mmol) when still at -78 °C and then allowed to warm to ambient temperature. The reaction was diluted with saturated Rochelle's salt solution (60 mL) and stirred for 16 h. The layers were separated, and the aqueous phase was extracted with dichloromethane (2 x 50 mL). The combined organic layers were dried through a hydrophobic frit and evaporated *in vacuo* to yield the crude product (913 mg). The residue was loaded in dichloromethane onto a 50 g SNAP cartridge and purified via Biotage SP4, eluting from 15-75% ethyl acetate/cyclohexane. The relevant fractions were combined and evaporated *in vacuo* to yield the pure product - (1-tosyl-1*H*-indol-4-yl)methanol (**103**, 901 mg, 2.84 mmol, 92% yield) as a white solid. LCMS (2 min Formic): Rt = 1.07 min, [M+Na]+ = 324.0. ^{1}H NMR (400 MHz, $CHCl_3$-*d*) δ ppm 7.97 (d, *J*=8.3 Hz,

1 H) 7.75 - 7.82 (m, 2 H) 7.62 (d, *J*=3.4 Hz, 1 H) 7.29 - 7.35 (m, 1 H) 7.21 - 7.27 (m, 3 H) 6.81 - 6.87 (m, 1 H) 4.91 (d, *J*=5.4 Hz, 2 H) 2.36 (s, 3 H) 1.69 (t, *J*=5.9 Hz, 1 H). Step 3: *4-(Bromomethyl)-1-tosyl-1H-indole* (**104**). (1-Tosyl-1*H*-indol-4-yl)methanol (**103**, 500 mg, 1.659 mmol) and HBr (3995 µL, 48% in water, 33.2 mmol) were heated at 80 °C monitoring by LCMS. Initial LCMS indicated formation of product and the reaction was heated for a further 4 h. The reaction mixture was poured onto water (10 mL) and the product was extracted with dichloromethane (3 x 20 mL). The combined organic portions were dried through a hydrophobic frit and evaporated *in vacuo* to yield the crude product - 4-(bromomethyl)-1-tosyl-1*H*-indole (**104**, 564 mg, 1.316 mmol, 79% yield) as a purple solid which was used without further purification. LCMS (2 min Formic): Rt = 1.35 min, [M-H]- = 362.0, 364.0. ^{1}H NMR (400 MHz, $CHCl_3$-*d*) δ ppm 7.90 - 8.04 (m, 1 H) 7.72 - 7.86 (m, 2 H) 7.68 (d, *J*=3.9 Hz, 1 H) 7.21 - 7.29 (m, 4 H) 6.85 (d, *J*=4.4 Hz, 1 H) 4.71 (s, 2 H) 2.37 (s, 3 H). Step 4: *N^5-Cyclopropyl-N^3-methyl-2-oxo-1-((1-tosyl-1H-indol-4-yl)methyl)-1,2-dihydropyridine-3,5-dicarboxamide* (**93**). To a solution of *N^5*-cyclopropyl-*N^3*-methyl-2-oxo-1,2-dihydropyridine-3,5-dicarboxamide (**87,** 100 mg, 0.425 mmol) in DMF (4.2 mL) was added potassium carbonate (118 mg, 0.850 mmol) and 4-(bromomethyl)-1-tosyl-1*H*-indole (**104**, 232 mg, 0.638 mmol) and the reaction was stirred at rt for 2.5 h. The reaction was quenched with water (77 µL, 4.25 mmol), poured onto water (60 mL) and the aqueous layer extracted with ethyl acetate (3 x 15 mL). The combined organic layers were washed with brine (2 x 5 mL), dried through a hydrophobic frit and evaporated *in vacuo*. The residue was loaded in dichloromethane onto a 25 g SNAP cartridge and purified *via* Biotage SP4 flash chromatography, eluting from 12-62 % (3:1 ethyl acetate : ethanol) / cyclohexane. The relevant fractions were combined and evaporated *in vacuo* to yield *N^5*-cyclopropyl-*N^3*-methyl-2-oxo-1-((1-tosyl-1*H*-indol-4-yl)methyl)-1,2-dihydropyridine-3,5-dicarboxamide (226 mg, 0.414 mmol, 97 % yield). LCMS (2 min Formic): Rt = 1.11 min, [MH]+ = 519.3. ^{1}H NMR (400 MHz, $CHCl_3$-*d*) δ ppm 9.46 - 9.63 (m, 1 H) 8.70 (d, *J*=2.4 Hz, 1 H) 8.40 (d, *J*=2.9 Hz, 1 H) 8.00 (d, *J*=8.3 Hz, 1 H) 7.75 - 7.88 (m, 2 H) 7.64 (d, *J*=3.4 Hz, 1 H) 7.28 - 7.34 (m, 1 H) 7.26 (d, *J*=7.8 Hz, 2 H) 7.11 (d, *J*=6.8 Hz, 1 H) 6.78 (dd, *J*=3.9, 1.0 Hz, 1 H) 6.56 (br s, 1 H) 5.47 (s, 2 H) 2.99 (d, *J*=4.9 Hz, 3 H) 2.79 - 2.88 (m, 1 H) 2.37 (s, 3 H) 0.78 - 0.90 (m, 2 H) 0.53 - 0.66 (m, 2 H). Step 5: *1-((1H-Indol-4-*

yl)methyl)-N^5-cyclopropyl-N^3-methyl-2-oxo-1,2-dihydropyridine-3,5-dicarboxamide (**56**). To a solution of N^5-cyclopropyl-N^3-methyl-2-oxo-1-((1-tosyl-1*H*-indol-4-yl)methyl)-1,2-dihydropyridine-3,5-dicarboxamide (**93**, 216 mg, 0.417 mmol) in methanol (771 µL) and THF (1543 µL) stirred at room temp was added solid cesium carbonate (543 mg, 1.666 mmol) in one charge. The reaction mixture was stirred at 70 °C for 30 min. The reaction mixture was concentrated *in vacuo* and taken up in ethyl acetate (15 mL) and water (30 mL). The aqueous layer was extracted with ethyl acetate (2 x 15 mL) and the combined organics were washed with brine (10 mL), dried through a hydrophobic frit and evaporated *in vacuo* to yield the desired product 1-((1*H*-indol-4-yl)methyl)-N^5-cyclopropyl-N^3-methyl-2-oxo-1,2-dihydropyridine-3,5-dicarboxamide (108 mg, 0.282 mmol, 68 % yield). LCMS (2 min High pH): Rt = 0.82 min, [MH]+ = 365.2. HRMS ($C_{20}H_{20}N_4O_3$): $[M+H]^+$ calculated 365.1614, found 365.1606. ^{1}H NMR (400 MHz, DMSO-d_6) δ ppm 11.25 (br s, 1 H) 9.45 (q, *J*=4.6 Hz, 1 H) 8.81 (d, *J*=2.9 Hz, 1 H) 8.58 (d, *J*=2.9 Hz, 1 H) 8.54 (d, *J*=3.9 Hz, 1 H) 7.35 - 7.41 (m, 2 H) 7.04 - 7.10 (m, 1 H) 6.83 (d, *J*=6.4 Hz, 1 H) 6.49 - 6.54 (m, 1 H) 5.55 (s, 2 H) 2.84 (d, *J*=4.9 Hz, 3 H) 2.78 (tq, *J*=7.4, 3.9 Hz, 1 H) 0.63 - 0.69 (m, 2 H) 0.51 - 0.57 (m, 2 H). ^{13}C NMR (176 MHz, DMSO-d_6) δ ppm 164.3, 163.7, 161.7, 144.4, 141.0, 136.4, 127.5, 126.5, 126.3, 121.4, 119.6, 118.7, 113.7, 112.0, 99.5, 51.0, 26.4, 23.5, 6.0 (2C).

1-((1H-Indol-7-yl)methyl)-N^5-cyclopropyl-N^3-methyl-2-oxo-1,2-dihydropyridine-3,5-dicarboxamide (**57**): Step 1: *Methyl 1-tosyl-1H-indole-7-carboxylate* (**107**). Methyl 1*H*-indole-7-carboxylate (1 g, 5.71 mmol, commercially available from, for example, Apollo Scientific) was dissolved in DMF (18.12 mL) at 0 °C. Sodium hydride (0.251 g, 60% dispersion in mineral oil, 6.28 mmol) was added in portions. The reaction was stirred at 0 °C for 10 min before warming to rt and stirring for 30 min. Tosyl-Cl (1.197 g, 6.28 mmol) was added and the reaction mixture was stirred for 2 h. The reaction was cooled back down to 0 °C and a further portion of sodium hydride (0.114 g, 60% dispersion in mineral oil, 2.85 mmol) was added portionwise. The reaction mixture was stirred for 10 min before warming to rt and stirring for 30 min. An additional portion of tosyl-Cl (0.544 g, 2.85 mmol) was added at this point. The reaction was stirred for a further 1.5 h. The reaction was quenched by the dropwise addition of water (5.14 mL, 285 mmol). The reaction was poured onto saturated aqueous lithium chloride (100 mL) and

the product was extracted with ethyl acetate (3 x 30 mL). The combined organic portions were dried through a hydrophobic frit and evaporated *in vacuo* to yield the crude product (2158 mg). The residue was dry loaded onto a 50 g SNAP silica cartridge and purified *via* Biotage SP4 flash chromatography, eluting from 0 - 25% ethyl acetate/ cyclohexane. The relevant fractions were combined and evaporated *in vacuo* to yield the pure product - methyl 1-tosyl-1*H*-indole-7-carboxylate (**107**, 1159 mg, 3.52 mmol, 62% yield) as a yellow solid. LCMS (2 min Formic): Rt = 1.18 min, $[MH]^+$ = 330.0. ^{1}H NMR (400 MHz, $CHCl_3$-*d*) δ ppm 7.57 - 7.63 (m, 3 H) 7.53 (dd, *J*=7.3, 1.0 Hz, 1 H) 7.50 (d, *J*=3.4 Hz, 1 H) 7.28 - 7.33 (m, 1 H) 7.15 - 7.21 (m, 2 H) 6.69 (d, *J*=3.9 Hz, 1 H) 3.96 (s, 3 H) 2.35 (s, 3 H). Step 2: *(1-Tosyl-1H-indol-7-yl)methanol* (**108**). A solution of methyl 1-tosyl-1*H*-indole-7-carboxylate (**107**, 1117 mg, 3.39 mmol) in DCM (33.913 mL) was cooled to -78 °C and DIBAL-H (14.92 mL, 1M in toluene, 14.92 mmol) was added dropwise over 15 min. The reaction mixture was stirred for 1.5 h more. The reaction was quenched with methanol (6.04 mL, 149 mmol) when still at -78 °C and then allowed to warm to ambient temperature. The reaction was diluted with Rochelle's salt solution (60 mL) and stirred for 16 h. The layers were separated, and the aqueous phase was extracted with dichloromethane (2 x 50 mL). The combined organic layers were dried through a hydrophobic frit and evaporated *in vacuo* to yield the crude product (1065 mg). The residue was loaded in dichloromethane and purified *via* Biotage SP4, eluting from 10 - 50% ethyl acetate/cyclohexane. The relevant fractions were combined and evaporated *in vacuo* to yield a clear oil. The product was air dried to yield (1-tosyl-1*H*-indol-7-yl)methanol (**108**, 901 mg, 2.84 mmol, 84% yield). LCMS (2 min Formic): Rt = 1.07 min, $[M-H]^-$ = 300.1. ^{1}H NMR (400 MHz, $CHCl_3$-*d*) δ ppm 7.72 (d, *J*=3.9 Hz, 1 H) 7.53 - 7.58 (m, 2 H) 7.51 (dd, *J*=7.6, 1.2 Hz, 1 H) 7.36 (dd, *J*=7.3, 1.5 Hz, 1 H) 7.20 - 7.30 (obs. m, 3 H) 6.75 (d, *J*=3.4 Hz, 1 H) 4.91 (d, *J*=7.3 Hz, 2 H) 3.23 (t, *J*=7.3 Hz, 1 H) 2.38 (s, 3 H). Step 3: *7-(Bromomethyl)-1-tosyl-1H-indole* (**109**). (1-Tosyl-1*H*-indol-7-yl)methanol (**108**, 500 mg, 1.659 mmol) and HBr (3995 µL, 48% in water, 33.2 mmol) were heated at 80 °C for 1 h. The reaction mixture was filtered through a sinter funnel and washed with water. The collected precipitate was dissolved in dichloromethane (100 mL), dried through a hydrophobic frit and evaporated *in vacuo* to yield the crude product 7-(bromomethyl)-1-tosyl-1*H*-indole (**109**, 602 mg,

1.322 mmol, 80 % yield) as a deep red oil which was used without further purification. LCMS (2 min Formic): Rt = 1.34 min, $[MH]^+$ = 364.0, 366.0. ^{1}H NMR (400 MHz, $CHCl_3$-*d*) δ ppm 7.75 (d, *J*=3.9 Hz, 1 H) 7.58 - 7.64 (m, 2 H) 7.49 (dd, *J*=7.8, 1.0 Hz, 1 H) 7.43 (dd, *J*=7.6, 1.2 Hz, 1 H) 7.21 - 7.29 (obs. m, 3 H) 6.72 (d, *J*=3.4 Hz, 1 H) 5.18 (s, 2 H) 2.37 (s, 3 H). Step 4: *5-Bromo-N-methyl-2-oxo-1-((1-tosyl-1H-indol-7-yl)methyl)-1,2-dihydropyridine-3-carboxamide* (**81**). Prepared from **67** (300 mg, 1.298 mmol) and 7-(bromomethyl)-1-tosyl-1*H*-indole (**109**, 568 mg, 1.558 mmol). using the same procedure as for **68**, to give 5-bromo-*N*-methyl-2-oxo-1-((1-tosyl-1*H*-indol-7-yl)methyl)-1,2-dihydropyridine-3-carboxamide (326 mg, 0.570 mmol, 44% yield) as an orange solid. LCMS (2 min Formic): Rt = 1.22 min, $[MH]^+$ = 513.9, 515.9. ^{1}H NMR (400 MHz, $CHCl_3$-*d*) δ ppm 9.59 (br s, 1 H) 8.57 (d, *J*=2.4 Hz, 1 H) 7.81 (d, *J*=3.9 Hz, 1 H) 7.58 (dd, *J*=7.6, 1.2 Hz, 1 H) 7.50 - 7.55 (m, 2 H) 7.21 - 7.28 (m, 3 H) 7.19 (d, *J*=2.9 Hz, 1 H) 6.87 (d, *J*=6.8 Hz, 1 H) 6.79 (d, *J*=3.4 Hz, 1 H) 5.68 (s, 2 H) 3.01 (d, *J*=4.9 Hz, 3 H) 2.38 (s, 3 H). *Step 5: N^5-Cyclopropyl-N^3-methyl-2-oxo-1-((1-tosyl-1H-indol-7-yl)methyl)-1,2-dihydropyridine-3,5-dicarboxamide* (**82**). Prepared from **81** (297 mg, 0.577 mmol) and cyclopropylamine (81 µL, 1.155 mmol) using the same procedure as for **35**, to give N^5-cyclopropyl-N^3-methyl-2-oxo-1-((1-tosyl-1*H*-indol-7-yl)methyl)-1,2-dihydropyridine-3,5-dicarboxamide (251 mg, 0.290 mmol, 50 % yield) as an orange solid which was used without further purification in subsequent chemistry. LCMS (2 min Formic): Rt = 1.09 min, $[MH]^+$ = 519.0. ^{1}H NMR (400 MHz, $CHCl_3$-*d*) δ ppm 9.54 (br d, *J*=4.9 Hz, 1 H) 8.72 (d, *J*=2.4 Hz, 1 H) 8.10 (d, *J*=2.9 Hz, 1 H) 7.76 (d, *J*=3.4 Hz, 1 H) 7.52 - 7.56 (m, 3 H) 7.17 - 7.26 (m, 3 H) 6.75 - 6.79 (m, 2 H) 6.48 (br s, 1 H) 5.74 (s, 2 H) 3.00 (d, *J*=4.9 Hz, 3 H) 2.85 (tq, *J*=7.1, 3.6 Hz, 1 H) 2.36 (s, 3 H) 0.82 - 0.89 (m, 2 H) 0.59 - 0.65 (m, 2 H). Step 6: *1-((1H-Indol-7-yl)methyl)-N^5-cyclopropyl-N^3-methyl-2-oxo-1,2-dihydropyridine-3,5-dicarboxamide* (**57**). Prepared from **82** (124 mg, 0.120 mmol) using the same procedure as for **56**, to give 1-((1*H*-indol-7-yl)methyl)-N^5-cyclopropyl-N^3-methyl-2-oxo-1,2-dihydropyridine-3,5-dicarboxamide (18.8 mg, 0.049 mmol, 41% yield) as a white solid. LCMS (2 min Formic): Rt = 0.91 min, $[MH]^+$ = 365.1. ^{1}H NMR (400 MHz, $CHCl_3$-*d*) δ ppm 9.94 (br s, 1 H) 9.56 (br d, *J*=4.9 Hz, 1 H) 8.69 (d, *J*=2.4 Hz, 1 H) 8.61 (d, *J*=2.4 Hz, 1 H) 7.69 (d, *J*=7.8 Hz, 1 H) 7.27 - 7.32 (obs. m, 2

H) 7.13 (dd, *J*=8.1, 7.1 Hz, 1 H) 6.58 (dd, *J*=3.2, 2.2 Hz, 1 H) 6.46 (br s, 1 H) 5.52 (s, 2 H) 3.06 (d, *J*=4.9 Hz, 3 H) 2.82 - 2.90 (m, 1 H) 0.83 - 0.89 (m, 2 H) 0.57 - 0.63 (m, 2 H).

1-((1H-Pyrrolo[3,2-c]pyridin-4-yl)methyl)-N^5-cyclopropyl-N^3-methyl-2-oxo-1,2-dihydropyridine-3,5-dicarboxamide (**58**): Step 1: *(1H-Pyrrolo[3,2-c]pyridin-4-yl)methanol, hydrochloride* (**126**). To a solution of 1*H*-pyrrolo[3,2-c]pyridine-4-carboxylic acid (400 mg, 2.47 mmol, commercially available from, for example, Sigma-Aldrich) in THF (16 mL), was added borane tetrahydrofuran complex (1M in THF, 4.93 mL, 4.93 mmol) at rt. The reaction was stirred at rt for 3 h. The reaction was then quenched with methanol (0.998 mL, 24.67 mmol) and hydrochloric acid (1M, 3.08 mL, 6.17 mmol) and stirred for 1 h at rt. The reaction mixture was left to stand overnight. A precipitate was noted in the reaction mixture which was filtered off to yield (1*H*-pyrrolo[3,2-c]pyridin-4-yl)methanol, hydrochloride (306 mg, 1.33 mmol, 54% yield) as an off-white solid which was used without further purification. LCMS (2 min High pH): Rt = 0.43 min, $[MH]^+$ = 149.1. Step 2: *1-((1H-Pyrrolo[3,2-c]pyridin-4-yl)methyl)-N^5-cyclopropyl-N^3-methyl-2-oxo-1,2-dihydropyridine-3,5-dicarboxamide* (**58**). To a suspension of *N^5*-cyclopropyl-*N^3*-methyl-2-oxo-1,2-dihydropyridine-3,5-dicarboxamide (**87**, 55 mg, 0.23 mmol) in acetonitrile (2.3 mL) was added (1*H*-pyrrolo[3,2-c]pyridin-4-yl)methanol hydrochloride (86 mg, 0.468 mmol), triphenylphosphine (184 mg, 0.70 mmol), triethylamine (0.068 mL, 0.49 mmol) and DIAD (0.136 mL, 0.701 mmol). The reaction was stirred at rt for 5 h. Further portions of triphenylphosphine (184 mg, 0.70 mmol) and DIAD (0.136 mL, 0.70 mmol) were added. After 21 h, the reaction mixture was poured onto saturated aqueous sodium bicarbonate (10 mL) and extracted with ethyl acetate (3 x 15 mL). The combined organics were dried through a hydrophobic frit and evaporated *in vacuo* to yield the crude product (727 mg). The residue was dry loaded in methanol onto a 50 g SNAP cartridge and purified by Biotage SP4 flash chromatography, eluting from 18-88% (80:20 DCM:2M methanolic ammonia) / DCM. Poor separation was achieved and all fractions containing product were recombined and evaporated *in vacuo* to yield a clear glass (41 mg). The sample was dissolved in 1:1 MeOH:DMSO (1 mL) and purified by MDAP (High pH). The solvent was dried under a stream of nitrogen to give 1-((1*H*-pyrrolo[3,2-c]pyridin-4-yl)methyl)-*N^5*-cyclopropyl-*N^3*-methyl-2-oxo-1,2-dihydropyridine-3,5-

dicarboxamide (3.2 mg, 8.32 µmol, 4% yield) as a white solid. LCMS (2 min High pH): Rt = 0.66 min, $[MH]^+$ = 366.4. ^{1}H NMR (400 MHz, DMSO-d_6) δ ppm 11.61 (br s, 1 H) 9.32 (q, *J*=4.7 Hz, 1 H) 8.84 (d, *J*=2.9 Hz, 1 H) 8.73 (d, *J*=2.4 Hz, 1 H) 8.56 (d, *J*=4.4 Hz, 1 H) 8.01 (d, *J*=5.4 Hz, 1 H) 7.49 (dd, *J*=2.9, 2.0 Hz, 1 H) 7.27 - 7.36 (m, 1 H) 6.67 (d, *J*=2.9 Hz, 1 H) 5.66 (s, 2 H) 2.84 (tq, *J*=7.4, 3.9 Hz, 1 H) 2.79 (d, *J*=4.9 Hz, 3 H) 0.66 - 0.72 (m, 2 H) 0.55 - 0.60 (m, 2 H).

N^5-Cyclopropyl-1-(indolin-4-ylmethyl)-N^3-methyl-2-oxo-1,2-dihydropyridine-3,5-dicarboxamide (**59**):

Step 1: tert-Butyl 4-(hydroxymethyl)indoline-1-carboxylate (**127**). Indolin-4-ylmethanol (301 mg, 2.018 mmol, commercially available from, for example, Fluorochem) was dissolved in DCM (5 mL), Boc-anhydride (660 mg, 3.03 mmol) was added and the reaction stirred at rt under N_2 for 2 h. The reaction was diluted with sat. aq. sodium bicarbonate (10 mL), extracted with DCM (2 x 10 mL), dried over a hydrophobic frit and concentrated to give an orange oil (776 mg). This was purified by chromatography on SiO_2 (Biotage SNAP 50 g cartridge, eluting with 0-50% EtOAc/cyclohexane). The appropriate fractions were concentrated to give *tert*-butyl 4-(hydroxymethyl)indoline-1-carboxylate (472 mg, 1.704 mmol, 84% yield) as a colourless oil. LCMS (2 min Formic): Rt = 1.00 min, $[MH]^+$ = 194.1. ^{1}H NMR (400 MHz, DMSO-d_6) δ ppm 7.52 (br. s., 1 H) 7.12 (t, J=7.7 Hz, 1 H) 6.95 (d, J=7.6 Hz, 1 H) 5.05 (t, J=5.5 Hz, 1 H) 4.42 (d, J=5.4 Hz, 2 H) 3.91 (t, J=8.7 Hz, 2 H) 3.00 (t, J=8.7 Hz, 2 H) 1.50 (s, 9 H). *Step 2: tert-Butyl 4-((5-(cyclopropylcarbamoyl)-3-(methylcarbamoyl)-2-oxopyridin-1(2H)-yl)methyl)indoline-1-carboxylate* (**92**). Prepared from **87** (50 mg, 0.213 mmol) and *tert*-butyl 4-(hydroxymethyl)indoline-1-carboxylate (**127**, 79 mg, 0.319 mmol) using the same procedure as for **91**, to give *tert*-butyl 4-((5-(cyclopropylcarbamoyl)-3-(methylcarbamoyl)-2-oxopyridin-1(2*H*)-yl)methyl)indoline-1-carboxylate (41 mg, 0.075 mmol, 35.1 % yield) as a colourless oil. LCMS (2 min Formic): Rt = 1.08 min, [MH]+ = 467.2. ^{1}H NMR (400 MHz, MeOH-d_4) δ ppm 8.83 (d, J=2.7 Hz, 1 H) 8.47 (d, J=2.7 Hz, 1 H) 7.60 - 7.71 (m, 1 H) 7.14 (t, J=7.9 Hz, 1 H) 6.73 (d, J=7.6 Hz, 1 H) 5.24 (s, 2 H) 4.00 (t, J=8.7 Hz, 2 H) 3.14 (t, J=8.7 Hz, 2 H) 2.93 (s, 3 H) 2.80 (tt, J=7.3, 3.7 Hz, 1 H) 1.56 (s, 9 H) 0.74 - 0.82 (m, 2 H) 0.58 - 0.65 (m, 2 H). *Step 3: N^5-Cyclopropyl-1-(indolin-4-ylmethyl)-N^3-methyl-2-oxo-1,2-dihydropyridine-3,5-dicarboxamide* (**59**). *tert*-Butyl 4-((5-(cyclopropylcarbamoyl)-3-(methylcarbamoyl)-2-oxopyridin-1(2*H*)-

yl)methyl)indoline-1-carboxylate (**92**, 43 mg, 0.092 mmol) and TFA (0.5 mL, 6.49 mmol) were stirred at rt in DCM for 30 min (2 mL). The reaction mixture was concentrated and loaded onto a SCX cartridge (5 g, pre-conditioned with MeOH) and eluted with MeOH (20 mL) followed by 2M NH_3 in MeOH (20 mL). The ammonia fractions containing product were combined and concentrated to give N^5-cyclopropyl-1-(indolin-4-ylmethyl)-N^3-methyl-2-oxo-1,2-dihydropyridine-3,5-dicarboxamide (30 mg, 0.074 mmol, 80% yield) as a yellow solid. LCMS (2 min Formic): Rt = 0.45 min, [MH]+ = 367.2. ^{1}H NMR (400 MHz, MeOH-d_4) δ ppm 8.81 (d, J=2.7 Hz, 1 H) 8.43 (d, J=2.7 Hz, 1 H) 6.97 (t, J=7.8 Hz, 1 H) 6.61 (d, J=7.8 Hz, 1 H) 6.47 (d, J=7.6 Hz, 1 H) 5.22 (s, 2 H) 3.49 (t, J=8.4 Hz, 2 H) 2.98 (t, J=8.4 Hz, 2 H) 2.94 (s, 3 H) 2.79 (tt, J=7.3, 3.8 Hz, 1 H) 0.74 - 0.81 (m, 2 H) 0.58 - 0.63 (m, 2 H).

X-ray Diffraction Study of 20

Data were collected with an Oxford Diffraction Gemini A Ultra diffractometer at 150(2)K using Cu-Kα X-radiation (λ = 1.54178 Å).

Crystal data and refinement summary for **20**: $C_{18}H_{19}N_3O_3$; M = 325.36; colourless needle from the slow evaporation of a solution of **20** in methanol and water; 0.24 x 0.04 x 0.01 mm; monoclinic; space group $P2_1/n$ (alt. $P2_1/c$, #14); a = 13.4672(4) Å, b = 5.79643(15) Å, c = 20.7574(6) Å, β = 97.299(3) °, V = 1607.23(8) Å^3; Z = 4; D_{calc} = 1.345 Mgm^{-3}; ϑ_{max} = 67.00 °; reflections collected = 11968; independent reflections = 2833; R_{int} = 0.0438; coverage = 99.1 %; restraints = 0; parameters = 227; S = 1.032; R_1 [$I>2\sigma(I)$] = 0.0384; wR_2 (all data) = 0.0940; and largest difference peak and hole = 0.240 and -0.190 eÅ^{-3}.

A description of the refinement and the full tables associated with the crystal structure are given in the Supporting Information. A crystallographic information file has been deposited with the Cambridge Crystallographic Data Centre. CCDC 2001550 contains the supplementary crystallographic data for this paper. The data can be obtained free of charge from The Cambridge Crystallographic Data Centre *via* www.ccdc.cam.ac.uk/structures.

BRD4 Mutant TR-FRET Assay[62]

Tandem bromodomains of 6His-Thr-BRD4(1−477) were expressed, with an appropriate mutation in BD2 (Y390A) to monitor compound binding to BD1, or in BD1 (97A) to monitor compound binding to BD2. Analogous Y→A mutants were used to measure binding to the other BET bromodomains: 6His-Thr-BRD2 (1−473 Y386A or Y113A), 6His-Thr-BRD3 (1−435 Y348A or Y73A), 6His-FLAG-Tev-BRDT (1−397 Y309A or Y66A). The AlexaFluor 647 labelled BET bromodomain ligand was prepared as follows: To a solution of AlexaFluor 647 hydroxysuccinimide ester in DMF was added a 1.8-fold excess of N-(5-aminopentyl)-2-((4*S*)-6-(4-chlorophenyl)-8-methoxy-1-methyl-4H-benzo[*f*][1,2,4]triazolo[4,3-*a*][1,4]-diazepin-4-yl)acetamide, also in DMF, and when thoroughly mixed, the solution was basified by the addition of a 3-fold excess of diisopropylethylamine. Reaction progress was followed by electrospray LC/MS, and when judged complete, the product was isolated and purified by reversed-phase C18 HPLC. The final compound was characterized by mass spectroscopy and analytical reversed-phase HPLC.

Compounds were titrated from 10 mM in 100% DMSO and 50 nL transferred to a low volume black 384 well micro titre plate using a Labcyte Echo 555. A Thermo Scientific Multidrop Combi was used to dispense 5 µL of 20 nM protein in an assay buffer of 50 mM HEPES, 150 mM NaCl, 5% glycerol, 1 mM DTT and 1 mM CHAPS, pH 7.4, and in the presence of 100 nM fluorescent ligand (~K_d concentration for the interaction between BRD4 BD1 and ligand). After equilibrating for 30 min in the dark at rt, the bromodomain protein:fluorescent ligand interaction was detected using TR-FRET following a 5 µL addition of 3 nM europium chelate labelled anti-6His antibody (Perkin Elmer, W1024, AD0111) in assay buffer. Time resolved fluorescence (TRF) was then detected on a TRF laser equipped Perkin Elmer Envision multimode plate reader (excitation = 337 nm; emission 1 = 615 nm; emission 2 = 665 nm; dual wavelength bias dichroic = 400 nm, 630 nm). TR-FRET ratio was calculated using the following equation: Ratio = ((Acceptor fluorescence at 665 nm) / (Donor fluorescence at 615 nm)) * 1000. TR-FRET ratio data were normalised to high (DMSO) and low (compound control derivative of I-BET762)

controls and IC_{50} values determined for each of the compounds tested by fitting the fluorescence ratio data to a four parameter model:

$$\mathbf{y} = \boldsymbol{A} + (\boldsymbol{B} - \boldsymbol{A})/(\mathbf{1} + (\mathbf{10}\text{^}\boldsymbol{c}/\boldsymbol{x})\text{^}\boldsymbol{D}\ )$$

where 'a' is the minimum, 'b' is the Hill slope, 'c' is the IC_{50} and 'd' is the maximum.

BRD4 SPR Assay

BRD4 SPR was measured using published protocols.[53] In brief SPR were performed using a Biacore S200 instrument (GE Healthcare) on CM5 chips (GE Healthcare) at 25 °C. Two proteins (1) 6His-Thr-Brd4 (1-477) Y390A and (2) His-tagged cleaved BRD4 (347-463), were immobilised onto the same CM5 to allow simultaneously affinity data to be obtained for BRD4-BD1 and BRD4-BD2 binding respectively . The top concentration used for triple dilution dose response titrations was 10 μM.

Physicochemical Properties

Permeability across a lipid membrane, chromatographic LogD at pH 7.4, and CLND solubility by precipitation into saline were measured using published protocols.[86-89]

FaSSIF solubility

Compounds were dissolved in DMSO at 2.5 mg/mL and then diluted in Fast State Simulated Intestinal Fluid (FaSSIF pH 6.5) at 125 μg/mL (final DMSO concentration is 5%). After 16 h of incubation at 25 °C, the suspension was filtered. The concentration of the compound was determined by a fast HPLC gradient. The ratio of the peak areas obtained from the standards and the sample filtrate was used to calculate the solubility of the compound.

All animal studies were ethically reviewed and carried out in accordance with Animals (Scientific Procedures) Act 1986 and the GSK Policy on the Care, Welfare and Treatment of Animals.

The human biological samples were sourced ethically and their research use was in accord with the terms of the informed consents under an IRB/EC approved protocol.

Intrinsic Clearance (CL_{int}) Measurements

The human biological samples were sourced ethically and their research use was in accord with the terms of the informed consents under an IRB/EC approved protocol.

Microsome Intrinsic Clearance data were determined by Cyprotex UK. To test the metabolic stability of **12**, it was incubated in male Wistar Han rat and mixed gender pooled human liver microsomes. Microsomes (final protein concentration 0.5 mg/mL), 0.1 M phosphate buffer pH7.4 and test compound (final substrate concentration = 0.5 µM) were pre-incubated at 37 °C prior to the addition of NADPH (final concentration = 1 mM) to initiate the reaction. The test compound was incubated for 0, 5, 15, 30 and 45 min. The control (minus NADPH) was incubated for 45 min only. The reactions were stopped by the addition of 50 µL methanol containing internal standard at the appropriate time points. Following protein precipitation, the compound remaining in the supernatants was measured using specific LC-MS/MS methods as a ratio to the internal standard in the absence of a calibration curve. Peak area ratios (Compound to IS) were fitted to an unweighted logarithmic decline in substrate. Using the first order rate constant, clearance was calculated by adjustment for protein concentration, volume of the incubation and hepatic scaling factor (52.5 mg microsomal protein/g liver for all species).

Hepatocyte Intrinsic Clearance data were determined by Cyprotex UK. Test compound (0.5 µM) was incubated with cryopreserved hepatocytes in suspension. Samples were removed at 6 time points over the course of a 60 min (rat) or 120 min (human) experiment and test compound analysed by LC-MS/MS. Cryopreserved pooled hepatocytes were purchased from a reputable commercial supplier and stored in liquid nitrogen prior to use. Williams E media supplemented with 2 mM L-glutamine and 25 mM HEPES and test compound (final substrate concentration 0.5 µM; final DMSO concentration 0.25%) was pre-incubated at 37 °C prior to the addition of a suspension of cryopreserved hepatocytes (final cell density 0.5 x 10^6 viable cells/mL in Williams E media supplemented with 2 mM L-glutamine and 25 mM HEPES) to initiate the reaction. The final incubation volume was 500 µL. The reactions were stopped by transferring 50 µL of incubate to 100 µL acetonitrile at the appropriate time points. The termination plates were centrifuged at 2500 rpm at 4 °C for 30 min to precipitate the protein. The

remaining incubate (200 µL) was crashed with 400 µL acetonitrile at the end of the incubation. Following protein precipitation, the sample supernatants were combined in cassettes of up to 4 compounds and analysed using Cyprotex generic LC-MS/MS conditions.

Intrinsic Clearance (CL_{int}) Data Analysis

From a plot of ln peak area ratio (compound peak area/internal standard peak area) against time, the gradient of the line was determined. Subsequently, half-life ($t_{½}$) and intrinsic clearance (CL_{int}) were calculated using the equations below:

Elimination rate constant (k) = (- gradient)

Half-life ($t_{½}$)(min) = $\frac{0.693}{k}$

Intrinsic clearance (CL_{int})(µL/min/million cells) = $\frac{V \times 0.693}{t_{½}}$

where V = Incubation volume (µL)/Number of cells

Fraction Unbound in Blood

Control blood from Wistar Han Rat and Beagle Dog were obtained on the day of experimentation from in house GSK stock animals. The fraction unbound in blood of each species was determined using rapid equilibrium dialysis technology (RED plate (Linden Bioscience, Woburn, MA) at a concentration of 200 & 1000 ng/mL. Blood was dialyzed against phosphate buffered saline solution by incubating the dialysis units at 37 °C for 4 h. Following incubation aliquots of blood and buffer were matrix matched prior to analysis by LC−MS/MS. The unbound fraction was determined using the peak area ratios in buffer and in blood as a mean value of the two concentrations investigated.

***in vivo* DMPK Studies**

All animal studies were ethically reviewed and carried out in accordance with Animals (Scientific Procedures) Act 1986 and the GSK Policy on the Care, Welfare and Treatment of Animals.

For all *in vivo* studies, the temperature and humidity were nominally maintained at 21 °C ± 2 °C and 55% ± 10%, respectively. The diet for rodents was 5LF2 Eurodent Diet 14% (PMI Labdiet, Richmond, IN) and for dogs was Harlan Teklad 2021C (HarlanTeklad, Madison, WI). There were no known contaminants in the diet or water at concentrations that could interfere with the outcome of the studies.

Rat surgical preparation for IV infusion study

Male Wistar Han rats (supplied by Charles River UK Ltd.) were surgically prepared at GSK with implanted cannulae in the femoral vein (for drug administration) and jugular vein (for blood sampling). The rats received Cefuroxime (116 mg/kg sc) and carprofen (7.5 mg/kg sc) as a preoperative antibiotic and analgesic, respectively. The rats were allowed to recover for at least 2 days prior to dosing and had free access to food and water throughout.

Rat IV n=1 PK study

Surgically prepared male Wistar Han Rats received a 1 h intravenous (iv) infusion of Compound of interest as a discrete dose, formulated in DMSO and 10% (w/v) Kleptose HPB in saline aq (2%:98% (v/v)) at a concentration of 0.2 mg/mL to achieve a target dose of 1 mg/kg. Serial blood samples (25 µL) were collected predose and up to 7 h after the start of the iv infusion. Diluted blood samples were analyzed for parent compound using a specific LC−MS/MS assay (LLQ = 2-10 ng/mL). At the end of the study the rats were euthanized by a Schedule 1 technique.

Rat PO n=3 PK study

3 naïve Male Wistar Han Rats (Female Lewis Rats for **56**) with no surgical preparation received an oral gavage administration of Compound of interest as a discrete dose, suspended in 1% (w/v) methylcellulose aq at a concentration of 0.6 mg/mL to achieve a target dose of 3 mg/kg (a

concentration of 2 mg/mL to achieve a target dose of 10 mg/kg for **56**). Serial blood samples (25 µL) were collected via temporary tail vein cannulation up to 7 h after oral dosing and additional blood sampling via tail vein venepuncture up to 24 h after oral dosing. Diluted blood samples were analysed for parent compound using a specific LC–MS/MS assay (LLQ = 2-10 ng/mL). At the end of the study the rats were euthanized by a Schedule 1 technique.

Rat IV PO n=3 crossover PK study

This study was conducted as a crossover design over two dosing occasions, with 5 days between dose administrations in 3 surgically prepared male Wistar Han Rats. On the first dosing occasion, rats each received a 1 h intravenous (iv) infusion of Compound 18 formulated in DMSO and 10% (w/v) Kleptose HPB in saline aq (2%:98% (v/v)) at a concentration of 0.2 mg/mL to achieve a target dose of 1 mg/kg. On the second dosing occasion, the same 3 rats were administered with Compound 18 suspended in 1% (w/v) methylcellulose 400 aq at a concentration of 0.6 mg/mL orally, at a target dose of 3 mg/kg. Serial blood samples (25 µL) were collected predose and up to 24 h after the start of the iv infusion and after oral dosing. Diluted blood samples were analysed using a specific LC–MS/MS assay (LLQ = 2 ng/mL). At the end of the study the rats were euthanized by a Schedule 1 technique.

Dog PK Study

One healthy, laboratory-bred, male Beagle dog (supplied by Harlan Laboratories, U.K.) was used. The dog was fasted overnight prior to each dose administration and fed approximately 4 h after the start of dosing and had free access to water throughout the study. This study was conducted as a crossover design, with 8 days between dose administrations. On the first dosing occasion, the dog received a 1 h intravenous (iv) infusion of **20** formulated in DMSO and 10% (w/v) Kleptose HPB in saline aq (2%:98% (v/v)), at a concentration of 0.1 mg/mL to achieve a target dose of 0.5 mg/kg. On a subsequent dosing occasion, the same dog was administered with **20**, suspended in 1% (w/v)

methylcellulose aq at a concentration of 0.1 mg/mL to achieve a target dose of 1 mg/kg. A temporary cannula was inserted into the cephalic vein from which serial blood samples (50 µL) were collected predose and up to 26 h after the start of dosing. After collection of the 2 h time point the cannula was removed and later time points were taken via direct venepuncture of the jugular vein. Diluted blood samples were analyzed for parent drug concentration using a specific LC−MS/MS assay (LLQ = 5 ng/mL). At the end of each study the dog was returned to the colony.

Blood Sample Analysis

Diluted blood samples (1:1 with water) were extracted using protein precipitation with acetonitrile containing an analytical internal standard. An aliquot of the supernatant was analyzed by reverse phase LC−MS/MS using a heat assisted electrospray interface in positive ion mode. Samples were assayed against calibration standards prepared in control blood.

PK Data Analysis from PK Studies

PK parameters were obtained from the blood concentration−time profiles using noncompartmental analysis with WinNonlin Professional 6.3 (Pharsight, Mountain View, CA).

hWB MCP-1 Assay

The human biological samples were sourced ethically and their research use was in accord with the terms of the informed consents under an IRB/EC approved protocol.

Compounds to be tested were diluted in 100% DMSO to give a range of appropriate concentrations at 140x the required final assay concentration, of which 1 µL was added to a 96 well tissue culture plate. 130 µL of human whole blood, collected into sodium heparin anticoagulant, (1 unit/mL final) was added to each well and plates were incubated at 37°C (5% C02) for 30 min before the addition of 10 µL of 2.8 µg/mL LPS (Salmonella Typhosa), diluted in complete RPMI 1640 (final concentration 200 ng/mL), to give a total volume of 140 µL per well. After further incubation for 24 h at 37 °C, 140 µL of

PBS was added to each well. The plates were sealed, shaken for 10 min and then centrifuged (2500 rpm x 10 min). 100 µL of the supernatant was removed and MCP-1 levels assayed immediately by immunoassay (MesoScale Discovery technology).

ASSOCIATED CONTENT

DiscoverX BROMOscan® Bromodomain Profiling of **20**, cross screening data of liability target panel for **20** and **56**, sequence alignment and differences of BET proteins, X-ray crystallographic data and selected LCMS and NMR Spectra (PDF)

Molecular formula strings (CSV)

PDB IDs : 6ZB0, 6ZB1, 6ZB2, 6ZB3

Authors will release the atomic coordinates upon article publication.AUTHOR INFORMATION

Corresponding Author

J.T.S: E-mail: jon.t.seal@gsk.com

S.J.A: E-mail: stephen.atkinson@astrazeneca.com

Present Addresses

Stephen Atkinson Current Address: Discovery Sciences, AstraZeneca, Cambridge, UK.

Tom Hayhow Current Address: Discovery Sciences, AstraZeneca, Cambridge, UK.

[#]Matthew Lindon: Research and Early Development, RIA, Biopharmaceuticals R&D, AstraZeneca, SE-431 83, Mölndal, Sweden

[‡] Simon Taylor Current Address: Drug Discovery Services Europe, Pharmaron, Hertford Road, Hoddesdon, EN11 9BU, UK.

Author Contributions

The manuscript was written through contributions of all authors. All authors have given approval to the final version of the manuscript.

Funding Sources

All authors were GlaxoSmithKline full-time employees when this study was performed.

ACKNOWLEDGMENT

We would like to thank members of Platform Technology & Science at GSK for protein reagent generation, assay and crystallisation support; Tony Cooper and Heather Barnett for support with chemistry arrays; Eric Hortense, Richard Briers, Steve Jackson and Sean Hindley for analytical and purification support; Sean Lynn, Richard Upton and Stephen Richards for assistance with NMR analysis; and William Clegg and Michael Probert (University of Newcastle) for the GSK-funded crystal structure of **20**.

ABBREVIATIONS

AMP, artificial membrane permeability; BAZ2B, bromodomain adjacent to zinc finger domain 2B; BD1, bromodomain 1 (N-terminal bromodomain); BD2, bromodomain 2 (C-terminal bromodomain); BET, bromo and extra-terminal domain; BRD2,3,4,T, bromodomain containing protein 2,3,4,T; BSEP, bile salt export pump; CHAPS, (3-((3-cholamidopropyl) dimethylammonio)-1-propanesulfonate); CL_b, blood clearance; CL_{int}, intrinsic clearance; CLND, chemiluminscent nitrogen detection; CMTP, 2-(tributylphosphoranylidene)acetonitrile; D, dose; DIAD, diisopropyl azodicarboxylate; dppb, 1,4-bis(diphenylphosphino)butane; EDC, N-(3-dimethylaminopropyl)-N'-ethylcarbodiimide; EDG, electron-donating group; EWG, electron-withdrawing group; FACS, flow cytometry staining buffer; FP, fluorescence polarisation, fu_b, fraction unbound in blood; GSH, glutathione; HATU, 1-[bis(dimethylamino)methylene]-1H-1,2,3-triazolo[4,5-b]pyridinium 3-oxid hexafluorophosphate; HepG2, human liver cancer cell line; HEPES, (4-(2-hydroxyethyl)-1-piperazineethanesulfonic acid); hWB, human whole blood; k, elimination rate constant; KAc, acetylated lysine; LLE_{at}, Astex lipophilic ligand efficiency; MCP-1/CCL2, monocyte chemoattractant protein-1; MDAP, mass-directed auto preparation; MDI, metabolism dependent inhibition; MLA, mouse lymphoma assay; RPMI, Roswell Park Memorial Institute; SPR, surface plasmon resonance; STAB, sodium triacetoxyborohydride; TDI, time dependent inhibition; TR-FRET, time resolved fluorescence resonance energy transfer, V, incubation volume; V_{ss}, volume of distribution at steady state; WPF, tryptophan-proline-phenylalanine; XRPD, X-ray powder diffraction; 2-MeTHF, 2-methyltetrahydrofuran.

REFERENCES

1. Fujisawa, T.; Filippakopoulos, P., Functions of bromodomain-containing proteins and their roles in homeostasis and cancer. *Nature Reviews Molecular Cell Biology* **2017,** *18*, 246-262.

2. Prinjha, R. K.; Witherington, J.; Lee, K., Place your BETs: the therapeutic potential of bromodomains. *Trends in Pharmacological Sciences* **2012,** *33* (3), 146-153.

3. Filippakopoulos, P.; Qi, J.; Picaud, S.; Shen, Y.; Smith, W. B.; Fedorov, O.; Morse, E. M.; Keates, T.; Hickman, T. T.; Felletar, I.; Philpott, M.; Munro, S.; McKeown, M. R.; Wang, Y.; Christie, A. L.; West, N.; Cameron, M. J.; Schwartz, B.; Heightman, T. D.; La Thangue, N.; French, C. A.; Wiest, O.; Kung, A. L.; Knapp, S.; Bradner, J. E., Selective inhibition of BET bromodomains. *Nature* **2010,** *468*, 1067.

4. Chaidos, A.; Caputo, V.; Gouvedenou, K.; Liu, B.; Marigo, I.; Chaudhry, M. S.; Rotolo, A.; Tough, D. F.; Smithers, N. N.; Bassil, A. K.; Chapman, T. D.; Harker, N. R.; Barbash, O.; Tummino, P.; Al-Mahdi, N.; Haynes, A. C.; Cutler, L.; Le, B.; Rahemtulla, A.; Roberts, I.; Kleijnen, M.; Witherington, J. J.; Parr, N. J.; Prinjha, R. K.; Karadimitris, A., Potent antimyeloma activity of the novel bromodomain inhibitors I-BET151 and I-BET762. *Blood* **2014,** *123* (5), 697.

5. Zuber, J.; Shi, J.; Wang, E.; Rappaport, A. R.; Herrmann, H.; Sison, E. A.; Magoon, D.; Qi, J.; Blatt, K.; Wunderlich, M.; Taylor, M. J.; Johns, C.; Chicas, A.; Mulloy, J. C.; Kogan, S. C.; Brown, P.; Valent, P.; Bradner, J. E.; Lowe, S. W.; Vakoc, C. R., RNAi screen identifies Brd4 as a therapeutic target in acute myeloid leukaemia. *Nature* **2011,** *478*, 524.

6. Cheng, Z.; Gong, Y.; Ma, Y.; Lu, K.; Lu, X.; Pierce, L. A.; Thompson, R. C.; Muller, S.; Knapp, S.; Wang, J., Inhibition of BET Bromodomain Targets Genetically Diverse Glioblastoma. *Clinical Cancer Research* **2013,** *19* (7), 1748.

7. da Motta, L. L.; Ledaki, I.; Purshouse, K.; Haider, S.; De Bastiani, M. A.; Baban, D.; Morotti, M.; Steers, G.; Wigfield, S.; Bridges, E.; Li, J. L.; Knapp, S.; Ebner, D.; Klamt, F.; Harris, A. L.; McIntyre, A., The BET inhibitor JQ1 selectively impairs tumour response to hypoxia and downregulates CA9 and angiogenesis in triple negative breast cancer. *Oncogene* **2016,** *36*, 122.

8. Rhyasen, G. W.; Hattersley, M. M.; Yao, Y.; Dulak, A.; Wang, W.; Petteruti, P.; Dale, I. L.; Boiko, S.; Cheung, T.; Zhang, J.; Wen, S.; Castriotta, L.; Lawson, D.; Collins, M.; Bao, L.; Ahdesmaki, M. J.; Walker, G.; Connor, G.; Yeh, T. C.; Rabow, A. A.; Dry, J. R.; Reimer, C.; Lyne, P.; Mills, G. B.; Fawell, S. E.; Waring, M. J.; Zinda, M.; Clark, E.; Chen, H., AZD5153: A Novel Bivalent BET Bromodomain Inhibitor Highly Active against Hematologic Malignancies. *Molecular Cancer Therapeutics* **2016,** *15* (11), 2563.

9. Boi, M.; Gaudio, E.; Bonetti, P.; Kwee, I.; Bernasconi, E.; Tarantelli, C.; Rinaldi, A.; Testoni, M.; Cascione, L.; Ponzoni, M.; Mensah, A. A.; Stathis, A.; Stussi, G.; Riveiro, M. E.; Herait, P.; Inghirami, G.; Cvitkovic, E.; Zucca, E.; Bertoni, F., The BET Bromodomain Inhibitor OTX015 Affects Pathogenetic Pathways in Preclinical B-cell Tumor Models and Synergizes with Targeted Drugs. *Clinical Cancer Research* **2015,** *21* (7), 1628.

10. Picaud, S.; Da Costa, D.; Thanasopoulou, A.; Filippakopoulos, P.; Fish, P. V.; Philpott, M.; Fedorov, O.; Brennan, P.; Bunnage, M. E.; Owen, D. R.; Bradner, J. E.; Taniere, P.; Sullivan, B.; Müller, S.; Schwaller, J.; Stankovic, T.; Knapp, S., PFI-1, a Highly Selective Protein Interaction Inhibitor, Targeting BET Bromodomains. *Cancer Research* **2013,** *73* (11), 3336.

11. Segura, M. F.; Fontanals-Cirera, B.; Gaziel-Sovran, A.; Guijarro, M. V.; Hanniford, D.; Zhang, G.; González-Gomez, P.; Morante, M.; Jubierre, L.; Zhang, W.; Darvishian, F.; Ohlmeyer, M.; Osman, I.; Zhou, M.-M.; Hernando, E., BRD4 Sustains Melanoma Proliferation and Represents a New Target for Epigenetic Therapy. *Cancer Research* **2013,** *73* (20), 6264.

12. Tough, D. F.; Tak, P. P.; Tarakhovsky, A.; Prinjha, R. K., Epigenetic drug discovery: breaking through the immune barrier. *Nature Reviews Drug Discovery* **2016,** *15*, 835.

13. Tough, D. F.; Prinjha, R. K., Immune disease-associated variants in gene enhancers point to BET epigenetic mechanisms for therapeutic intervention. *Epigenomics* **2016,** *9* (4), 573-584.

14. Mele, D. A.; Salmeron, A.; Ghosh, S.; Huang, H.-R.; Bryant, B. M.; Lora, J. M., BET bromodomain inhibition suppresses T(H)17-mediated pathology. *The Journal of Experimental Medicine* **2013,** *210* (11), 2181-2190.

15. Bandukwala, H. S.; Gagnon, J.; Togher, S.; Greenbaum, J. A.; Lamperti, E. D.; Parr, N. J.; Molesworth, A. M. H.; Smithers, N.; Lee, K.; Witherington, J.; Tough, D. F.; Prinjha, R. K.; Peters, B.; Rao, A., Selective inhibition of CD4+ T-cell cytokine production and autoimmunity by BET protein and c-Myc inhibitors. *Proceedings of the National Academy of Sciences* **2012,** *109* (36), 14532.

16. Chan, C. H.; Fang, C.; Qiao, Y.; Yarilina, A.; Prinjha, R. K.; Ivashkiv, L. B., BET bromodomain inhibition suppresses transcriptional responses to cytokine-Jak-STAT signaling in a gene-specific manner in human monocytes. *European Journal of Immunology* **2015,** *45* (1), 287-297.

17. Schilderink, R.; Bell, M.; Reginato, E.; Patten, C.; Rioja, I.; Hilbers, F. W.; Kabala, P. A.; Reedquist, K. A.; Tough, D. F.; Tak, P. P.; Prinjha, R. K.; de Jonge, W. J., BET bromodomain inhibition reduces maturation and enhances tolerogenic properties of human and mouse dendritic cells. *Molecular Immunology* **2016,** *79*, 66-76.

18. Belkina, A. C.; Nikolajczyk, B. S.; Denis, G. V., BET Protein Function Is Required for Inflammation: Brd2 Genetic Disruption and BET Inhibitor JQ1 Impair Mouse Macrophage Inflammatory Responses. *The Journal of Immunology* **2013,** *190* (7), 3670.

19. Klein, K.; Kabala, P. A.; Grabiec, A. M.; Gay, R. E.; Kolling, C.; Lin, L.-L.; Gay, S.; Tak, P. P.; Prinjha, R. K.; Ospelt, C.; Reedquist, K. A., The bromodomain protein inhibitor I-BET151 suppresses expression of inflammatory genes and matrix degrading enzymes in rheumatoid arthritis synovial fibroblasts. *Annals of the Rheumatic Diseases* **2016,** *75* (2), 422.

20. Nicodeme, E.; Jeffrey, K. L.; Schaefer, U.; Beinke, S.; Dewell, S.; Chung, C.-w.; Chandwani, R.; Marazzi, I.; Wilson, P.; Coste, H.; White, J.; Kirilovsky, J.; Rice, C. M.; Lora, J. M.; Prinjha, R. K.; Lee, K.; Tarakhovsky, A., Suppression of inflammation by a synthetic histone mimic. *Nature* **2010,** *468*, 1119.

21. Meng, S.; Zhang, L.; Tang, Y.; Tu, Q.; Zheng, L.; Yu, L.; Murray, D.; Cheng, J.; Kim, S. H.; Zhou, X.; Chen, J., BET Inhibitor JQ1 Blocks Inflammation and Bone Destruction. *Journal of Dental Research* **2014,** *93* (7), 657-662.

22. Nadeem, A.; Al-Harbi, N. O.; Al-Harbi, M. M.; El-Sherbeeny, A. M.; Ahmad, S. F.; Siddiqui, N.; Ansari, M. A.; Zoheir, K. M. A.; Attia, S. M.; Al-Hosaini, K. A.; Al-Sharary, S. D., Imiquimod-induced

psoriasis-like skin inflammation is suppressed by BET bromodomain inhibitor in mice through RORC/IL-17A pathway modulation. *Pharmacological Research* **2015,** *99*, 248-257.

23. Zhang, Q.-g.; Qian, J.; Zhu, Y.-c., Targeting bromodomain-containing protein 4 (BRD4) benefits rheumatoid arthritis. *Immunology Letters* **2015,** *166* (2), 103-108.

24. Liu, Z.; Wang, P.; Chen, H.; Wold, E. A.; Tian, B.; Brasier, A. R.; Zhou, J., Drug Discovery Targeting Bromodomain-Containing Protein 4. *Journal of Medicinal Chemistry* **2017,** *60* (11), 4533-4558.

25. Doroshow, D. B.; Eder, J. P.; LoRusso, P. M., BET inhibitors: a novel epigenetic approach. *Annals of Oncology* **2017,** *28* (8), 1776-1787.

26. Alqahtani, A.; Choucair, K.; Ashraf, M.; Hammouda, D. M.; Alloghbi, A.; Khan, T.; Senzer, N.; Nemunaitis, J., Bromodomain and Extra-Terminal Motif Inhibitors: A Review of Preclinical and Clinical Advances in Cancer Therapy. *Future Science OA* **2019,** *5* (3), FSO372.

27. Andrieu, G.; Belkina, A. C.; Denis, G. V., Clinical Trials for BET Inhibitors Run Ahead of the Science. *Drug Discovery Today: Technologies* **2016,** *19*, 45-50.

28. Postel-Vinay, S.; Herbschleb, K.; Massard, C.; Woodcock, V.; Soria, J.-C.; Walter, A. O.; Ewerton, F.; Poelman, M.; Benson, N.; Ocker, M.; Wilkinson, G.; Middleton, M., First-in-Human Phase I Study of the Bromodomain and Extraterminal Motif Inhibitor BAY 1238097: Emerging Pharmacokinetic/Pharmacodynamic Relationship and Early Termination due to Unexpected Toxicity. *Eur. J. Cancer* **2019,** *109*, 103-110.

29. Odenike, O.; Wolff, J. E.; Borthakur, G.; Aldoss, I. T.; Rizzieri, D.; Prebet, T.; Hu, B.; Dinh, M.; Chen, X.; Modi, D.; Freise, K. J.; Jonas, B. A., Results from the First-in-Human Study of Mivebresib (ABBV-075), a Pan-Inhibitor of Bromodomain and Extra Terminal Proteins, in Patients with Relapsed/Refractory Acute Myeloid Leukemia. *J. Clin. Oncol.* **2019,** *37* (15_suppl), 7030-7030.

30. Amans, D.; Atkinson, S. J.; Harrison, L. A.; Hirst, D. J.; Law, R. P.; Lindon, M.; Preston, A.; Seal, J. T.; Wellaway, C. R. Preparation of acylaminotetrahydroquinoline derivatives for use as bromodomain inhibitors. WO2014140076A1, 2014.

31. Atkinson, S. J.; Demont, E. H.; Harrison, L. A.; Hayhow, T. G. C.; House, D.; Lindon, M. J.; Preston, A. G.; Seal, J. T.; Wall, I. D.; Watson, R. J.; Woolven, J. M. Preparation of pyridinone-dicarboxamide for use as bromodomain inhibitors. WO2017050714A1, 2017.

32. Atkinson, S. J.; Aylott, H. E.; Cooper, A. W. J.; Demont, E. H.; Harrison, L. A.; Hayhow, T. G. C.; Lindon, M. J.; Preston, A. G.; Seal, J. T.; Wall, I. D.; Watson, R. J.; Woolven, J. M. Preparation of pyridinone dicarboxamide derivatives for use as bromodomain inhibitors. WO2017037116A1, 2017.

33. Amans, D.; Bamborough, P.; Barker, M. D.; Bit, R. A.; Brown, J. A.; Campbell, M.; Garton, N. S.; Lindon, M. J.; Shipley, T. J.; Theodoulou, N. H.; Wellaway, C. R.; Westaway, S. M. Preparation of furopyridines as bromodomain inhibitors useful in treating cancer, inflammation, and autoimmune disorders. WO2014140077A1, 2014.

34. Wang, L.; Dai, Y.; Holms, J.; Liu, D.; McClellan, W.; McDaniel, K.; Hasvold, L.; Fidanze, S. D.; Sheppard, G.; Marjanovic, J. Preparation of pyrrolopyridinone derivatives as bromodomain inhibitors. WO2014206345A1, 2014.

35. Siegel, S.; Baeurle, S.; Cleve, A.; Haendler, B.; Fernandez-Montalvan, A. E. Preparation of 1-phenyl-3H-2,3-benzodiazepines and their use as bromodomain inhibitors. WO2015121268A1, 2015.

36. Combs, A. P.; Sparks, R. B.; Maduskuie, T. P., Jr.; Rodgers, J. D. Preparation of tricyclic heterocycles as bet protein inhibitors. WO2014143768A1, 2014.

37. Gerner Seitzberg, J.; Titilola Akinleminu Kronborg, T.; Poljak, V.; Friberg, G.; Teuber, L. Heterocyclic compounds as bromodomain Inhibitors and their preparation. WO2016016316A1, 2016.

38. Gacias, M.; Gerona-Navarro, G.; Plotnikov, Alexander N.; Zhang, G.; Zeng, L.; Kaur, J.; Moy, G.; Rusinova, E.; Rodriguez, Y.; Matikainen, B.; Vincek, A.; Joshua, J.; Casaccia, P.; Zhou, M.-M., Selective Chemical Modulation of Gene Transcription Favors Oligodendrocyte Lineage Progression. *Chemistry & Biology* **2014,** *21* (7), 841-854.

39. Cheung, K.; Lu, G.; Sharma, R.; Vincek, A.; Zhang, R.; Plotnikov, A. N.; Zhang, F.; Zhang, Q.; Ju, Y.; Hu, Y.; Zhao, L.; Han, X.; Meslamani, J.; Xu, F.; Jaganathan, A.; Shen, T.; Zhu, H.; Rusinova, E.; Zeng, L.; Zhou, J.; Yang, J.; Peng, L.; Ohlmeyer, M.; Walsh, M. J.; Zhang, D. Y.; Xiong, H.; Zhou, M.-M., BET N-

terminal bromodomain inhibition selectively blocks Th17 cell differentiation and ameliorates colitis in mice. *Proceedings of the National Academy of Sciences* **2017,** *114* (11), 2952.

40. Hügle, M.; Lucas, X.; Weitzel, G.; Ostrovskyi, D.; Breit, B.; Gerhardt, S.; Einsle, O.; Günther, S.; Wohlwend, D., 4-Acyl Pyrrole Derivatives Yield Novel Vectors for Designing Inhibitors of the Acetyl-Lysine Recognition Site of BRD4(1). *Journal of Medicinal Chemistry* **2016,** *59* (4), 1518-1530.

41. Raux, B.; Voitovich, Y.; Derviaux, C.; Lugari, A.; Rebuffet, E.; Milhas, S.; Priet, S.; Roux, T.; Trinquet, E.; Guillemot, J.-C.; Knapp, S.; Brunel, J.-M.; Fedorov, A. Y.; Collette, Y.; Roche, P.; Betzi, S.; Combes, S.; Morelli, X., Exploring Selective Inhibition of the First Bromodomain of the Human Bromodomain and Extra-terminal Domain (BET) Proteins. *Journal of Medicinal Chemistry* **2016,** *59* (4), 1634-1641.

42. Zhang, G.; Plotnikov, A. N.; Rusinova, E.; Shen, T.; Morohashi, K.; Joshua, J.; Zeng, L.; Mujtaba, S.; Ohlmeyer, M.; Zhou, M.-M., Structure-Guided Design of Potent Diazobenzene Inhibitors for the BET Bromodomains. *Journal of Medicinal Chemistry* **2013,** *56* (22), 9251-9264.

43. Divakaran, A.; Talluri, S. K.; Ayoub, A. M.; Mishra, N. K.; Cui, H.; Widen, J. C.; Berndt, N.; Zhu, J.-Y.; Carlson, A. S.; Topczewski, J. J.; Schonbrunn, E. K.; Harki, D. A.; Pomerantz, W. C. K., Molecular Basis for the N-Terminal Bromodomain-and-Extra-Terminal-Family Selectivity of a Dual Kinase–Bromodomain Inhibitor. *Journal of Medicinal Chemistry* **2018,** *61* (20), 9316-9334.

44. Wellaway, C. R.; Bamborough, P.; Bernard, S.; Chung, C.-w.; Craggs, P. D.; Cutler, L.; Demont, E. H.; Evans, J. P.; Gordon, L.; Karamshi, B.; Lewis, A. J.; Lindon, M. J.; Mitchell, D. J.; Rioja, I.; Soden, P. E.; Taylor, S.; Watson, R. J.; Willis, R.; Woolven, J. M.; Wyspianska, B. S.; Kerr, W. J.; Prinjha, R. K., Structure-based Design of a Bromodomain and Extraterminal Domain (BET) Inhibitor Selective for the N-terminal Bromodomains that Retains an Anti-inflammatory and Anti-proliferative Phenotype. *J. Med. Chem.* **2020,** *Submitted*.

45. Baud, M. G. J.; Lin-Shiao, E.; Zengerle, M.; Tallant, C.; Ciulli, A., New Synthetic Routes to Triazolo-benzodiazepine Analogues: Expanding the Scope of the Bump-and-Hole Approach for

Selective Bromo and Extra-Terminal (BET) Bromodomain Inhibition. *J. Med. Chem.* **2016,** *59* (4), 1492-1500.

46. Picaud, S.; Wells, C.; Felletar, I.; Brotherton, D.; Martin, S.; Savitsky, P.; Diez-Dacal, B.; Philpott, M.; Bountra, C.; Lingard, H.; Fedorov, O.; Müller, S.; Brennan, P. E.; Knapp, S.; Filippakopoulos, P., RVX-208, an inhibitor of BET transcriptional regulators with selectivity for the second bromodomain. *Proceedings of the National Academy of Sciences* **2013,** *110* (49), 19754.

47. Law, R. P.; Atkinson, S. J.; Bamborough, P.; Chung, C.-w.; Demont, E. H.; Gordon, L. J.; Lindon, M.; Prinjha, R. K.; Watson, A. J. B.; Hirst, D. J., Discovery of Tetrahydroquinoxalines as Bromodomain and Extra-Terminal Domain (BET) Inhibitors with Selectivity for the Second Bromodomain. *Journal of Medicinal Chemistry* **2018,** *61* (10), 4317-4334.

48. Faivre, E. J.; McDaniel, K. F.; Albert, D. H.; Mantena, S. R.; Plotnik, J. P.; Wilcox, D.; Zhang, L.; Bui, M. H.; Sheppard, G. S.; Wang, L.; Sehgal, V.; Lin, X.; Huang, X.; Lu, X.; Uziel, T.; Hessler, P.; Lam, L. T.; Bellin, R. J.; Mehta, G.; Fidanze, S.; Pratt, J. K.; Liu, D.; Hasvold, L. A.; Sun, C.; Panchal, S. C.; Nicolette, J. J.; Fossey, S. L.; Park, C. H.; Longenecker, K.; Bigelow, L.; Torrent, M.; Rosenberg, S. H.; Kati, W. M.; Shen, Y., Selective inhibition of the BD2 bromodomain of BET proteins in prostate cancer. *Nature* **2020,** *578* (7794), 306-310.

49. Sheppard, G. S.; Wang, L.; Fidanze, S. D.; Hasvold, L. A.; Liu, D.; Pratt, J. K.; Park, C. H.; Longenecker, K. L.; Qiu, W.; Torrent, M.; Kovar, P.; Bui, M.; Faivre, E. J.; Huang, X.; Lin, X.; Wilcox, D.; Zhang, L.; Shen, Y.; Albert, D. H.; Magoc, T. J.; Rajaraman, G.; Kati, W. M.; McDaniel, K. F., Discovery of N-Ethyl-4-[2-(4-fluoro-2,6-dimethyl-phenoxy)-5-(1-hydroxy-1-methyl-ethyl)phenyl]-6-methyl-7-oxo-1H-pyrrolo[2,3-c]pyridine-2-carboxamide (ABBV-744), a BET Bromodomain Inhibitor with Selectivity for the Second Bromodomain. *J. Med. Chem.* **2020**.

50. Chen, D.; Lu, T.; Yan, Z.; Lu, W.; Zhou, F.; Lyu, X.; Xu, B.; Jiang, H.; Chen, K.; Luo, C.; Zhao, Y., Discovery, Structural Insight, and Bioactivities of BY27 as a Selective Inhibitor of the Second Bromodomains of BET Proteins. *Eur. J. Med. Chem.* **2019,** *182*, 111633.

51. Kharenko, O. A.; Gesner, E. M.; Patel, R. G.; Norek, K.; White, A.; Fontano, E.; Suto, R. K.; Young, P. R.; McLure, K. G.; Hansen, H. C., RVX-297- a novel BD2 selective inhibitor of BET bromodomains. *Biochemical and Biophysical Research Communications* **2016,** *477* (1), 62-67.

52. Jahagirdar, R.; Attwell, S.; Marusic, S.; Bendele, A.; Shenoy, N.; McLure, K. G.; Gilham, D.; Norek, K.; Hansen, H. C.; Yu, R.; Tobin, J.; Wagner, G. S.; Young, P. R.; Wong, N. C. W.; Kulikowski, E., RVX-297, a BET Bromodomain Inhibitor, Has Therapeutic Effects in Preclinical Models of Acute Inflammation and Autoimmune Disease. *Molecular Pharmacology* **2017,** *92* (6), 694.

53. Gilan, O.; Rioja, I.; Knezevic, K.; Bell, M. J.; Yeung, M. M.; Harker, N. R.; Lam, E. Y. N.; Chung, C.-w.; Bamborough, P.; Petretich, M.; Urh, M.; Atkinson, S. J.; Bassil, A. K.; Roberts, E. J.; Vassiliadis, D.; Burr, M. L.; Preston, A. G. S.; Wellaway, C.; Werner, T.; Gray, J. R.; Michon, A.-M.; Gobbetti, T.; Kumar, V.; Soden, P. E.; Haynes, A.; Vappiani, J.; Tough, D. F.; Taylor, S.; Dawson, S.-J.; Bantscheff, M.; Lindon, M.; Drewes, G.; Demont, E. H.; Daniels, D. L.; Grandi, P.; Prinjha, R. K.; Dawson, M. A., Selective Targeting of BD1 and BD2 of the BET Proteins in Cancer and Immuno-Inflammation. *Science* **2020,** *368* (6489), 387-394.

54. Miller, T. C. R.; Simon, B.; Rybin, V.; Grötsch, H.; Curtet, S.; Khochbin, S.; Carlomagno, T.; Müller, C. W., A bromodomain–DNA interaction facilitates acetylation-dependent bivalent nucleosome recognition by the BET protein BRDT. *Nature Communications* **2016,** *7*, 13855.

55. Baud, M. G. J.; Lin-Shiao, E.; Cardote, T.; Tallant, C.; Pschibul, A.; Chan, K.-H.; Zengerle, M.; Garcia, J. R.; Kwan, T. T. L.; Ferguson, F. M.; Ciulli, A., A bump-and-hole approach to engineer controlled selectivity of BET bromodomain chemical probes. *Science* **2014,** *346* (6209), 638.

56. Runcie, A. C.; Zengerle, M.; Chan, K. H.; Testa, A.; van Beurden, L.; Baud, M. G. J.; Epemolu, O.; Ellis, L. C. J.; Read, K. D.; Coulthard, V.; Brien, A.; Ciulli, A., Optimization of a "bump-and-hole" approach to allele-selective BET bromodomain inhibition. *Chemical Science* **2018**.

57. Olp, M. D.; Jackson, V.; Smith, B. C., Nucleosome Scaffolding by Brd4 Tandem Bromodomains in Acetylation-Dependent Chromatin Compartmentalization. *bioRxiv* **2019**, 699967.

58. Kuntz, I. D.; Chen, K.; Sharp, K. A.; Kollman, P. A., The maximal affinity of ligands. *Proceedings of the National Academy of Sciences* **1999,** *96* (18), 9997.

59. Hopkins, A. L.; Groom, C. R.; Alex, A., Ligand efficiency: a useful metric for lead selection. *Drug Discovery Today* **2004,** *9* (10), 430-431.

60. Mortenson, P. N.; Murray, C. W., Assessing the lipophilicity of fragments and early hits. *Journal of Computer-Aided Molecular Design* **2011,** *25* (7), 663-667.

61. Young, R. J.; Green, D. V. S.; Luscombe, C. N.; Hill, A. P., Getting Physical in Drug Discovery II: The Impact of Chromatographic Hydrophobicity Measurements and Aromaticity. *Drug Discovery Today* **2011,** *16* (17), 822-830.

62. Chung, C.-w.; Coste, H.; White, J. H.; Mirguet, O.; Wilde, J.; Gosmini, R. L.; Delves, C.; Magny, S. M.; Woodward, R.; Hughes, S. A.; Boursier, E. V.; Flynn, H.; Bouillot, A. M.; Bamborough, P.; Brusq, J.-M. G.; Gellibert, F. J.; Jones, E. J.; Riou, A. M.; Homes, P.; Martin, S. L.; Uings, I. J.; Toum, J.; Clément, C. A.; Boullay, A.-B.; Grimley, R. L.; Blandel, F. M.; Prinjha, R. K.; Lee, K.; Kirilovsky, J.; Nicodeme, E., Discovery and Characterization of Small Molecule Inhibitors of the BET Family Bromodomains. *Journal of Medicinal Chemistry* **2011,** *54* (11), 3827-3838.

63. Filippakopoulos, P.; Knapp, S., Targeting bromodomains: epigenetic readers of lysine acetylation. *Nature Reviews Drug Discovery* **2014,** *13*, 337.

64. Filippakopoulos, P.; Picaud, S.; Mangos, M.; Keates, T.; Lambert, J.-P.; Barsyte-Lovejoy, D.; Felletar, I.; Volkmer, R.; Müller, S.; Pawson, T.; Gingras, A.-C.; Arrowsmith, Cheryl H.; Knapp, S., Histone Recognition and Large-Scale Structural Analysis of the Human Bromodomain Family. *Cell* **2012,** *149* (1), 214-231.

65. Ferguson, F. M.; Fedorov, O.; Chaikuad, A.; Philpott, M.; Muniz, J. R. C.; Felletar, I.; von Delft, F.; Heightman, T.; Knapp, S.; Abell, C.; Ciulli, A., Targeting Low-Druggability Bromodomains: Fragment Based Screening and Inhibitor Design against the BAZ2B Bromodomain. *J. Med. Chem.* **2013,** *56* (24), 10183-10187.

66. Preston, A.; Atkinson, S. J.; Seal, J.; Mitchell, D. J.; Watson, R. J.; Gray, J. R. J.; Woolven, J.; Wall, I.; Chung, C.-w.; Bamborough, Paul; Rianjongdee, F.; Taylor, S.; Michon, A.-M.; Grandi, P.; Rioja, I.; Gordon, L.; Jones, E. J.; Craggs, P. D.; Prinjha, R. K.; Lindon, M.; Demont, E. H., The Design and Synthesis of a Highly Selective and In Vivo Capable Inhibitor of the Second Bromodomain (BD2) of the Bromodomain and Extra Terminal Domain (BET) Family of Proteins. *J. Med. Chem.* **2020,** *Submitted*.

67. Veber, D. F.; Johnson, S. R.; Cheng, H.-Y.; Smith, B. R.; Ward, K. W.; Kopple, K. D., Molecular Properties That Influence the Oral Bioavailability of Drug Candidates. *Journal of Medicinal Chemistry* **2002,** *45* (12), 2615-2623.

68. Hill, A. P.; Young, R. J., Getting physical in drug discovery: a contemporary perspective on solubility and hydrophobicity. *Drug Discovery Today* **2010,** *15* (15), 648-655.

69. Skipper, P. L.; Kim, M. Y.; Sun, H. L. P.; Wogan, G. N.; Tannenbaum, S. R., Monocyclic aromatic amines as potential human carcinogens: old is new again. *Carcinogenesis* **2010,** *31* (1), 50-58.

70. Smith, D. A.; Di, L.; Kerns, E. H., The effect of plasma protein binding on in vivo efficacy: misconceptions in drug discovery. *Nature Reviews Drug Discovery* **2010,** *9*, 929.

71. Ueda, T.; Konishi, H.; Manabe, K., Trichlorophenyl Formate: Highly Reactive and Easily Accessible Crystalline CO Surrogate for Palladium-Catalyzed Carbonylation of Aryl/Alkenyl Halides and Triflates. *Organic Letters* **2012,** *14* (20), 5370-5373.

72. Schoenberg, A.; Bartoletti, I.; Heck, R. F., Palladium-catalyzed carboalkoxylation of aryl, benzyl, and vinylic halides. *The Journal of Organic Chemistry* **1974,** *39* (23), 3318-3326.

73. Baburajan, P.; Elango, K. P., Co2(CO)8 as a convenient in situ CO source for the direct synthesis of benzamides from aryl halides (Br/I) via aminocarbonylation. *Tetrahedron Letters* **2014,** *55* (5), 1006-1010.

74. Krasnaya, Z. A., Interaction of 5-Acetyl(alkoxycarbonyl)-3-alkoxycarbonyl-6-methylpyridin-2(1H)-ones with Primary Aromatic Amines and Hydrazine Hydrate. *Chemistry of Heterocyclic Compounds* **2004,** *40* (9), 1155-1161.

75. Malmqvist, M., Biospecific interaction analysis using biosensor technology. *Nature* **1993,** *361*, 186.

76. Ames, B. N., Identifying environmental chemicals causing mutations and cancer. *Science* **1979,** *204* (4393), 587.

77. Clive, D.; Flamm, W. G.; Machesko, M. R.; Bernheim, N. J., A mutational assay system using the thymidine kinase locus in mouse lymphoma cells. *Mutation Research/Fundamental and Molecular Mechanisms of Mutagenesis* **1972,** *16* (1), 77-87.

78. Chen, T.; Guo, X.; Moore, M., *The Mouse Lymphoma Assay*. 2014; p 323-342.

79. Stieger, B., Role of the bile salt export pump, BSEP, in acquired forms of cholestasis. *Drug Metabolism Reviews* **2010,** *42* (3), 437-445.

80. Baillie, T. A., Metabolism and Toxicity of Drugs. Two Decades of Progress in Industrial Drug Metabolism. *Chemical Research in Toxicology* **2008,** *21* (1), 129-137.

81. Masubuchi, Y.; Horie, T., Toxicological Significance of Mechanism-Based Inactivation of Cytochrome P450 Enzymes by Drugs. *Critical Reviews in Toxicology* **2007,** *37* (5), 389-412.

82. Murray, M., Drug-Mediated Inactivation of Cytochrome P450. *Clinical and Experimental Pharmacology and Physiology* **1997,** *24* (7), 465-470.

83. Dalvie, D. K.; Kalgutkar, A. S.; Khojasteh-Bakht, S. C.; Obach, R. S.; O'Donnell, J. P., Biotransformation Reactions of Five-Membered Aromatic Heterocyclic Rings. *Chemical Research in Toxicology* **2002,** *15* (3), 269-299.

84. Deshmane, S. L.; Kremlev, S.; Amini, S.; Sawaya, B. E., Monocyte Chemoattractant Protein-1 (MCP-1): An Overview. *Journal of Interferon & Cytokine Research* **2009,** *29* (6), 313-326.

85. Anderson, K. W.; Fotouhi, N.; Gillespie, P.; Goodnow, R. A., Jr.; Guertin, K. R.; Haynes, N.-E.; Myers, M. P.; Pietranico-Cole, S. L.; Qi, L.; Rossman, P. L.; Scott, N. R.; Thakkar, K. C.; Tilley, J. W.; Zhang, Q. Preparation of Pyrazole-4-carboxamide Derivatives as 11-Beta-Hydroxysteroid Dehydrogenase Form I (11-beta-HSD1) Inhibitors. WO2007107470A2, 2007.

86. Camurri, G.; Zaramella, A., High-Throughput Liquid Chromatography/Mass Spectrometry Method for the Determination of the Chromatographic Hydrophobicity Index. *Anal. Chem.* **2001,** *73* (15), 3716-3722.

87. Valko, K.; Nunhuck, S.; Bevan, C.; Abraham, M. H.; Reynolds, D. P., Fast Gradient HPLC Method to Determine Compounds Binding to Human Serum Albumin. Relationships with Octanol/Water and Immobilized Artificial Membrane Lipophilicity. *J. Pharm. Sci.* **2003,** *92* (11), 2236-2248.

88. Bamborough, P.; Chung, C.-w.; Demont, E. H.; Furze, R. C.; Bannister, A. J.; Che, K. H.; Diallo, H.; Douault, C.; Grandi, P.; Kouzarides, T.; Michon, A.-M.; Mitchell, D. J.; Prinjha, R. K.; Rau, C.; Robson, S.; Sheppard, R. J.; Upton, R.; Watson, R. J., A Chemical Probe for the ATAD2 Bromodomain. *Angew. Chem. Int. Ed.* **2016,** *55* (38), 11382-11386.

89. Bamborough, P.; Chung, C.-w.; Furze, R. C.; Grandi, P.; Michon, A.-M.; Sheppard, R. J.; Barnett, H.; Diallo, H.; Dixon, D. P.; Douault, C.; Jones, E. J.; Karamshi, B.; Mitchell, D. J.; Prinjha, R. K.; Rau, C.; Watson, R. J.; Werner, T.; Demont, E. H., Structure-Based Optimization of Naphthyridones into Potent ATAD2 Bromodomain Inhibitors. *Journal of Medicinal Chemistry* **2015,** *58* (15), 6151-6178.

TOC Graphic:

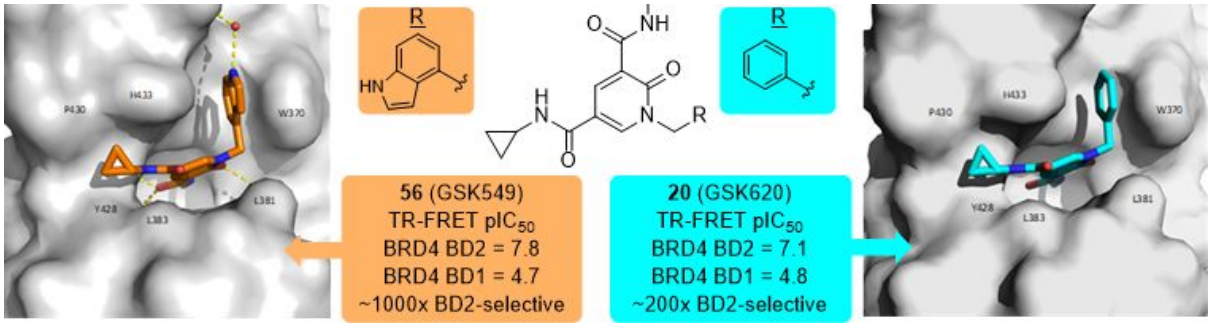
R
HN
O
NH
H
N
O
O
N
R
R
56 (GSK549)
TR-FRET pIC50
BRD4 BD2 = 7.8
BRD4 BD1 = 4.7
~1000x BD2-selective
20 (GSK620)
TR-FRET pIC50
BRD4 BD2 = 7.1
BRD4 BD1 = 4.8
~200x BD2-selective